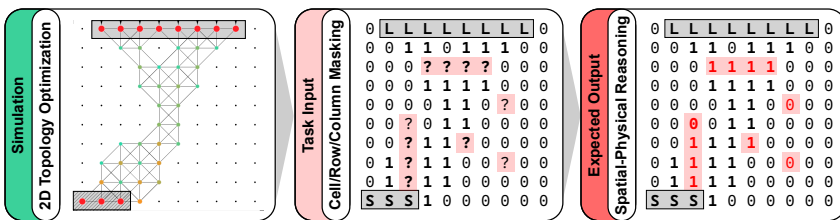


SPHYR: SPATIAL-PHYSICAL REASONING BENCHMARK ON MATERIAL DISTRIBUTION

000
001
002
003
004
005 **Anonymous authors**
006 Paper under double-blind review
007
008
009
010

ABSTRACT

011 We introduce a novel dataset designed to benchmark the physical and spatial reason-
012 ing capabilities of Large Language Models (LLM) based on topology optimization,
013 a method for computing optimal material distributions within a design space under
014 prescribed loads and supports. In this dataset, LLMs are provided with conditions
015 such as 2D boundary, applied forces and supports, and must reason about the result-
016 ing optimal material distribution. The dataset includes a variety of tasks, ranging
017 from filling in masked regions within partial structures to predicting complete
018 material distributions. Solving these tasks requires understanding the flow of forces
019 and the required material distribution under given constraints, without access to
020 simulation tools or explicit physical models, challenging models to reason about
021 structural stability and spatial organization. Our dataset targets the evaluation of
022 spatial and physical reasoning abilities in 2D settings, offering a complementary
023 perspective to traditional language and logic benchmarks¹.
024



025
026
027
028
029
030
031
032 Figure 1: Topology Optimization is used to calculate material distribution. Masking individual cells,
033 rows, columns or the complete distribution space offer challenging spatial physical reasoning tasks.
034
035
036

1 INTRODUCTION

038 Large language models (LLMs) have achieved strong performance on linguistic and logical tasks, but
039 their ability to reason about physical systems and spatial structures remains underexplored Zhang et al.
040 (2025). Existing benchmarks primarily probe either visual perception or text-based commonsense
041 knowledge, but few explicitly test reasoning grounded in physical constraints.

042 For example, visual question-answering benchmarks such as CLEVR focus on object attributes
043 and spatial relations in synthetic scenes Johnson et al. (2016), while intuitive physics datasets like
044 IntPhys and Physion evaluate models’ ability to predict or assess the plausibility of physical events in
045 videos Riochet et al. (2020); Bear et al. (2022). Interactive environments such as PHYRE Bakhtin
046 et al. (2019) and stability-focused datasets like ShapeStacks Groth et al. (2018) further probe causal
047 reasoning and contact mechanics, whereas text-based datasets such as PIQA Bisk et al. (2019) and
048 PhysReason Zhang et al. (2025) target physical commonsense and multi-step problem solving in
049 language form.

050 Existing benchmarks have advanced our understanding of physical reasoning in LLMs, but they
051 largely focus on object dynamics, intuitive physics, or qualitative predictions. They do not evaluate

052 ¹Huggingface Dataset: anonymized
053 Data Generation and Model Evaluation Code: <https://anonymous.4open.science/r/SPhyR-587C>

whether models can reason about how forces should be supported and transmitted through a structure, a capability fundamental to engineering and design. This gap leaves untested a crucial class of reasoning that requires integrating spatial layout with structural principles such as load paths, stiffness, and stability. Beyond physical reasoning, recent work like ARC-AGI-2 Chollet et al. (2025) has introduced grid-based tasks for testing abstract reasoning and generalization. While unrelated to physics, this work highlights the value of structured 2D representations for isolating reasoning capabilities. We build on this intuition but shift the focus from symbolic transformations to spatially grounded physical reasoning.

To address this gap, we introduce **SPhyR**, a new benchmark for evaluating spatial and physical reasoning in LLMs. SPhyR formulates topology optimization-inspired tasks in a grid-based format, where models must infer how to distribute material to support specified forces and constraints. By testing whether models can reason about load paths, stability, and structural connectivity from descriptions alone, SPhyR bridges the gap between language-based reasoning and physically grounded design tasks. We benchmark state-of-the-art LLMs on SPhyR and reveal fundamental limitations in their ability to integrate spatial and physical reasoning.

2 RELATED WORK

Benchmarks for Physical and Spatial Reasoning A wide range of benchmarks probe models' understanding of physical and spatial reasoning (Table 1). CLEVR Johnson et al. (2016) evaluates visual reasoning about objects and spatial relations in synthetic scenes, while CLEVRER Yi et al. (2020) extends this to temporal and causal reasoning in videos. IntPhys Riochet et al. (2020) and Physion Bear et al. (2022) test whether models can predict or assess the plausibility of physical events, while ShapeStacks Groth et al. (2018) targets block stability prediction. In interactive settings, PHYRE Bakhtin et al. (2019) challenges agents to solve 2D physics puzzles by reasoning about actions and causal effects. Language-based datasets such as PIQA Bisk et al. (2019) and PhysReason Zhang et al. (2025) shift the focus from perception to textual physical reasoning, evaluating knowledge of everyday object interactions and multi-step physics problem solving, respectively.

While these benchmarks advance physical reasoning evaluation, they largely focus on event prediction or commonsense reasoning. None require models to determine optimal material arrangements under explicit load and support constraints - a capability crucial for real-world engineering reasoning.

Benchmark	Format	Physical Reasoning	Spatial Reasoning	Notes
CLEVR (2017)	Visual QA	✗	✓	Scene reasoning
CLEVRER (2020)	Video QA	✓	✓	Causal events
IntPhys (2018)	Video plausibility	✓	✓	Violation detection
Physion (2021)	Video prediction	✓	✓	Object behavior prediction
ShapeStacks (2016)	Image classification	✓	✓	Block stability
PHYRE (2019)	2D physics puzzles	✓	✓	Action planning
PIQA (2020)	Text QA	✓	✗	Physical commonsense
PhysReason (2023)	Text QA	✓	✗	Multi-step physics
SPhyR (ours)	Structured prediction	✓	✓	Material distribution

Table 1: Comparison of existing benchmarks evaluating physical and spatial reasoning. Our proposed dataset (**SPhyR**) focuses specifically on material distribution reasoning under boundary conditions, combining spatial and physical understanding in structured tasks.

Topology Optimization as a Benchmark Topology optimization (TO) Bendsøe & Sigmund (2004) is a well-established method for computing optimal material layouts in a domain under specified forces and supports. Prior work on Machine Learning (ML) in this space has focused on accelerating solvers or generating high-quality designs Banga et al. (2018); Rawat & Shen (2019). Our work repurposes topology optimization as a reasoning benchmark rather than a design tool. By framing it as a grid-based prediction problem, SPhyR tests whether LLMs can infer material distributions solely from boundary conditions and physical constraints - without access to solvers or simulation engines. This setup complements existing physical reasoning benchmarks by embedding spatial and physical structure into tasks that require more than pattern recognition.

108 **Machine Learning for Topology Optimization** Prior machine learning work for Topology Optimization (TO) has focused on developing fast, high-fidelity solvers that can predict optimized material layouts with orders-of-magnitude speedup over conventional methods Banga et al. (2018);
 109 Rawat & Shen (2019); Zhang et al. (2020). These domain-specific approaches rely on embedding
 110 explicit structural knowledge, such as physics-informed loss functions or compliance constraints, into
 111 the model architecture and training process. In contrast, SPhyR evaluates general-purpose LLMs in
 112 a zero-shot setting, probing whether emergent, implicit physical knowledge acquired during broad
 113 training can substitute for explicitly learned physics.
 114

116 **Structured Reasoning Beyond Physics** Finally, our work connects to broader research on structured reasoning in grid-based environments. ARC-AGI-2 Chollet et al. (2025) tests abstract reasoning
 117 and generalization in symbolic, non-physical tasks. While ARC-AGI-2 and SPhyR share a structured
 118 representation, SPhyR introduces grounded physical constraints, bridging the gap between abstract
 119 symbolic reasoning and the physically grounded reasoning required for real-world design.
 120

122 3 PROBLEM SETUP

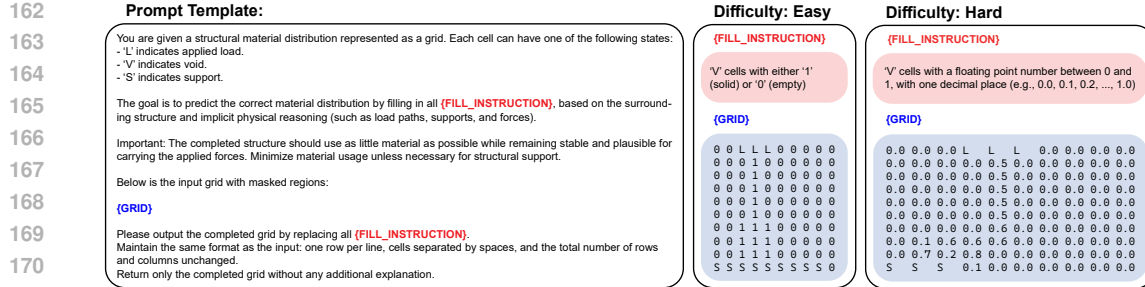
124 **Topology Optimization Task** Topology optimization determines an optimal material distribution
 125 within a domain under prescribed forces and supports. All dataset samples are generated using
 126 Millipede’s density-based SIMP formulation, solving a minimum-compliance problem with a fixed
 127 volume fraction (Appendix B for solver parameters). This yields well-defined, single-objective
 128 solutions that capture characteristic load paths and material connectivity.
 129

130 In this work, we repurpose these topology optimization instances as reasoning tasks for LLMs.
 131 Instead of performing numerical optimization, models must predict plausible material distributions
 132 from forces, supports, and boundaries alone, requiring them to infer principles of load transfer,
 133 stability, and efficient material use, approximating the behavior of minimum-compliance topology
 134 optimization without access to simulation tools.

135 **Input and Output Specification** Each task instance in our benchmark is defined by a set of
 136 boundary conditions and a corresponding material distribution. The **inputs** provided to the model are:
 137 **2D boundaries**: A discretized 2D grid representing the spatial extent of the structure, **fixed supports**:
 138 Locations within the boundaries that act as load bearing supports and **applied forces**: Locations
 139 within the boundaries specifying external loads. The **output** expected from the model is a partial or
 140 complete **material distribution** over the domain grid, indicating where material should be placed to
 141 form a material optimized, that is minimum material distributed, but stable structure under the given
 142 boundary conditions. All inputs and outputs are represented in structured formats suitable for LLMs,
 143 through textual descriptions and serialized grids. No direct access to simulation results or numerical
 144 solvers is provided.

145 **Reasoning Challenges** The tasks in our benchmark require a combination of physical and spatial
 146 reasoning that poses significant challenges for current large language models. First, models must infer
 147 how forces propagate through the structure, deciding where material is necessary to maintain stability
 148 and support loads. This involves understanding force paths, support connectivity, and load transfer-
 149 concepts that are rarely encountered in typical LLM training data. Second, models must reason
 150 spatially about the layout of material across a 2D grid. Predicting plausible completions requires
 151 local coherence (e.g., avoiding isolated material islands) as well as global structural organization
 152 (e.g., maintaining continuous load paths from forces to supports). Moreover, models must solve these
 153 tasks without explicit simulation tools or numerical methods. Instead, they must generalize from the
 154 provided boundary conditions and partial observations, synthesizing structures that satisfy implicit
 155 physical constraints. These reasoning demands span from local (individual cells or lines) to global
 156 (complete structures), creating a rich and graded challenge space for evaluating LLM capabilities
 157 beyond language-based tasks.

158 **Task Variations** We define several task variations according to the nature and extent of the masked
 159 regions in the material distribution, and categorize them into two difficulty levels: easy and hard.
 160 Easy is distribution based on binary values such as material or no material, while hard is based on a
 161 continuous value range, 0 to 1. **N-Random Cell(s)**: Predict the material state of N randomly masked
 162 cell(s), where N is one of 1, 5 or 10. **N-Random Row(s)**: Predict the material state of N randomly



172 Figure 2: Prompt template used across all tasks and difficulty levels, showing instructions and grid
 173 format as served to models for evaluation.

174
 175
 176 masked row(s), where N is one of 1 or 3. **N-Random Columns(s):** Predict the material state of N
 177 randomly masked columns(s), where N is one of 1 or 3. **Full Structure Prediction:** Predict the
 178 complete material distribution based only on boundary conditions. These variations allow us to
 179 systematically probe local and global reasoning abilities, from single-cell predictions to complex
 180 structural synthesis (Appendix C for samples).

181 4 DATASET DESCRIPTION

182 The SPhyR dataset was generated by solving 2D topology optimization problems, creating material
 183 distributions under various boundary conditions using the density-based solver Millipede Michalatos
 184 & Kaijima (2024). We constructed a set of 2D samples by systematically varying the positions
 185 of applied forces and supports, focusing on load-support scenarios typical of structural building
 186 design (load from the top, support on the bottom, ranging from 3 to 6 cells in width). Each material
 187 distribution was optimized for stiffness and efficiency using 10 solver iteration steps. The inherent
 188 variability in these boundary conditions ensures that tasks require generalization beyond memorization
 189 of fixed patterns (Appendix B, for detailed solver parameters).

190 **Dataset Statistics** The dataset consists of 10×10 structural optimization grids, balancing computational
 191 tractability with sufficient spatial complexity. In total, the dataset contains **1296** samples for
 192 all task variations and difficulties. These samples are organized into task-specific subsets, including
 193 cell completion, row/column completion, and full structure prediction, across both easy and hard
 194 difficulty levels. The full list of eight subject types (e.g., 1 Random Cell, 3 Random Row) and their
 195 descriptions is provided in Table C. Each sample includes structured representations of the boundary
 196 conditions and the corresponding ground truth material distribution.

197 **Input and Output Formats** Each sample in the dataset is represented as a structured input-output
 198 pair designed for compatibility with large language models. Samples are grouped into task-specific
 199 subjects, enabling targeted evaluation of different reasoning challenges.

200 The input consists of a natural language prompt that describes the task and defines the structural
 201 grid format. Within this grid, different symbols indicate key physical roles: **L** marks an applied
 202 load, **S** a support, and **V** (void) a masked cell whose material state must be predicted. Regions with
 203 known material values, whether binary or continuous, depending on the task difficulty (easy/hard),
 204 are explicitly included in the grid. The prompt provides clear instructions emphasizing structural
 205 plausibility and material efficiency, along with a grid where each row appears on a separate line and
 206 cell values are space-separated.

207 The expected output is a completed version of the same grid, where all **V** cells are replaced by
 208 predicted values (1 or 0) while preserving the original structure and formatting. No explanation or
 209 commentary is included in the output-only the raw grid content.

210 Each subject is labeled with a difficulty level. In easy variants, the ground truth material distribution is
 211 binary, focusing on high-level structural placement and discrete spatial reasoning. In hard variants, the
 212 underlying distributions are continuous or involve more complex structural dependencies, requiring
 213 finer-grained predictions and deeper reasoning about stress propagation and global support (Figure 2,
 214 for prompt template and Appendix J, E.1, for detailed model prompt and completion samples).

216 5 EVALUATION SETUP
217218 5.1 EVALUATION METRICS
219

220 We evaluate model performance using three complementary families of metrics for a holistic as-
221 sessment of both symbolic accuracy and structural realism: (1) **Reconstruction Accuracy Metrics**,
222 quantifying cell-wise agreement with the ground truth, including measures of fidelity, penalization,
223 and difficulty weighting; (2) **Topological Validity Metrics**, assessing global structural soundness
224 through load-support connectivity and grid validity; and (3) **Physics-Approximating Metrics**, es-
225 timating the structural efficiency via gravity-aligned load-transfer paths. This comprehensive suite
226 ensures robustness against simple pattern-matching success.

227 **Reconstruction Accuracy Metrics** We assess reconstruction fidelity using several grid-level
228 measures based on cellwise agreement between the predicted grid \hat{G} and the ground-truth grid G^*
229 (Appendix ??, for prompt, completion and calculation scenarios).

- 231 • **Exact Match** \uparrow (**EM**): Binary indicator of perfect reconstruction:

$$232 \quad 233 \quad 234 \quad \text{EM} = \begin{cases} 1, & \text{if } \hat{G} = G^*, \\ 0, & \text{otherwise.} \end{cases}$$

- 235 • **Difference Ratio (DiffRatio)**: Fraction of incorrect cells normalized by total ground-truth
236 mass:

$$237 \quad 238 \quad 239 \quad \text{DiffRatio} = 1 - \frac{D(\hat{G}, G^*)}{\sum_{i,j} g_{ij}^*},$$

240 where $D(A, B)$ counts cellwise mismatches. *Higher is better* (1 indicates perfect match).

- 241 • **Relative Difference Ratio (RelDiffRatio)**: A softer variant that measures numeric deviation:

$$242 \quad 243 \quad 244 \quad \text{RelDiffRatio} = 1 - \frac{D_{\text{rel}}(\hat{G}, G^*)}{\sum_{i,j} g_{ij}^*},$$

245 where D_{rel} accumulates $|a_{ij} - b_{ij}|$ for numeric cells and counts categorical mismatches
246 (L, S, V) as 1. *Higher is better*.

- 247 • **Penalized Difference Ratio (PenDiffRatio)**: Penalty-weighted version increasing the cost
248 of modifying or introducing new load, support, or void cells:

$$249 \quad 250 \quad 251 \quad \text{PenDiffRatio} = 1 - \frac{D_{\text{pen}}(\hat{G}, G^*)}{\sum_{i,j} g_{ij}^*},$$

252 where D_{pen} multiplies L, S , or V cell errors by a penalty (typically $3\times$). *Higher is better*.

- 253 • **Difficulty-Weighted Difference Ratios**: Optional variants that multiply each cell’s contribu-
254 tion by its local difficulty weight (see DWCS below). These versions emphasize correctness
255 in structurally ambiguous or high-difficulty regions. *Higher is better*.

256 **Topological Validity Metrics** Beyond pixelwise accuracy, we evaluate the structural and connectiv-
257 ity properties of the reconstructed topology (Appendix D.3, for prompt, completion and calculation
258 scenarios):

- 259 • **Grid Validity (ValidGrid)**: Boolean check ensuring \hat{G} matches G^* in shape and uses only
260 admissible values (L, S , or $[0, 1]$). *True is desired*.
- 261 • **Load-Support Connectivity (LSConn)**: True if any load cell (L) connects to any support
262 (S) through contiguous solid cells ($> 0, L$, or S):

$$264 \quad 265 \quad 266 \quad \text{LSConn} = \begin{cases} 1, & \exists \text{ load-support path through solids,} \\ 0, & \text{otherwise.} \end{cases}$$

267 *True is desired*.

- 268 • **Directional Load-Support Connectivity (DirLSConn)**: Same as LSConn, but restricted
269 to force paths aligned with the gravity vector g inferred from dataset rotation metadata. *True*
is *desired*.

- **Isolated Cluster Count (N_{islands}):** Number of solid-cell clusters disconnected from any load or support, found via 4-connectivity. *Lower is better*.
- **Difficulty Score (DWCS):** Average difficulty weight for originally masked cells:

$$\text{DWCS} = \frac{1}{|\mathcal{V}|} \sum_{(i,j) \in \mathcal{V}} w_{ij}, \quad w_{ij} \in \{1, 2, 3\}.$$

Higher DWCS implies the reconstruction region is more complex or ambiguous; it reflects task difficulty rather than model quality. *Higher indicates harder samples.*

Physics-Approximating Metrics To estimate the physical plausibility of predicted topologies, we approximate directional load-support efficiency using a force-path traversal cost. We calculate the average minimum directional cost for each load to reach a support, computed via a gravity-aligned Dijkstra traversal with angular and depth penalties. Unsupported loads receive a large but finite penalty (Appendix D.1 for EPCEff calculation details, and D.3, for prompt, completion and calculation scenarios).

- **Force Path Cost Average Efficiency Ratio (FPCEff):** Relative efficiency of predicted vs. ground-truth structures:

$$\text{FPCEff} = \text{clip}_{[0,1]} \left(\frac{C_{\text{avg}}^*}{\hat{C}_{\text{avg}}} \right),$$

where C_{avg}^* and \hat{C}_{avg} are average load-support path costs in G^* and \hat{G} respectively. *Higher is better.*

Category	Metric Name	Type / Range	Desired Trend
Reconstruction	Exact Match (EM)	Boolean {0,1}	True
	Difference Ratio (DiffRatio)	Float [0,1]	Higher is better
	Penalized Difference Ratio (PenDiffRatio)	Float [0,1]	Higher is better
	Relative Difference Ratio (RelDiffRatio)	Float [0,1]	Higher is better
	Difficulty-Weighted Diff. Ratio	Float [0,1]	Higher is better
	Difficulty-Weighted Rel. Diff. Ratio	Float [0,1]	Higher is better
Topology	Valid Grid (ValidGrid)	Boolean {0,1}	True
	Load-Support Connectivity (LSConn)	Boolean {0,1}	True
	Directional L-S Connectivity (DirLSConn)	Boolean {0,1}	True
	Isolated Clusters (N_{islands})	Integer ≥ 0	Lower is better
	Difficulty Score (DWCS)	Float [1,3] avg.	Higher is harder
Physics-Approx.	Force Path Cost Efficiency (FPCEff)	Float [0,1]	Higher is better

Table 2: Summary of all evaluation metrics by category, with their types, typical ranges, and optimization direction.

5.2 EXPERIMENTS

To establish baseline performance, we evaluate a broad set of contemporary language models in a zero-shot setting. From OpenAI, we include GPT-3.5 Brown et al. (2020), GPT-4.1 OpenAI et al. (2024a), and GPT-4o OpenAI et al. (2024b), representing successive generations with improved reasoning and multimodal capabilities. From Anthropic, we test Claude 3.7 Sonnet anthropic (2025a) and Claude Opus 4 anthropic (2025b), the strongest in the Claude family. From Google DeepMind, we include Gemini 1.5 Pro Team et al. (2024) and Gemini 2.5 Pro Comanici et al. (2025), designed for complex multimodal reasoning. We also assess DeepSeek-R1 DeepSeek-AI et al. (2025), an open-source model for scientific and engineering tasks, and Perplexity Sonar Team (2025a) and Sonar Reasoning Team (2025b), tuned for information-seeking and multi-step reasoning. Models are prompted (Appendix J) with structured descriptions of boundary conditions, forces, and supports, without simulation tools or external knowledge. A random subset of **100** examples spanning all task variations, difficulties and all models are evaluated under identical conditions via publicly available APIs (Table 3). Performance is measured using the metrics defined in Section 5.1.

324
325

6 RESULTS AND ANALYSIS

326
327
328
329
330

We present quantitative results in Table 3 and analyze failure modes qualitatively. Detailed results on few-shot prompting, rotation, and physics-enhanced and -neutral prompt design are discussed in the subsequent sections and further expanded in the Appendix.

331
332
333
334
335

Table 3: Zero-Shot Performance on SPhyR 2D Tasks (Easy vs. Hard). Top-performing LLMs (Claude, Gemini) maintain high Load-Support Connectivity, demonstrating core topological understanding. However, performance degrades sharply on Hard tasks, with negative Difference Ratios (red) confirming inefficient material hallucination and structural over-designing across all models. (\uparrow indicates better, \downarrow indicates worse).

Task	Metric	Easy						Hard					
		GPT 4.1	Claude Opus 4	Gemini 2.5 Pro	DeepSeek-R1	Perplexity-Sonar	GPT 4.1	Claude Opus 4	Gemini 2.5 Pro	DeepSeek-R1	Perplexity-Sonar		
1 Random Cell	Exact Match \uparrow	26	82	81	58	52	13	77	76	37	13		
	Difference Ratio (%) \uparrow	95.47	99.05	99.03	97.37	93.28	88.14	95.45	96.70	91.44	80.07		
	Relative Difference Ratio (%) \uparrow	95.47	99.05	99.03	97.37	93.28	96.05	96.72	97.88	96.51	88.98		
	Penalized Difference Ratio (%) \uparrow	94.82	98.40	98.37	96.71	92.03	92.44	93.11	94.31	92.90	85.12		
	Average Difficulty Score	1.99	1.99	1.99	1.99	1.99	1.99	1.99	1.99	1.96	1.96		
	Difficulty Weighted Difference Ratio (%) \uparrow	63.51	65.51	65.47	64.54	60.95	56.05	56.97	58.87	59.41	52.28		
	Difficulty Weighted Relative Difference Ratio (%) \uparrow	63.31	65.51	65.47	64.54	61.92	62.49	62.25	60.01	62.43	58.26		
	Valid Output Grid \uparrow	100.00	100.00	100.00	100.00	96.00	100.00	99.00	100.00	100.00	94.00		
	Load-Support Connectivity (%) \uparrow	100.00	100.00	100.00	100.00	95.00	99.00	98.00	100.00	100.00	99.00	93.00	
	Load-Support Directional Connectivity (%) \uparrow	100.00	100.00	100.00	100.00	95.00	99.00	98.00	100.00	100.00	99.00	93.00	
	Average Isolated Clusters Count \downarrow	0.32	0.00	0.00	0.15	0.16	0.44	0.00	0.01	0.26	0.37		
	Force Path Cost Average Efficiency Ratio (%) \uparrow	99.94	99.94	99.94	99.86	94.84	98.93	97.91	99.92	98.93	92.93		
5 Random Cells	Exact Match \uparrow	1	45	39	15	10	0	30	37	5	3		
	Difference Ratio (%) \uparrow	75.87	95.76	95.08	88.16	75.79	83.23	87.27	83.19	65.68	88.29		
	Relative Difference Ratio (%) \uparrow	75.87	95.76	95.08	88.16	75.79	75.68	91.58	89.98	86.83	70.37		
	Penalized Difference Ratio (%) \uparrow	69.37	89.26	88.59	81.66	68.84	61.72	78.42	75.62	71.73	57.71		
	Average Difficulty Score	1.89	1.89	1.89	1.89	1.89	1.97	1.97	1.96	1.97	1.97		
	Difficulty Weighted Difference Ratio (%) \uparrow	48.77	59.89	59.48	55.56	47.57	23.41	56.17	52.60	41.52	24.87		
	Difficulty Weighted Relative Difference Ratio (%) \uparrow	48.77	59.89	59.48	55.56	47.57	50.95	57.85	57.87	54.19	45.99		
	Valid Output Grid \uparrow	100.00	100.00	100.00	100.00	99.00	100.00	99.00	100.00	100.00	99.00		
	Load-Support Connectivity (%) \uparrow	100.00	100.00	100.00	100.00	95.00	100.00	99.00	100.00	100.00	99.00		
	Load-Support Directional Connectivity (%) \uparrow	100.00	100.00	100.00	100.00	95.00	100.00	99.00	100.00	100.00	99.00		
	Average Isolated Clusters Count \downarrow	1.64	0.00	0.00	0.44	0.37	1.88	0.00	0.03	0.56	1.22		
	Force Path Cost Average Efficiency Ratio (%) \uparrow	99.72	99.70	99.75	97.50	78.42	98.55	97.84	98.25	97.94	94.98		
10 Random Cells	Exact Match \uparrow	0	15	13	2	1	0	13	14	3	0		
	Difference Ratio (%) \uparrow	59.82	89.08	88.88	78.78	72.68	51.37	79.91	82.80	74.22	42.43		
	Relative Difference Ratio (%) \uparrow	59.82	89.08	88.88	78.78	72.68	59.85	79.91	82.50	74.29	42.37		
	Penalized Difference Ratio (%) \uparrow	47.02	67.41	70.31	65.95	59.85	47.02	70.31	72.01	71.94	2.01		
	Average Difficulty Score	1.97	1.97	1.97	1.97	1.97	2.07	2.01	1.94	2.01	1.97		
	Difficulty Weighted Difference Ratio (%) \uparrow	40.24	58.23	58.06	51.72	47.81	34.45	52.88	52.66	48.86	29.03		
	Difficulty Weighted Relative Difference Ratio (%) \uparrow	40.24	58.23	58.06	51.72	47.81	50.05	49.05	45.14	45.37	17.05		
	Valid Output Grid \uparrow	100.00	100.00	100.00	100.00	99.00	100.00	99.00	100.00	100.00	99.00		
	Load-Support Connectivity (%) \uparrow	100.00	100.00	100.00	100.00	95.00	100.00	99.00	100.00	100.00	95.00		
	Load-Support Directional Connectivity (%) \uparrow	100.00	100.00	100.00	100.00	95.00	100.00	99.00	100.00	100.00	95.00		
	Average Isolated Clusters Count \downarrow	2.27	0.00	0.00	0.46	0.40	2.82	0.01	0.02	0.69	1.20		
	Force Path Cost Average Efficiency Ratio (%) \uparrow	98.28	99.06	99.31	88.72	73.62	98.13	91.98	99.34	83.93	56.25		
1 Random Row	Exact Match \uparrow	20	52	44	14	21	2	49	46	34	7		
	Difference Ratio (%) \uparrow	84.50	94.92	93.90	73.09	77.87	18.44	80.55	71.69	73.13	27.07		
	Relative Difference Ratio (%) \uparrow	84.50	94.92	93.90	73.09	77.87	73.91	94.39	93.86	94.13	74.82		
	Penalized Difference Ratio (%) \uparrow	84.50	94.92	93.90	73.09	77.65	73.91	94.39	93.86	94.13	74.82		
	Average Difficulty Score	1.94	1.94	1.94	1.94	1.94	1.92	1.92	1.92	1.99	1.92		
	Difficulty Weighted Difference Ratio (%) \uparrow	54.72	64.04	60.55	47.90	46.05	11.00	49.25	45.14	45.37	17.05		
	Difficulty Weighted Relative Difference Ratio (%) \uparrow	54.72	64.04	60.55	47.90	46.05	47.88	61.04	61.91	60.94	57.99		
	Valid Output Grid \uparrow	97.00	100.00	100.00	100.00	91.00	98.00	100.00	100.00	100.00	91.00		
	Load-Support Connectivity (%) \uparrow	97.00	100.00	100.00	100.00	97.00	100.00	99.00	100.00	100.00	96.00		
	Load-Support Directional Connectivity (%) \uparrow	97.00	100.00	100.00	100.00	97.00	100.00	99.00	100.00	100.00	96.00		
	Average Isolated Clusters Count \downarrow	0.01	0.00	0.00	0.27	0.28	0.03	0.00	0.00	0.00	0.01	0.01	
	Force Path Cost Average Efficiency Ratio (%) \uparrow	94.09	99.68	97.54	69.22	73.47	99.99	96.97	99.87	61.31	95.91		
3 Random Rows	Exact Match \uparrow	6	35	29	20	24	0	21	26	15	3		
	Difference Ratio (%) \uparrow	50.31	88.64	84.09	62.64	62.25	-102.36	32.01	18.75	16.98	-106.35		
	Relative Difference Ratio (%) \uparrow	50.31	88.64	84.09	62.64	74.23	23.74	84.70	77.42	76.37	46.20		
	Penalized Difference Ratio (%) \uparrow	50.31	88.64	82.84	62.04	73.99	23.74	84.70	77.42	76.37	45.35		
	Average Difficulty Score	1.89	1.89	1.92	1.89	1.99	1.99	1.99	1.95	1.99	1.99		
	Difficulty Weighted Difference Ratio (%) \uparrow	37.91	55.31	53.52	39.27	46.97	-107.71	17.50	9.64	8.49	-71.32		
	Difficulty Weighted Relative Difference Ratio (%) \uparrow	37.91	55.31	53.52	39.27	46.97	17.09	55.67	49.98	49.88	30.87		
	Valid Output Grid \uparrow	90.00	100.00	99.00	100.00	100.00	100.00	100.00	100.00	100.00	98.00		
	Load-Support Connectivity (%) \uparrow	95.00	100.00	98.00	69.00	74.00	100.00	97.00	100.00	100.00	96.00		
	Load-Support Directional Connectivity (%) \uparrow	95.00	100.00	98.00	69.00	74.00	100.00	97.00	100.00	100.00	96.00		
	Average Isolated Clusters Count \downarrow	0.01	0.00	0.01	0.06	0.09	0.00	0.00	0.01	0.06	0.06	0.05	
	Force Path Cost Average Efficiency Ratio (%) \uparrow	94.09	99.00	97.30	97.61	86.51	94.44	100.00	100.00	88.00	90.00		
1 Random Column	Exact Match \uparrow	0	23	26	8	12	0	21	26	15	3		
	Difference Ratio (%) \uparrow	51.92	83.09	81.95	63.38	67.71	-34.24	37.46	20.55	44.93	29.07	-26.12	
	Relative Difference Ratio (%) \uparrow	51.92	83.09	81.95	63.38	67.71	29.24	26.68	72.53	60.88	36.26		
	Penalized Difference Ratio (%) \uparrow	47.23	71.51	73.05	55.52	53.69	-31.05	31.45	46.17	27.99	42.42		
	Average Difficulty Score	1.90	1.90	1.95	1.90	1.90	2.13	1.37	2.13	2.13	2.13		
	Difficulty Weighted Difference Ratio (%) \uparrow	36.02	50.85	48.21	40.90	44.12	-23.21	14.68	15.91	10.73	26.35		
	Difficulty Weighted Relative Difference Ratio (%) \uparrow	36.02	50.85	48.21	40.90	44.12	22.54	37.62	40.27	38.36	26.35		
	Valid Output Grid \uparrow	100.00	100.00	98.00	97.00	97.00	99.00	99.00	100.00	97.00	91.00		
	Load-Support Connectivity (%) \uparrow	100.00	100.00	98.00	97.00	97.00	99.00	99.00	100.00	97.00	90.00		
	Load-Support Directional Connectivity (%) \uparrow	100.00	100.00	98.00	97.00	97.00	99.00	99.00	100.00	97.00	90.00		
	Average Isolated Clusters Count \downarrow	0.13	0.00	0.00	0.08	0.06	0.00	0.00	0.01	0.01	0.04		
	Force Path Cost Average Efficiency Ratio (%) \uparrow	99.55	94.90	97.30	97.61	86.51	94.44	99.48	93.47	88.37			
3 Random Columns	Exact Match \uparrow	1	5	3	2	1	0	7	3	5	1		
	Difference Ratio (%) \uparrow	2.46	58.69	52.03	18.34	24.01	-238.99	-17.63	-56.28	-22.76	-142.17		
	Relative Difference Ratio (%) \uparrow	2.46	58.69	52.03	18.34	24.01	-35.52	31.78	20.55	22.87	-18.10</		

378 6.1 QUANTITATIVE RESULTS
379380 **General Performance Trends** Table 3 presents model performance across all task variations
381 using the metrics defined in Section 5.1. As expected, performance degrades as task complexity
382 increases; "Easy" (binary) tasks consistently yield higher accuracy than "Hard" (continuous) variants.
383 Top-performing models like Claude Opus 4 and Gemini 2.5 Pro achieve near-perfect Load-Support
384 Connectivity (>98%) and Valid Grid scores on easy tasks, suggesting that while they fail to replicate
385 the exact ground-truth geometry (low Exact Match), they successfully reason about global structural
386 integrity and force propagation (Appendix F, for additional plots).
387388 **The Hard Task Anomaly and Material Hallucination** A critical observation in the hard (continuous)
389 tasks is the prevalence of negative Difference Ratios across almost all models. Physically,
390 this result implies significant over-designing: rather than converging on efficient load paths, models
391 tend to "smear" material across the void, producing dense, non-optimal clusters. This hallucination
392 of mass suggests that while models grasp the concept of filling space, they lack the physical intuition
393 to minimize volume while maintaining stability, a core tenet of topology optimization.
394395 **DeepSeek-R1 and the Limits of Chain-of-Thought** Notably, DeepSeek-R1, a model optimized
396 for reasoning, exhibits a strong performance drop between easy and hard tasks. While it maintains
397 reasonable connectivity on binary tasks, its performance collapses on continuous distributions (Table
398 3). We hypothesize that the model's Chain-of-Thought (CoT) process struggles to ground floating-
399 point grid representations into spatial intuition. Instead of visualizing the physical load path, the
400 model likely attempts arithmetic or symbolic manipulation of the density values. This symbolic
401 approach fails to capture the global topological constraints required for stability, resulting in outputs
402 that are computationally "reasoned" but structurally incoherent.
403404 **Rotation Experiments and Gravity Bias** Among localized tasks, row completions consistently
405 outperform column completions. Our rotation experiments ($k = 3, 270^\circ$) reveal that this is not merely
406 a formatting artifact but a "gravity bias." When loads are applied horizontally (simulating a cantilever
407 or rotated structure), models frequently fail to reorient their structural intuition, attempting to build
408 "downward" relative to the grid rather than in the direction of the force vector L . This indicates that
409 models rely heavily on memorized visual patterns of vertical buildings rather than reasoning about
410 the directed vector of applied forces (Appendix G, for additional rotation experiment results).
411412 **Few-Shot Experiments** To investigate the in-context learning capabilities of the models, we
413 performed few-shot experiments complementary to the zero-shot baseline. In this setting, we
414 prepended $k = 1$ and $k = 3$ randomly selected input-output pairs from the dataset to the prompt
415 before presenting the target test instance. The examples were drawn from the same task variation (e.g.,
416 3 Random Row) and difficulty level (easy or hard) as the query. This approach evaluates whether
417 models can improve their spatial reasoning and output formatting by observing valid load-path
418 distributions, thereby allowing us to quantify the extent to which physical constraints can be inferred
419 from examples versus explicit instructions (Appendix H, for additional few-shot experiment results).
420421 **Physics-Enhanced vs. Physics-Neutral Prompts** Counter-intuitively, our prompt ablation studies
422 reveal that physics-enhanced prompts, those augmented with terminology like "stress," "load path,"
423 and "equilibrium", actually degraded performance on harder tasks compared to the base prompt.
424 While the Physics-Neutral setting suffered in connectivity metrics, the failure of the Enhanced
425 prompt suggests that models do not ground physical jargon to the visual grid. Instead, terms like
426 "stress" likely act as semantic distractors, shifting the model's focus away from the necessary spatial
427 pattern-matching and leading to worse topological validity (Appendix I, for details).
428429 6.2 QUALITATIVE ANALYSIS OF FAILURE MODES
430431 To complement the quantitative metrics, we visually inspected model predictions to identify recurring
432 patterns of reasoning failure. We observed three distinct failure modes that explain the performance
433 gaps reported in Table 3.

432 **The "Smearing" Effect in Continuous Tasks** In hard (continuous) tasks, models frequently fail
 433 to commit to a defined structure. Instead of placing high-density material in critical load paths, they
 434 distribute low-density values (0.1 – 0.3) broadly across the void (Appendix J.15). This "smearing"
 435 behavior results in the negative Difference Ratios observed quantitatively; the models appear to be
 436 minimizing risk by filling space rather than optimizing for stiffness, effectively hallucinating material
 437 where none is needed.

438 **Disconnected Islands and Local Bias** A common error in lower-performing models (e.g., Perplex-
 439 ity Sonar, DeepSeek-R1 on hard tasks) is the generation of "floating islands", clusters of material
 440 completely disconnected from supports. This confirms: these models are operating primarily on local
 441 pattern consistency (placing a 1 next to another 1) rather than global constraint satisfaction. They fail
 442 to trace the load path $L \rightarrow S$ back to a fixed point, violating fundamental equilibrium principles.
 443

444 **Gravity Bias in Rotated Scenarios** Qualitative inspection of the rotated experiments (270°) reveals
 445 a strong directional bias. Even when the load L is applied horizontally from the left, models often
 446 attempt to build "downward" relative to the grid layout, ignoring the rotated force vector. This results
 447 in structures that "hang" into empty space or connect to non-existent supports at the bottom of the grid,
 448 providing strong evidence that the models are relying on visual memorization of vertical architectural
 449 forms rather than physical reasoning.

450 **Over-Constrained "Safety"** Conversely, top-performing models like Gemini 2.5 Pro often "over-
 451 build," creating blocky, wall-like structures rather than truss-like efficient designs. While this strategy
 452 achieves high Load-Support Connectivity (resulting in high success rates), it fails the efficiency
 453 objective of topology optimization, treating the task as a "fill-the-gap" segmentation problem rather
 454 than a minimum-compliance optimization problem.
 455

456 7 DISCUSSION

459 The quantitative and qualitative results highlight fundamental gaps between linguistic reasoning and
 460 physical-spatial understanding in Large Language Models.

461 **Lack of Grounded Physical Understanding** The failure of physics-enhanced prompts and the
 462 struggle with hard tasks suggest that current LLMs do not possess a grounded model of physics.
 463 When a model reads "load path", it does not translate this into a constraint satisfaction problem on
 464 the grid; it treats it as a textual token associated with general engineering contexts. Consequently,
 465 models perform best when the task is framed as a visual pattern completion (base prompt) rather than
 466 a physics simulation problem.
 467

468 **Visual Memorization vs. Force Reasoning** The "gravity bias" observed in our rotation experiments
 469 confirms that models are solving SPhyR tasks primarily through visual memorization of architectural
 470 forms (e.g., columns support beams from below) rather than first-principles reasoning about force
 471 vectors. When the "floor" is moved to the "wall" (rotated setup), the model's heuristic fails, proving
 472 that it is not tracing the force L to the support S , but rather completing a learned image schema.
 473

474 **The Challenge of Continuous Optimization** The "smearing" effect and negative Difference Ratios
 475 in continuous tasks highlight a specific deficiency in LLM spatial reasoning: the inability to perform
 476 gradient-like optimization. While models can predict discrete binary occupancy (material vs. void)
 477 based on connectivity rules, they cannot intuitively minimize compliance or volume in a continuous
 478 space. This remains a significant barrier for using LLMs in generative design and engineering
 479 applications where efficiency is paramount.

480 8 CONCLUSION

483 SPhyR reveals that while LLMs exhibit strong general reasoning, they fail to integrate spatial layout
 484 with grounded physical constraints. Observed failure modes (e.g., gravity bias, material smearing)
 485 confirm reliance on visual pattern matching over global force-directed reasoning, necessitating future
 work on geometric constraint satisfaction.

486 REFERENCES
487

488 anthropic. Claude 3.7 Sonnet and Claude Code, February 2025a. URL <https://www.anthropic.com/news/clause-3-7-sonnet>.

489 anthropic. Introducing Claude 4, May 2025b. URL <https://www.anthropic.com/news/clause-4>.

490 Anton Bakhtin, Laurens van der Maaten, Justin Johnson, Laura Gustafson, and Ross Girshick.
491 PHYRE: A New Benchmark for Physical Reasoning, August 2019. URL <http://arxiv.org/abs/1908.05656>. arXiv:1908.05656 [cs].

492 Saurabh Banga, Harsh Gehani, Sanket Bhilare, Sagar Patel, and Levent Kara. 3D Topology Optimization using Convolutional Neural Networks, August 2018. URL <http://arxiv.org/abs/1808.07440>. arXiv:1808.07440 [cs].

493 Daniel M. Bear, Elias Wang, Damian Mrowca, Felix J. Binder, Hsiao-Yu Fish Tung, R. T. Pramod,
494 Cameron Holdaway, Sirui Tao, Kevin Smith, Fan-Yun Sun, Li Fei-Fei, Nancy Kanwisher, Joshua B.
495 Tenenbaum, Daniel L. K. Yamins, and Judith E. Fan. Physion: Evaluating Physical Prediction from
496 Vision in Humans and Machines, June 2022. URL <http://arxiv.org/abs/2106.08261>.
497 arXiv:2106.08261 [cs].

498 Martin P. Bendsøe and Ole Sigmund. *Topology Optimization*. Springer, Berlin, Heidelberg, 2004.
499 ISBN 978-3-642-07698-5 978-3-662-05086-6. doi: 10.1007/978-3-662-05086-6. URL <http://link.springer.com/10.1007/978-3-662-05086-6>.

500 Yonatan Bisk, Rowan Zellers, Ronan Le Bras, Jianfeng Gao, and Yejin Choi. PIQA: Reasoning about
501 Physical Commonsense in Natural Language, November 2019. URL <http://arxiv.org/abs/1911.11641>. arXiv:1911.11641 [cs].

502 Tom B. Brown, Benjamin Mann, Nick Ryder, Melanie Subbiah, Jared Kaplan, Prafulla Dhariwal,
503 Arvind Neelakantan, Pranav Shyam, Girish Sastry, Amanda Askell, Sandhini Agarwal, Ariel
504 Herbert-Voss, Gretchen Krueger, Tom Henighan, Rewon Child, Aditya Ramesh, Daniel M. Ziegler,
505 Jeffrey Wu, Clemens Winter, Christopher Hesse, Mark Chen, Eric Sigler, Mateusz Litwin, Scott
506 Gray, Benjamin Chess, Jack Clark, Christopher Berner, Sam McCandlish, Alec Radford, Ilya
507 Sutskever, and Dario Amodei. Language Models are Few-Shot Learners, July 2020. URL
508 <http://arxiv.org/abs/2005.14165>. arXiv:2005.14165 [cs].

509 Francois Chollet, Mike Knoop, Gregory Kamradt, Bryan Landers, and Henry Pinkard. ARC-AGI-2:
510 A New Challenge for Frontier AI Reasoning Systems, May 2025. URL <http://arxiv.org/abs/2505.11831>. arXiv:2505.11831 [cs].

511 Gheorghe Comanici, Eric Bieber, Mike Schaeckermann, Ice Pasupat, Noveen Sachdeva, Inderjit
512 Dhillon, Marcel Blistein, Ori Ram, Dan Zhang, Evan Rosen, Luke Marrs, Sam Petulla, Colin
513 Gaffney, Asaf Aharoni, Nathan Lintz, Tiago Cardal Pais, Henrik Jacobsson, Idan Szpektor, Nan
514 Jiang Jiang, Krishna Haridasan, Ahmed Omran, Nikunj Saunshi, Dara Bahri, Gaurav Mishra, Eric
515 Chu, Toby Boyd, Brad Hekman, Aaron Parisi, Chaoyi Zhang, Kornraphop Kawintiranon, Tania
516 Bedrax-Weiss, Oliver Wang, Ya Xu, Ollie Purkiss, Uri Mendlovic, Ilai Deutel, Nam Nguyen, Adam
517 Langley, Flip Korn, Lucia Rossazza, Alexandre Ramé, Sagar Waghmare, Helen Miller, Nathan
518 Byrd, Ashrith Sheshan, Raia Hadsell Sangnie Bhardwaj, Pawel Janus, Tero Rissa, Dan Horgan,
519 Sharon Silver, Ayzaan Wahid, Sergey Brin, Yves Raimond, Klemen Kloboves, Cindy Wang,
520 Nitesh Bharadwaj Gundavarapu, Ilia Shumailov, Bo Wang, Mantas Pajarskas, Joe Heyward, Martin
521 Nikoltchev, Maciej Kula, Hao Zhou, Zachary Garrett, Sushant Kafle, Sercan Arik, Ankita Goel,
522 Mingyao Yang, Jiho Park, Koji Kojima, Parsa Mahmoudieh, Koray Kavukcuoglu, Grace Chen,
523 Doug Fritz, Anton Bulyenov, Sudeshna Roy, Dimitris Paparas, Hadar Shemtov, Bo-Juen Chen,
524 Robin Strudel, David Reitter, Aurko Roy, Andrey Vlasov, Changwan Ryu, Chas Leichner, Haichuan
525 Yang, Zelda Mariet, Denis Vnukov, Tim Sohn, Amy Stuart, Wei Liang, Minmin Chen, Praynaa
526 Rawlani, Christy Koh, J. D. Co-Reyes, Guangda Lai, Praseem Banzal, Dimitrios Vytiniotis, Jieru
527 Mei, Mu Cai, Mohammed Badawi, Corey Fry, Ale Hartman, Daniel Zheng, Eric Jia, James Keeling,
528 Annie Louis, Ying Chen, Efren Robles, Wei-Chih Hung, Howard Zhou, Nikita Saxena, Sonam
529 Goenka, Olivia Ma, Zach Fisher, Mor Hazan Taege, Emily Graves, David Steiner, Yujia Li, Sarah
530 Nguyen, Rahul Sukthankar, Joe Stanton, Ali Eslami, Gloria Shen, Berkin Akin, Alexey Guseynov,

540 Yiqian Zhou, Jean-Baptiste Alayrac, Armand Joulin, Efrat Farkash, Ashish Thapliyal, Stephen
 541 Roller, Noam Shazeer, Todor Davchev, Terry Koo, Hannah Forbes-Pollard, Kartik Audhkhasi,
 542 Greg Farquhar, Adi Mayrav Gilady, Maggie Song, John Aslanides, Piermaria Mendolicchio,
 543 Alicia Parrish, John Blitzer, Pramod Gupta, Xiaoen Ju, Xiaochen Yang, Puranjay Datta, Andrea
 544 Tacchetti, Sanket Vaibhav Mehta, Gregory Dibb, Shubham Gupta, Federico Piccinini, Raia Hadsell,
 545 Sujee Rajayogam, Jiepu Jiang, Patrick Griffin, Patrik Sundberg, Jamie Hayes, Alexey Frolov,
 546 Tian Xie, Adam Zhang, Kingshuk Dasgupta, Uday Kalra, Lior Shani, Klaus Macherey, Tzu-
 547 Kuo Huang, Liam MacDermed, Karthik Duddu, Paulo Zaccchello, Zi Yang, Jessica Lo, Kai Hui,
 548 Matej Kastelic, Derek Gasaway, Qijun Tan, Summer Yue, Pablo Barrio, John Wieting, Weel
 549 Yang, Andrew Nystrom, Solomon Demmessie, Anselm Levskaya, Fabio Viola, Chetan Tekur,
 550 Greg Billock, George Necula, Mandar Joshi, Rylan Schaeffer, Swachhand Lokhande, Christina
 551 Sorokin, Pradeep Shenoy, Mia Chen, Mark Collier, Hongji Li, Taylor Bos, Nevan Wickers,
 552 Sun Jae Lee, Angéline Pouget, Santhosh Thangaraj, Kyriakos Axiotis, Phil Crone, Rachel Sterneck,
 553 Nikolai Chinaev, Victoria Krakovna, Oleksandr Ferludin, Ian Gemp, Stephanie Winkler, Dan
 554 Goldberg, Ivan Korotkov, Kefan Xiao, Malika Mehrotra, Sandeep Mariserla, Vihari Piratla, Terry
 555 Thurk, Khiem Pham, Hongxu Ma, Alexandre Senges, Ravi Kumar, Clemens Meyer, Ellie Talius,
 556 Nuo Wang Pierse, Ballie Sandhu, Horia Toma, Kuo Lin, Swaroop Nath, Tom Stone, Dorsa Sadigh,
 557 Nikita Gupta, Arthur Guez, Avi Singh, Matt Thomas, Tom Duerig, Yuan Gong, Richard Tanburn,
 558 Lydia Lihui Zhang, Phuong Dao, Mohamed Hammad, Sirui Xie, Shruti Rijhwani, Ben Murdoch,
 559 Duhyeon Kim, Will Thompson, Heng-Tze Cheng, Daniel Sohn, Pablo Sprechmann, Qiantong
 560 Xu, Srinivas Tadepalli, Peter Young, Ye Zhang, Hansa Srinivasan, Miranda Aperghis, Aditya
 561 Ayyar, Hen Fitoussi, Ryan Burnell, David Madras, Mike Dusenberry, Xi Xiong, Tayo Oguntebi,
 562 Ben Albrecht, Jörg Bornschein, Jovana Mitrović, Mason Dimarco, Bhargav Kanagal Shamanna,
 563 Premal Shah, Eren Sezener, Shyam Upadhyay, Dave Lacey, Craig Schiff, Sébastien Baur, Sanjay
 564 Ganapathy, Eva Schnider, Mateo Wirth, Connor Schenck, Andrey Simanovsky, Yi-Xuan Tan,
 565 Philipp Fränken, Dennis Duan, Bharath Mankalale, Nikhil Dhawan, Kevin Sequeira, Zichuan
 566 Wei, Shivanker Goel, Caglar Unlu, Yukun Zhu, Haitian Sun, Ananth Balashankar, Kurt Shuster,
 567 Megh Umekar, Mahmoud Alnahlawi, Aäron van den Oord, Kelly Chen, Yuexiang Zhai, Zihang
 568 Dai, Kuang-Huei Lee, Eric Doi, Lukas Zilka, Rohith Vallu, Disha Shrivastava, Jason Lee, Hisham
 569 Husain, Honglei Zhuang, Vincent Cohen-Addad, Jarred Barber, James Atwood, Adam Sadovsky,
 570 Quentin Wellens, Steven Hand, Arunkumar Rajendran, Aybuke Turker, C. J. Carey, Yuanzhong Xu,
 571 Hagen Soltau, Zefei Li, Xinying Song, Conglong Li, Iurii Kemaev, Sasha Brown, Andrea Burns,
 572 Viorica Patraucean, Piotr Stanczyk, Renga Aravamudhan, Mathieu Blondel, Hila Noga, Lorenzo
 573 Blanco, Will Song, Michael Isard, Mandar Sharma, Reid Hayes, Dalia El Badawy, Avery Lamp,
 574 Itay Laish, Olga Kozlova, Kelvin Chan, Sahil Singla, Srinivas Sunkara, Mayank Upadhyay, Chang
 575 Liu, Aijun Bai, Jarek Wilkiewicz, Martin Zlocha, Jeremiah Liu, Zhuowan Li, Haiguang Li, Omer
 576 Barak, Ganna Raboshchuk, Jiho Choi, Fangyu Liu, Erik Jue, Mohit Sharma, Andreea Marzoca,
 577 Robert Busa-Fekete, Anna Korsun, Andre Elisseeff, Zhe Shen, Sara Mc Carthy, Kay Lamerigts,
 578 Anahita Hosseini, Hanzhao Lin, Charlie Chen, Fan Yang, Kushal Chauhan, Mark Omernick,
 579 Dawei Jia, Karina Zainullina, Demis Hassabis, Danny Vainstein, Ehsan Amid, Xiang Zhou, Ronny
 580 Votel, Eszter Vértes, Xinjian Li, Zongwei Zhou, Angeliki Lazaridou, Brendan McMahan, Arjun
 581 Narayanan, Hubert Soyer, Sujoy Basu, Kayi Lee, Bryan Perozzi, Qin Cao, Leonard Berrada, Rahul
 582 Arya, Ke Chen, Katrina Xu, Matthias Lochbrunner, Alex Hofer, Sahand Sharifzadeh, Renjie
 583 Wu, Sally Goldman, Pranjal Awasthi, Xuezhi Wang, Yan Wu, Claire Sha, Biao Zhang, Maciej
 584 Mikuła, Filippo Graziano, Siobhan McLaughlin, Irene Giannoumis, Youhei Namiki, Chase Malik,
 585 Carey Radebaugh, Jamie Hall, Ramiro Leal-Cavazos, Jianmin Chen, Vikas Sindhwani, David Kao,
 586 David Greene, Jordan Griffith, Chris Welty, Ceslee Montgomery, Toshihiro Yoshino, Liangzhe
 587 Yuan, Noah Goodman, Assaf Hurwitz Michaely, Kevin Lee, K. P. Sawhney, Wei Chen, Zheng
 588 Zheng, Megan Shum, Nikolay Savinov, Etienne Pot, Alex Pak, Morteza Zadimoghaddam, Sijal
 589 Bhatnagar, Yoad Lewenberg, Blair Kutzman, Ji Liu, Lesley Katzen, Jeremy Selier, Josip Djolonga,
 590 Dmitry Lepikhin, Kelvin Xu, Jacky Liang, Jiewen Tan, Benoit Schillings, Muge Ersoy, Pete
 591 Blois, Bernd Bandemer, Abhimanyu Singh, Sergei Lebedev, Pankaj Joshi, Adam R. Brown, Evan
 592 Palmer, Shreya Pathak, Komal Jalan, Fedir Zubach, Shuba Lall, Randall Parker, Alok Gunjan,
 593 Sergey Rogulenko, Sumit Sanghai, Zhaoqi Leng, Zoltan Egyed, Shixin Li, Maria Ivanova, Kostas
 Andriopoulos, Jin Xie, Elan Rosenfeld, Auriel Wright, Ankur Sharma, Xinyang Geng, Yicheng
 Wang, Sam Kwei, Renke Pan, Yujing Zhang, Gabby Wang, Xi Liu, Chak Yeung, Elizabeth Cole,
 Aviv Rosenberg, Zhen Yang, Phil Chen, George Polovets, Pranav Nair, Rohun Saxena, Josh Smith,
 Shuo-yiin Chang, Aroma Mahendru, Svetlana Grant, Anand Iyer, Irene Cai, Jed McGiffin, Jiaming
 Shen, Alanna Walton, Antonious Grgis, Oliver Woodman, Rosemary Ke, Mike Kwong, Louis

594 Rouillard, Jinmeng Rao, Zhihao Li, Yuntao Xu, Flavien Prost, Chi Zou, Ziwei Ji, Alberto Magni,
 595 Tyler Liechty, Dan A. Calian, Deepak Ramachandran, Igor Krivokon, Hui Huang, Terry Chen,
 596 Anja Hauth, Anastasija Ilić, Weijuan Xi, Hyeontaek Lim, Vlad-Doru Ion, Pooya Moradi, Metin
 597 Toksoz-Exley, Kalesha Bullard, Miltos Allamanis, Xiaomeng Yang, Sophie Wang, Zhi Hong,
 598 Anita Gergely, Cheng Li, Bhavishya Mittal, Vitaly Kovalev, Victor Ungureanu, Jane Labanowski,
 599 Jan Wassenberg, Nicolas Lacasse, Geoffrey Cideron, Petar Dević, Annie Marsden, Lynn Nguyen,
 600 Michael Fink, Yin Zhong, Tatsuya Kiyono, Desi Ivanov, Sally Ma, Max Bain, Kiran Yalasangi,
 601 Jennifer She, Anastasia Petrushkina, Mayank Lunayach, Carla Bromberg, Sarah Hodkinson,
 602 Vilobh Meshram, Daniel Vlasic, Austin Kyker, Steve Xu, Jeff Stanway, Zuguang Yang, Kai Zhao,
 603 Matthew Tung, Seth Odoom, Yasuhisa Fujii, Justin Gilmer, Eunyoung Kim, Felix Halim, Quoc Le,
 604 Bernd Bohnet, Seliem El-Sayed, Behnam Neyshabur, Malcolm Reynolds, Dean Reich, Yang Xu,
 605 Erica Moreira, Anuj Sharma, Zeyu Liu, Mohammad Javad Hosseini, Naina Raisinghani, Yi Su,
 606 Ni Lao, Daniel Formoso, Marco Gelmi, Almog Gueta, Tapomay Dey, Elena Gribovskaya, Domagoj
 607 Ćevid, Sidharth Mudgal, Garrett Bingham, Jianling Wang, Anurag Kumar, Alex Cullum, Feng Han,
 608 Konstantinos Bousmalis, Diego Cedillo, Grace Chu, Vladimir Magay, Paul Michel, Ester Hlavnova,
 609 Daniele Calandriello, Setareh Ariafar, Kaisheng Yao, Vikash Sehwag, Arpi Vezer, Agustin Dal
 610 Lago, Zhenkai Zhu, Paul Kishan Rubenstein, Allen Porter, Anirudh Baddepudi, Oriana Riva,
 611 Mihai Dorin Istin, Chih-Kuan Yeh, Zhi Li, Andrew Howard, Nilpa Jha, Jeremy Chen, Raoul de
 612 Liedekerke, Zafarali Ahmed, Mikel Rodriguez, Tanuj Bhatia, Bangju Wang, Ali Elqursh, David
 613 Klinghoffer, Peter Chen, Pushmeet Kohli, Te I, Weiyang Zhang, Zack Nado, Jilin Chen, Maxwell
 614 Chen, George Zhang, Aayush Singh, Adam Hillier, Federico Lebron, Yiqing Tao, Ting Liu, Gabriel
 615 Dulac-Arnold, Jingwei Zhang, Shashi Narayan, Buhuang Liu, Orhan Firat, Abhishek Bhowmick,
 616 Bingyuan Liu, Hao Zhang, Zizhao Zhang, Georges Rotival, Nathan Howard, Anu Sinha, Alexander
 617 Grushetsky, Benjamin Beyret, Keerthana Gopalakrishnan, James Zhao, Kyle He, Szabolcs Payrits,
 618 Zaid Nabulsi, Zhaoyi Zhang, Weijie Chen, Edward Lee, Nova Fallen, Sreenivas Gollapudi, Aurick
 619 Zhou, Filip Pavetić, Thomas Köppe, Shiyu Huang, Rama Pasumarthi, Nick Fernando, Felix
 620 Fischer, Daria Čurko, Yang Gao, James Svensson, Austin Stone, Haroon Qureshi, Abhishek
 621 Sinha, Apoorv Kulshreshtha, Martin Matysiak, Jieming Mao, Carl Saroufim, Aleksandra Faust,
 622 Qingnan Duan, Gil Fidel, Kaan Katircioglu, Raphaël Lopez Kaufman, Dhruv Shah, Weize Kong,
 623 Abhishek Bapna, Gellért Weisz, Emma Dunleavy, Praneet Dutta, Tianqi Liu, Rahma Chaabouni,
 624 Carolina Parada, Marcus Wu, Alexandra Belias, Alessandro Bissacco, Stanislav Fort, Li Xiao,
 625 Fantine Huot, Chris Knutson, Yochai Blau, Gang Li, Jennifer Prendki, Juliette Love, Yinlam
 626 Chow, Pichi Charoenpanit, Hidetoshi Shimokawa, Vincent Coriou, Karol Gregor, Tomas Izo, Arjun
 627 Akula, Mario Pinto, Chris Hahn, Dominik Paulus, Jiaxian Guo, Neha Sharma, Cho-Jui Hsieh,
 628 Adaeze Chukwuka, Kazuma Hashimoto, Nathalie Rauschmayr, Ling Wu, Christof Angermueller,
 629 Yulong Wang, Sebastian Gerlach, Michael Pliskin, Daniil Mirylenka, Min Ma, Lexi Baugher,
 630 Bryan Gale, Shaan Bijwadia, Nemanja Rakićević, David Wood, Jane Park, Chung-Ching Chang,
 631 Babi Seal, Chris Tar, Kacper Krasowiak, Yiwen Song, Georgi Stephanov, Gary Wang, Marcello
 632 Maggioni, Stein Xudong Lin, Felix Wu, Shachi Paul, Zixuan Jiang, Shubham Agrawal, Bilal Piot,
 633 Alex Feng, Cheolmin Kim, Tulsee Doshi, Jonathan Lai, Chuqiao, Xu, Sharad Vikram, Ciprian
 634 Chelba, Sebastian Krause, Vincent Zhuang, Jack Rae, Timo Denk, Adrian Collister, Lotte Weerts,
 635 Xianghong Luo, Yifeng Lu, Håvard Gernes, Nitish Gupta, Terry Spitz, Avinatan Hassidim, Lihao
 636 Liang, Izhak Shafran, Peter Humphreys, Kenny Vassigh, Phil Wallis, Virat Shejwalkar, Nicolas
 637 Perez-Nieves, Rachel Hornung, Melissa Tan, Beka Westberg, Andy Ly, Richard Zhang, Brian
 638 Farris, Jongbin Park, Alec Kosik, Zeynep Cankara, Andrii Maksai, Yunhan Xu, Albin Cassirer,
 639 Sergi Caelles, Abbas Abdolmaleki, Mencher Chiang, Alex Fabrikant, Shravya Shetty, Luheng
 640 He, Mai Giménez, Hadi Hashemi, Sheena Panthaplatzel, Yana Kulizhskaya, Salil Deshmukh,
 641 Daniele Pighin, Robin Alazard, Disha Jindal, Seb Noury, Pradeep Kumar S, Siyang Qin, Xerxes
 642 Dotiwalla, Stephen Spencer, Mohammad Babaeizadeh, Blake JianHang Chen, Vaibhav Mehta,
 643 Jennie Lees, Andrew Leach, Penporn Koanantakool, Ilia Akolzin, Ramona Comanescu, Junwhan
 644 Ahn, Alexey Svyatkovskiy, Basil Mustafa, David D'Ambrosio, Shiva Mohan Reddy Garlapati,
 645 Pascal Lamblin, Alekh Agarwal, Shuang Song, Pier Giuseppe Sessa, Pauline Coquinot, John
 646 Maggs, Hussain Masoom, Divya Pitta, Yaqing Wang, Patrick Morris-Suzuki, Billy Porter, Johnson
 647 Jia, Jeffrey Dudek, Raghavender R, Cosmin Paduraru, Alan Ansell, Tolga Bolukbasi, Tony Lu,
 648 Ramya Ganeshan, Zi Wang, Henry Griffiths, Rodrigo Benenson, Yifan He, James Swirhun, George
 649 Papamakarios, Aditya Chawla, Kuntal Sengupta, Yan Wang, Vedrana Milutinovic, Igor Mordatch,
 650 Zhipeng Jia, Jamie Smith, Will Ng, Shitij Nigam, Matt Young, Eugen Vušak, Blake Hechtman,
 651 Sheela Goenka, Avital Zipori, Kareem Ayoub, Ashok Popat, Trilok Acharya, Luo Yu, Dawn
 652 Bloxwich, Hugo Song, Paul Roit, Haiqiong Li, Aviel Boag, Nigamaa Nayakanti, Bilva Chandra,

648 Tianli Ding, Aahil Mehta, Cath Hope, Jiageng Zhang, Idan Heimlich Shtacher, Kartikeya Badola,
 649 Ryo Nakashima, Andrei Sozanschi, Iulia Comă, Ante Žužul, Emily Caveness, Julian Odell,
 650 Matthew Watson, Dario de Cesare, Phillip Lippe, Derek Lockhart, Siddharth Verma, Huizhong
 651 Chen, Sean Sun, Lin Zhuo, Aditya Shah, Prakhar Gupta, Alex Muzio, Ning Niu, Amir Zait,
 652 Abhinav Singh, Meenu Gaba, Fan Ye, Prajit Ramachandran, Mohammad Saleh, Raluca Ada Popa,
 653 Ayush Dubey, Frederick Liu, Sara Javanmardi, Mark Epstein, Ross Hemsley, Richard Green,
 654 Nishant Ranka, Eden Cohen, Chuyuan Kelly Fu, Sanjay Ghemawat, Jed Borovik, James Martens,
 655 Anthony Chen, Pranav Shyam, André Susano Pinto, Ming-Hsuan Yang, Alexandru Țifrea, David
 656 Du, Boqing Gong, Ayushi Agarwal, Seungyeon Kim, Christian Frank, Saloni Shah, Xiaodan Song,
 657 Zhiwei Deng, Ales Mikhalap, Kleopatra Chatziprimou, Timothy Chung, Toni Creswell, Susan
 658 Zhang, Yennie Jun, Carl Lebsack, Will Truong, Slavica Andačić, Itay Yona, Marco Fornoni, Rong
 659 Rong, Serge Toropov, Afzal Shama Soudagar, Andrew Audibert, Salah Zaïem, Zaheer Abbas,
 660 Andrei Rusu, Sahitya Potluri, Shitao Weng, Anastasios Kementsietsidis, Anton Tsitsulin, Daiyi
 661 Peng, Natalie Ha, Sanil Jain, Tejasvi Latkar, Simeon Ivanov, Cory McLean, Anirudh GP, Rajesh
 662 Venkataraman, Canoe Liu, Dilip Krishnan, Joel D’sa, Roey Yogev, Paul Collins, Benjamin Lee,
 663 Lewis Ho, Carl Doersch, Gal Yona, Shawn Gao, Felipe Tiengo Ferreira, Adnan Ozturk, Hannah
 664 Muckenheim, Ce Zheng, Gargi Balasubramaniam, Mudit Bansal, George van den Driessche, Sivan
 665 Eiger, Salem Haykal, Vedant Misra, Abhimanyu Goyal, Danilo Martins, Gary Leung, Jonas
 666 Valfridsson, Four Flynn, Will Bishop, Chenxi Pang, Yoni Halpern, Honglin Yu, Lawrence Moore,
 667 Yuvein, Zhu, Sridhar Thiagarajan, Yoel Drori, Zhisheng Xiao, Lucio Dery, Rolf Jagerman, Jing
 668 Lu, Eric Ge, Vaibhav Aggarwal, Arjun Khare, Vinh Tran, Oded Elyada, Ferran Alet, James Rubin,
 669 Ian Chou, David Tian, Libin Bai, Lawrence Chan, Lukasz Lew, Karolis Misiunas, Taylan Bilal,
 670 Aniket Ray, Sindhu Raghuram, Alex Castro-Ros, Viral Carpenter, C. J. Zheng, Michael Kilgore,
 671 Josef Broder, Emily Xue, Praveen Kallakuri, Dheeru Dua, Nancy Yuen, Steve Chien, John Schultz,
 672 Saurabh Agrawal, Reut Tsarfaty, Jingcao Hu, Ajay Kannan, Dror Marcus, Nisarg Kothari, Baochen
 673 Sun, Ben Horn, Matko Bošnjak, Ferjad Naeem, Dean Hirsch, Lewis Chiang, Boya Fang, Jie Han,
 674 Qifei Wang, Ben Hora, Antoine He, Mario Lučić, Beer Changpinyo, Anshuman Tripathi, John
 675 Youssef, Chester Kwak, Philippe Schlattner, Cat Graves, Rémi Leblond, Wenjun Zeng, Anders
 676 Andreassen, Gabriel Rasskin, Yue Song, Eddie Cao, Junhyuk Oh, Matt Hoffman, Wojtek Skut,
 677 Yichi Zhang, Jon Stritar, Xingyu Cai, Saarthak Khanna, Kathie Wang, Shriya Sharma, Christian
 678 Reisswig, Younghoon Jun, Aman Prasad, Tatiana Sholokhova, Preeti Singh, Adi Gerzi Rosenthal,
 679 Anian Ruoss, Françoise Beaufays, Sean Kirmani, Dongkai Chen, Johan Schalkwyk, Jonathan
 680 Herzig, Been Kim, Josh Jacob, Damien Vincent, Adrian N. Reyes, Ivana Balazevic, Léonard
 681 Hussenot, Jon Schneider, Parker Barnes, Luis Castro, Spandana Raj Babbula, Simon Green,
 682 Serkan Cabi, Nico Duduta, Danny Driess, Rich Galt, Noam Velan, Junjie Wang, Hongyang Jiao,
 683 Matthew Mauger, Du Phan, Miteyan Patel, Vlado Galić, Jerry Chang, Eyal Marcus, Matt Harvey,
 684 Julian Salazar, Elahe Dabir, Suraj Satishkumar Sheth, Amol Mandhane, Hanie Sedghi, Jeremiah
 685 Willcock, Amir Zandieh, Shruthi Prabhakara, Aida Amini, Antoine Miech, Victor Stone, Massimo
 686 Nicosia, Paul Niemczyk, Ying Xiao, Lucy Kim, Sławek Kwasiborski, Vikas Verma, Ada Maksutaj
 687 Oflazer, Christoph Hirnschall, Peter Sung, Lu Liu, Richard Everett, Michiel Bakker, Ágoston
 688 Weisz, Yufei Wang, Vivek Sampathkumar, Uri Shaham, Bibo Xu, Yasemin Altun, Mingqiu Wang,
 689 Takaaki Saeki, Guanjie Chen, Emanuel Taropa, Shanthal Vasanth, Sophia Austin, Lu Huang,
 690 Goran Petrovic, Qingyun Dou, Daniel Golovin, Grigory Rozhdestvenskiy, Allie Culp, Will Wu,
 691 Motoki Sano, Divya Jain, Julia Proskurnia, Sébastien Cevey, Alejandro Cruzado Ruiz, Piyush Patil,
 692 Mahdi Mirzazadeh, Eric Ni, Javier Snaider, Lijie Fan, Alexandre Fréchette, A. J. Pierigiovanni,
 693 Shariq Iqbal, Kenton Lee, Claudio Fantacci, Jinwei Xing, Lisa Wang, Alex Irpan, David Raposo,
 694 Yi Luan, Zhuoyuan Chen, Harish Ganapathy, Kevin Hui, Jiazhong Nie, Isabelle Guyon, Heming
 695 Ge, Roopali Vij, Hui Zheng, Dayeong Lee, Alfonso Castaño, Khuslen Baatarsukh, Gabriel
 696 Ibagon, Alexandra Chronopoulou, Nicholas FitzGerald, Shashank Viswanadha, Safeen Huda,
 697 Rivka Moroshko, Georgi Stoyanov, Prateek Kolhar, Alain Vaucher, Ishaan Watts, Adhi Kuncoro,
 698 Henryk Michalewski, Satish Kambala, Bat-Orgil Batsaikhan, Alek Andreev, Irina Jurenka, Maigo
 699 Le, Qihang Chen, Wael Al Jishi, Sarah Chakera, Zhe Chen, Aditya Kini, Vikas Yadav, Aditya
 700 Siddhant, Ilia Labzovsky, Balaji Lakshminarayanan, Carrie Grimes Bostock, Pankil Botadra,
 701 Ankesh Anand, Colton Bishop, Sam Conway-Rahman, Mohit Agarwal, Yani Donchev, Achintya
 Singhal, Félix de Chaumont Quirky, Natalia Ponomareva, Nishant Agrawal, Bin Ni, Kalpesh
 Krishna, Masha Samsikova, John Karro, Yilun Du, Tamara von Glehn, Caden Lu, Christopher A.
 Choquette-Choo, Zhen Qin, Tingnan Zhang, Sicheng Li, Divya Tyam, Swaroop Mishra, Wing
 Lowe, Colin Ji, Weiyi Wang, Manaal Faruqui, Ambrose Slone, Valentin Dalibard, Arunachalam
 Narayanaswamy, John Lambert, Pierre-Antoine Manzagol, Dan Karliner, Andrew Bolt, Ivan

702 Lobov, Aditya Kusupati, Chang Ye, Xuan Yang, Heiga Zen, Nelson George, Mukul Bhutani,
 703 Olivier Lacombe, Robert Riachi, Gagan Bansal, Rachel Soh, Yue Gao, Yang Yu, Adams Yu,
 704 Emily Nottage, Tania Rojas-Esponda, James Noraky, Manish Gupta, Ragha Kotikalapudi, Jichuan
 705 Chang, Sanja Deur, Dan Graur, Alex Mossin, Erin Farnese, Ricardo Figueira, Alexandre Moufarek,
 706 Austin Huang, Patrik Zochbauer, Ben Ingram, Tongzhou Chen, Zelin Wu, Adrià Puigdomènec,
 707 Leland Rechis, Da Yu, Sri Gayatri Sundara Padmanabhan, Rui Zhu, Chu-ling Ko, Andrea Banino,
 708 Samira Daruki, Aarush Selvan, Dhruva Bhaswar, Daniel Hernandez Diaz, Chen Su, Salvatore
 709 Scellato, Jennifer Brennan, Woohyun Han, Grace Chung, Priyanka Agrawal, Urvashi Khandelwal,
 710 Khe Chai Sim, Morgane Lustman, Sam Ritter, Kelvin Guu, Jiawei Xia, Prateek Jain, Emma Wang,
 711 Tyrone Hill, Mirko Rossini, Marija Kostelac, Tautvydas Misiunas, Amit Sabne, Kyuyeun Kim,
 712 Ahmet Iscen, Congchao Wang, José Leal, Ashwin Sreevatsa, Utku Evcı, Manfred Warmuth, Saket
 713 Joshi, Daniel Suo, James Lottes, Garrett Honke, Brendan Jou, Stefani Karp, Jieru Hu, Himanshu
 714 Sahni, Adrien Ali Taïga, William Kong, Samrat Ghosh, Renshen Wang, Jay Pavagadhi, Natalie
 715 Axelsson, Nikolai Grigorev, Patrick Siegler, Rebecca Lin, Guohui Wang, Emilio Parisotto, Sharath
 716 Maddineni, Krishan Subudhi, Eyal Ben-David, Elena Pochernina, Orgad Keller, Thi Avrahami,
 717 Zhe Yuan, Pulkit Mehta, Jialu Liu, Sherry Yang, Wendy Kan, Katherine Lee, Tom Funkhouser,
 718 Derek Cheng, Hongzhi Shi, Archit Sharma, Joe Kelley, Matan Eyal, Yury Malkov, Corentin Tallec,
 719 Yuval Bahat, Shen Yan, Xintian, Wu, David Lindner, Chengda Wu, Avi Caciularu, Xiyang Luo,
 720 Rodolphe Jenatton, Tim Zaman, Yingying Bi, Ilya Kornakov, Ganesh Mallya, Daisuke Ikeda, Itay
 721 Karo, Anima Singh, Colin Evans, Praneeth Netrapalli, Vincent Nallatamby, Isaac Tian, Yannis
 722 Assael, Vikas Raunak, Victor Carbune, Ioana Bica, Lior Madmoni, Dee Cattle, Snchit Grover,
 723 Krishna Somandepalli, Sid Lall, Amelio Vázquez-Reina, Riccardo Patana, Jiaqi Mu, Pranav Talluri,
 724 Maggie Tran, Rajeev Aggarwal, R. J. Skerry-Ryan, Jun Xu, Mike Burrows, Xiaoyue Pan, Edouard
 725 Yvinec, Di Lu, Zhiying Zhang, Duc Dung Nguyen, Hairong Mu, Gabriel Barcik, Helen Ran,
 726 Lauren Beltrone, Krzysztof Choromanski, Dia Kharrat, Samuel Albanie, Sean Purser-haskell,
 727 David Bieber, Carrie Zhang, Jing Wang, Tom Hudson, Zhiyuan Zhang, Han Fu, Johannes Mauerer,
 728 Mohammad Hossein Bateni, A. J. Maschinot, Bing Wang, Muye Zhu, Arjun Pillai, Tobias Weyand,
 729 Shuang Liu, Oscar Akerlund, Fred Bertsch, Vittal Premachandran, Alicia Jin, Vincent Roulet,
 730 Peter de Boursac, Shubham Mittal, Ndaba Ndebele, Georgi Karadzhov, Sahra Ghalebikesabi,
 731 Ricky Liang, Allen Wu, Yale Cong, Nimesh Ghelani, Sumeet Singh, Bahar Fatemi, Warren, Chen,
 732 Charles Kwong, Alexey Kolganov, Steve Li, Richard Song, Chenkai Kuang, Sobhan Miryoosefi,
 733 Dale Webster, James Wendt, Arkadiusz Socala, Guolong Su, Artur Mendonça, Abhinav Gupta,
 734 Xiaowei Li, Tomy Tsai, Qiong, Hu, Kai Kang, Angie Chen, Sertan Girgin, Yongqin Xian, Andrew
 735 Lee, Nolan Ramsden, Leslie Baker, Madeleine Clare Elish, Varvara Krayvanova, Rishabh Joshi,
 736 Jiri Simsa, Yao-Yuan Yang, Piotr Ambroszczyk, Dipankar Ghosh, Arjun Kar, Yuan Shangguan,
 737 Yumeya Yamamori, Yaroslav Akulov, Andy Brock, Haotian Tang, Siddharth Vashishtha, Rich
 738 Munoz, Andreas Steiner, Kalyan Andra, Daniel Eppens, Qixuan Feng, Hayato Kobayashi, Sasha
 739 Goldshtain, Mona El Mahdy, Xin Wang, Jilei, Wang, Richard Killam, Tom Kwiatkowski, Kavya
 740 Kopparapu, Serena Zhan, Chao Jia, Alexei Bendebury, Sheryl Luo, Adrià Recasens, Timothy
 741 Knight, Jing Chen, Mohak Patel, YaGuang Li, Ben Withbroe, Dean Weesner, Kush Bhatia, Jie
 742 Ren, Danielle Eisenbud, Ebrahim Songhori, Yanhua Sun, Travis Choma, Tasos Kementsietsidis,
 743 Lucas Manning, Brian Roark, Wael Farhan, Jie Feng, Susheel Tatineni, James Cobon-Kerr, Yunjie
 744 Li, Lisa Anne Hendricks, Isaac Noble, Chris Breaux, Nate Kushman, Liqian Peng, Fuzhao Xue,
 745 Taylor Tobin, Jamie Rogers, Josh Lipschultz, Chris Alberti, Alexey Vlaskin, Mostafa Dehghani,
 746 Roshan Sharma, Tris Warkentin, Chen-Yu Lee, Benigno Uria, Da-Cheng Juan, Angad Chandorkar,
 747 Hila Sheftel, Ruibo Liu, Elnaz Davoodi, Borja De Balle Pigem, Kedar Dhamdhere, David Ross,
 748 Jonathan Hoech, Mahdis Mahdieh, Li Liu, Qiuji Li, Liam McCafferty, Chenxi Liu, Markus
 749 Mircea, Yunting Song, Omkar Savant, Alaa Saade, Colin Cherry, Vincent Hellendoorn, Siddharth
 750 Goyal, Paul Pucciarelli, David Vilar Torres, Zohar Yahav, Hyo Lee, Lars Lowe Sjoesund, Christo
 751 Kirov, Bo Chang, Deepanway Ghoshal, Lu Li, Gilles Baechler, Sébastien Pereira, Tara Sainath,
 752 Anudhyan Boral, Dominik Grewe, Afief Halumi, Nguyen Minh Phu, Tianxiao Shen, Marco Tulio
 753 Ribeiro, Dhriti Varma, Alex Kaskasoli, Vlad Feinberg, Navneet Potti, Jarrod Kahn, Matheus
 754 Wisniewski, Shakir Mohamed, Arnar Mar Hrafnkelsson, Bobak Shahriari, Jean-Baptiste Lespiau,
 755 Lisa Patel, Legg Yeung, Tom Paine, Lantao Mei, Alex Ramirez, Rakesh Shivanna, Li Zhong, Josh
 Woodward, Guilherme Tubone, Samira Khan, Heng Chen, Elizabeth Nielsen, Catalin Ionescu,
 Utsav Prabhu, Mingcen Gao, Qingze Wang, Sean Augenstein, Neesha Subramaniam, Jason Chang,
 Fotis Iliopoulos, Jiaming Luo, Myriam Khan, Weicheng Kuo, Denis Teplyashin, Florence Perot,
 Logan Kilpatrick, Amir Globerson, Hongkun Yu, Anfal Siddiqui, Nick Sukhanov, Arun Kandoor,
 Umang Gupta, Marco Andreetto, Moran Ambar, Donnie Kim, Paweł Wesołowski, Sarah Perrin,

756 Ben Limonchik, Wei Fan, Jim Stephan, Ian Stewart-Binks, Ryan Kappedal, Tong He, Sarah Cogan,
 757 Romina Datta, Tong Zhou, Jiayu Ye, Leandro Kieliger, Ana Ramalho, Kyle Kastner, Fabian
 758 Mentzer, Wei-Jen Ko, Arun Suggala, Tianhao Zhou, Shiraz Butt, Hana Strejček, Lior Belenki,
 759 Subhashini Venugopalan, Mingyang Ling, Evgenii Eltyshev, Yunxiao Deng, Geza Kovacs, Mukund
 760 Raghavachari, Hanjun Dai, Tal Schuster, Steven Schwarcz, Richard Nguyen, Arthur Nguyen, Gavin
 761 Buttimore, Shrestha Basu Mallick, Sudeep Gandhe, Seth Benjamin, Michal Jastrzebski, Le Yan,
 762 Sugato Basu, Chris Apps, Isabel Edkins, James Allingham, Immanuel Odisho, Tomas Kociský,
 763 Jewel Zhao, Linting Xue, Apoorv Reddy, Chrysovalantis Anastasiou, Aviel Atias, Sam Redmond,
 764 Kieran Milan, Nicolas Heess, Herman Schmit, Allan Dafoe, Daniel Andor, Tynan Gangwani,
 765 Anca Dragan, Sheng Zhang, Ashyana Kachra, Gang Wu, Siyang Xue, Kevin Aydin, Siqi Liu,
 766 Yuxiang Zhou, Mahan Malahi, Austin Wu, Siddharth Gopal, Candice Schumann, Peter Stys,
 767 Alek Wang, Mirek Olšák, Dangyi Liu, Christian Schallhart, Yiran Mao, Demetra Brady, Hao
 768 Xu, Tomas Mery, Chawin Sitawarin, Siva Velusamy, Tom Cobley, Alex Zhai, Christian Walder,
 769 Nitzan Katz, Ganesh Jawahar, Chinmay Kulkarni, Antoine Yang, Adam Paszke, Yinan Wang,
 770 Bogdan Damoc, Zalán Borsos, Ray Smith, Jinning Li, Mansi Gupta, Andrei Kapishnikov, Sushant
 771 Prakash, Florian Luisier, Rishabh Agarwal, Will Grathwohl, Kuangyuan Chen, Kehang Han,
 772 Nikhil Mehta, Andrew Over, Shekoofeh Azizi, Lei Meng, Niccolò Dal Santo, Kelvin Zheng, Jane
 773 Shapiro, Igor Petrovski, Jeffrey Hui, Amin Ghafouri, Jasper Snoek, James Qin, Mandy Jordan,
 774 Caitlin Sikora, Jonathan Malmaud, Yuheng Kuang, Aga Świertlik, Ruoxin Sang, Chongyang Shi,
 775 Leon Li, Andrew Rosenberg, Shubin Zhao, Andy Crawford, Jan-Thorsten Peter, Yun Lei, Xavier
 776 Garcia, Long Le, Todd Wang, Julien Amelot, Dave Orr, Praneeth Kacham, Dana Alon, Gladys
 777 Tyen, Abhinav Arora, James Lyon, Alex Kurakin, Mimi Ly, Theo Guidroz, Zhipeng Yan, Rina
 778 Panigrahy, Pingmei Xu, Thais Kagohara, Yong Cheng, Eric Noland, Jinhyuk Lee, Jonathan Lee,
 779 Cathy Yip, Maria Wang, Efrat Nehoran, Alexander Bykovsky, Zhihao Shan, Ankit Bhagatwala,
 780 Chaochao Yan, Jie Tan, Guillermo Garrido, Dan Ethier, Nate Hurley, Grace Vesom, Xu Chen,
 781 Siyuan Qiao, Abhishek Nayyar, Julian Walker, Paramjit Sandhu, Mihaela Rosca, Danny Swisher,
 782 Mikhail Dektiarev, Josh Dillon, George-Cristian Muraru, Manuel Tragut, Artiom Myaskovsky,
 783 David Reid, Marko Velic, Owen Xiao, Jasmine George, Mark Brand, Jing Li, Wenhao Yu, Shane
 784 Gu, Xiang Deng, François-Xavier Aubet, Soheil Hassas Yeganeh, Fred Alcober, Celine Smith,
 785 Trevor Cohn, Kay McKinney, Michael Tschanen, Ramesh Sampath, Gowoon Cheon, Liangchen
 786 Luo, Luyang Liu, Jordi Orbay, Hui Peng, Gabriela Botea, Xiaofan Zhang, Charles Yoon, Cesar
 787 Magalhaes, Paweł Stradomski, Ian Mackinnon, Steven Hemingray, Kumaran Venkatesan, Rhys
 788 May, Jaeyoun Kim, Alex Druinsky, Jingchen Ye, Zheng Xu, Terry Huang, Jad Al Abdallah, Adil
 789 Dostmohamed, Rachana Fellinger, Tsendsuren Munkhdalai, Akanksha Maurya, Peter Garst, Yin
 790 Zhang, Maxim Krikun, Simon Bucher, Aditya Srikanth Veerubhotla, Yixin Liu, Sheng Li, Nishesh
 791 Gupta, Jakub Adamek, Hanwen Chen, Bennett Orlando, Aleksandr Zaks, Joost van Amersfoort,
 792 Josh Camp, Hui Wan, HyunJeong Choe, Zhichun Wu, Kate Olszewska, Weiren Yu, Archita Vadali,
 793 Martin Scholz, Daniel De Freitas, Jason Lin, Amy Hua, Xin Liu, Frank Ding, Yichao Zhou, Boone
 794 Severson, Katerina Tsihlas, Samuel Yang, Tammo Spalink, Varun Yerram, Helena Pankov, Rory
 795 Blevins, Ben Vargas, Sarthak Jauhari, Matt Miecnikowski, Ming Zhang, Sandeep Kumar, Clement
 796 Farabet, Charline Le Lan, Sebastian Flennerhag, Yonatan Bitton, Ada Ma, Arthur Bražinskas,
 797 Eli Collins, Niharika Ahuja, Sneha Kudugunta, Anna Bortsova, Minh Giang, Wanzheng Zhu,
 798 Li Lao, Scott Pollom, Yifan Ding, Wei He, Lizzeth Bellot, Joana Iljazi, Ramya Sree Boppana,
 799 Shan Han, Tara Thompson, Amr Khalifa, Anna Bulanova, Blagoj Mitrevski, Bo Pang, Emma
 800 Cooney, Tian Shi, Rey Coaguila, Tamar Yakar, Marc'aurelio Ranzato, Nikola Momchev, Chris
 801 Rawles, Zachary Charles, Young Maeng, Yuan Zhang, Rishabh Bansal, Xiaokai Zhao, Brian
 802 Albert, Yuan Yuan, Sudheendra Vijayanarasimhan, Roy Hirsch, Vinay Ramasesh, Kiran Vodrahalli,
 803 Xingyu Wang, Arushi Gupta, D. J. Strouse, Jianmo Ni, Roma Patel, Gabe Taubman, Zhouyuan
 804 Huo, Dero Gharibian, Marianne Monteiro, Hoi Lam, Shobha Vasudevan, Aditi Chaudhary, Isabela
 805 Albuquerque, Kilol Gupta, Sebastian Riedel, Chaitra Hegde, Avraham Ruderman, András György,
 806 Marcus Wainwright, Ashwin Chaugule, Burcu Karagol Ayan, Tomer Levinboim, Sam Shleifer,
 807 Yogesh Kalley, Vahab Mirrokni, Abhishek Rao, Prabakar Radhakrishnan, Jay Hartford, Jialin
 808 Wu, Zhenhai Zhu, Francesco Bertolini, Hao Xiong, Nicolas Serrano, Hamish Tomlinson, Myle
 809 Ott, Yifan Chang, Mark Graham, Jian Li, Marco Liang, Xiangzhu Long, Sebastian Borgeaud,
 Yanif Ahmad, Alex Grills, Diana Mincu, Martin Izzard, Yuan Liu, Jinyu Xie, Louis O'Bryan,

810 Sameera Ponda, Simon Tong, Michelle Liu, Dan Malkin, Khalid Salama, Yuankai Chen, Rohan
 811 Anil, Anand Rao, Rigel Swavely, Misha Bilenko, Nina Anderson, Tat Tan, Jing Xie, Xing Wu,
 812 Lijun Yu, Oriol Vinyals, Andrey Ryabtsev, Rumen Dangovski, Kate Baumli, Daniel Keysers,
 813 Christian Wright, Zoe Ashwood, Betty Chan, Artem Shtefan, Yaohui Guo, Ankur Bapna, Radu
 814 Soricut, Steven Pecht, Sabela Ramos, Rui Wang, Jiahao Cai, Trieu Trinh, Paul Barham, Linda
 815 Friso, Eli Stickgold, Xiangzhuo Ding, Siamak Shakeri, Diego Ardila, Eleftheria Briakou, Phil
 816 Culliton, Adam Raveret, Jingyu Cui, David Saxton, Subhrajit Roy, Javad Azizi, Pengcheng Yin,
 817 Lucia Loher, Andrew Bunner, Min Choi, Faruk Ahmed, Eric Li, Yin Li, Shengyang Dai, Michael
 818 Elabd, Sriram Ganapathy, Shivani Agrawal, Yiqing Hua, Paige Kunkle, Sujeevan Rajayogam, Arun
 819 Ahuja, Arthur Conmy, Alex Vasiloff, Parker Beak, Christopher Yew, Jayaram Mudigonda, Bartek
 820 Wydrowski, Jon Blanton, Zhengdong Wang, Yann Dauphin, Zhuo Xu, Martin Polacek, Xi Chen,
 821 Hexiang Hu, Pauline Sho, Markus Kunesch, Mehdi Hafezi Manshadi, Eliza Rutherford, Bo Li,
 822 Sissie Hsiao, Iain Barr, Alex Tudor, Matija Kecman, Arsha Nagrani, Vladimir Pchelin, Martin
 823 Sundermeyer, Aishwarya P. S, Abhijit Karmarkar, Yi Gao, Grishma Chole, Olivier Bachem, Isabel
 824 Gao, Arturo BC, Matt Dibb, Mauro Verzetti, Felix Hernandez-Campos, Yana Lunts, Matthew
 825 Johnson, Julia Di Trapani, Raphael Koster, Idan Brusilovsky, Binbin Xiong, Megha Mohabey, Han
 826 Ke, Joe Zou, Tea Sabolić, Víctor Campos, John Palowitch, Alex Morris, Linhai Qiu, Pranavaraj
 827 Ponnuramu, Fangtao Li, Vivek Sharma, Kiranbir Sodhia, Kaan Tekelioglu, Aleksandr Chuklin,
 828 Madhavi Yenugula, Erika Gemzer, Theofilos Strinopoulos, Sam El-Husseini, Huiyu Wang, Yan
 829 Zhong, Edouard Leurent, Paul Natsev, Weijun Wang, Dre Mahaarachchi, Tao Zhu, Songyou Peng,
 830 Sami Alabd, Cheng-Chun Lee, Anthony Brohan, Arthur Szlam, G. S. Oh, Anton Kovsharov, Jenny
 831 Lee, Renee Wong, Megan Barnes, Gregory Thornton, Felix Gimeno, Omer Levy, Martin Sevenich,
 832 Melvin Johnson, Jonathan Mallinson, Robert Dadashi, Ziyue Wang, Qingchun Ren, Preethi Lahoti,
 833 Arka Dhar, Josh Feldman, Dan Zheng, Thatcher Ulrich, Liviu Panait, Michiel Blokzijl, Cip
 834 Baetu, Josip Matak, Jitendra Harlalka, Maulik Shah, Tal Marian, Daniel von Dincklage, Cosmo
 835 Du, Ruy Ley-Wild, Bethanie Brownfield, Max Schumacher, Yury Stuken, Shadi Noghabi, Sonal
 836 Gupta, Xiaoqi Ren, Eric Malmi, Felix Weissberger, Blanca Huergo, Maria Bauza, Thomas
 837 Lampe, Arthur Douillard, Mojtaba Seyedhosseini, Roy Frostig, Zoubin Ghahramani, Kelvin
 838 Nguyen, Kashyap Krishnakumar, Chengxi Ye, Rahul Gupta, Alireza Nazari, Robert Geirhos, Pete
 839 Shaw, Ahmed Eleryan, Dima Damen, Jennimaria Palomaki, Ted Xiao, Qiyin Wu, Quan Yuan,
 840 Phoenix Meadowlark, Matthew Bilotti, Raymond Lin, Mukund Sridhar, Yannick Schroecker,
 841 Da-Woon Chung, Jincheng Luo, Trevor Strohman, Tianlin Liu, Anne Zheng, Jesse Emond, Wei
 842 Wang, Andrew Lampinen, Toshiyuki Fukuzawa, Folawiyo Campbell-Ajala, Monica Roy, James
 843 Lee-Thorp, Lily Wang, Iftekhar Naim, Tony, Nguy~ê, Guy Bensky, Aditya Gupta, Dominika
 844 Rogozińska, Justin Fu, Thanumalayan Sankaranarayana Pillai, Petar Veličković, Shahar Drath,
 845 Philipp Neubeck, Vaibhav Tulsyan, Arseniy Klimovskiy, Don Metzler, Sage Stevens, Angel Yeh,
 846 Junwei Yuan, Tianhe Yu, Kelvin Zhang, Alec Go, Vincent Tsang, Ying Xu, Andy Wan, Isaac
 847 Galatzer-Levy, Sam Sobell, Abodunrinwa Toki, Elizabeth Salesky, Wenlei Zhou, Diego Antognini,
 848 Sholto Douglas, Shimu Wu, Adam Lelkes, Frank Kim, Paul Cavallaro, Ana Salazar, Yuchi Liu,
 849 James Besley, Tiziana Refice, Yiling Jia, Zhang Li, Michal Sokolik, Arvind Kannan, Jon Simon,
 850 Jo Chick, Avia Aharon, Meet Gandhi, Mayank Daswani, Keyvan Amiri, Vighnesh Birodkar, Abe
 851 Ittycheriah, Peter Grabowski, Oscar Chang, Charles Sutton, Zhixin, Lai, Umesh Telang, Susie
 852 Sargsyan, Tao Jiang, Raphael Hoffmann, Nicole Brichtova, Matteo Hessel, Jonathan Halcrow,
 853 Sammy Jerome, Geoff Brown, Alex Tomala, Elena Buchatskaya, Dian Yu, Sachit Menon, Pol
 854 Moreno, Yugu Liao, Vicky Zayats, Luming Tang, S. Q. Mah, Ashish Shenoy, Alex Siegman,
 855 Majid Hadian, Okwan Kwon, Tao Tu, Nima Khajehnouri, Ryan Foley, Parisa Haghani, Zhongru
 856 Wu, Vaishakh Keshava, Khyatti Gupta, Tony Bruguier, Rui Yao, Danny Karmen, Luisa Zintgraf,
 857 Zhicheng Wang, Enrique Piquerias, Junehyuk Jung, Jenny Brennan, Diego Machado, Marissa
 858 Giustina, M. H. Tessler, Kamyu Lee, Qiao Zhang, Joss Moore, Kaspar Daugaard, Alexander
 859 Frömmgen, Jennifer Beattie, Fred Zhang, Daniel Kasenberg, Ty Geri, Danfeng Qin, Gaurav Singh
 860 Tomar, Tom Ouyang, Tianli Yu, Luowei Zhou, Rajiv Mathews, Andy Davis, Yaoyiran Li, Jai
 861 Gupta, Damion Yates, Linda Deng, Elizabeth Kemp, Ga-Young Joung, Sergei Vassilvitskii, Mandy
 862 Guo, Pallavi LV, Dave Dopson, Sami Lachgar, Lara McConaughey, Himadri Choudhury, Dragos
 863 Dena, Aaron Cohen, Joshua Ainslie, Sergey Levi, Parthasarathy Gopavarapu, Polina Zablotskaia,
 Hugo Vallet, Sanaz Bahargam, Xiaodan Tang, Nenad Tomasev, Ethan Dyer, Daniel Balle, Hongrae
 Lee, William Bono, Jorge Gonzalez Mendez, Vadim Zubov, Shentao Yang, Ivor Rendulic, Yanyan
 Zheng, Andrew Hogue, Golan Pundak, Ralph Leith, Avishkar Bhoopchand, Michael Han, Mislav
 Žanić, Tom Schaul, Manolis Delakis, Tejas Iyer, Guanyu Wang, Harman Singh, Abdelrahman
 Abdelhamed, Tara Thomas, Siddhartha Brahma, Hilal Dib, Naveen Kumar, Wenxuan Zhou, Liang

864 Bai, Pushkar Mishra, Jiao Sun, Valentin Anklin, Roykrong Sukkerd, Lauren Agubuzu, Anton
 865 Briukhov, Anmol Gulati, Maximilian Sieb, Fabio Pardo, Sara Nasso, Junquan Chen, Kexin Zhu,
 866 Tiberiu Sosea, Alex Goldin, Keith Rush, Spurthi Amba Hombaiah, Andreas Noever, Allan Zhou,
 867 Sam Haves, Mary Phuong, Jake Ades, Yi-ting Chen, Lin Yang, Joseph Pagadura, Stan Bileschi,
 868 Victor Cotruta, Rachel Saputro, Arijit Pramanik, Sean Ammirati, Dan Garrette, Kevin Villela, Tim
 869 Blyth, Canfer Akbulut, Neha Jha, Alban Rustemi, Arissa Wongpanich, Chirag Nagpal, Yonghui
 870 Wu, Morgane Rivière, Sergey Kishchenko, Pranesh Srinivasan, Alice Chen, Animesh Sinha, Trang
 871 Pham, Bill Jia, Tom Hennigan, Anton Bakalov, Nithya Attaluri, Drew Garmon, Daniel Rodriguez,
 872 Dawid Wegner, Wenhao Jia, Evan Senter, Noah Fiedel, Denis Petek, Yuchuan Liu, Cassidy Hardin,
 873 Harshal Tushar Lehri, Joao Carreira, Sara Smoot, Marcel Prasetya, Nami Akazawa, Anca Stefanou, Chi-Hua Ho, Anelia Angelova, Kate Lin, Min Kim, Charles Chen, Marcin Sieniek, Alice Li, Tongfei Guo, Sorin Baltateanu, Pouya Tafti, Michael Wunder, Nadav Olmert, Divyansh Shukla, Jingwei Shen, Neel Kovelamudi, Balaji Venkatraman, Seth Neel, Romal Thoppilan, Jerome Connor, Frederik Benzing, Axel Stjerngren, Golnaz Ghiasi, Alex Polozov, Joshua Howland, Theophane Weber, Justin Chiu, Ganesh Poomal Girirajan, Andreas Terzis, Pidong Wang, Fangda Li, Yoav Ben Shalom, Dinesh Tewari, Matthew Denton, Roei Aharoni, Norbert Kalb, Heri Zhao, Junlin Zhang, Angelos Filos, Matthew Rahtz, Lalit Jain, Connie Fan, Vitor Rodrigues, Ruth Wang, Richard Shin, Jacob Austin, Roman Ring, Mariella Sanchez-Vargas, Mehadi Hassen, Ido Kessler, Uri Alon, Gufeng Zhang, Wenhua Chen, Yenai Ma, Xiancang Si, Le Hou, Azalia Mirhoseini, Marc Wilson, Geoff Bacon, Becca Roelofs, Lei Shu, Gautam Vasudevan, Jonas Adler, Artur Dwornik, Tayfun Terzi, Matt Lawlor, Harry Askham, Mike Bernico, Xuanyi Dong, Chris Hidey, Kevin Kilgour, Gaël Liu, Surya Bhupatiraju, Luke Leonhard, Siqi Zuo, Partha Talukdar, Qing Wei, Aliaksei Severyn, Vít Listík, Jong Lee, Aditya Tripathi, S. K. Park, Yossi Matias, Hao Liu, Alex Ruiz, Rajesh Jayaram, Jackson Tolins, Pierre Marcenac, Yiming Wang, Bryan Seybold, Henry Prior, Deepak Sharma, Jack Weber, Mikhail Sirotenko, Yunhsuan Sung, Dayou Du, Ellie Pavlick, Stefan Zinke, Markus Freitag, Max Dylla, Montse Gonzalez Arenas, Natan Potikha, Omer Goldman, Connie Tao, Rachita Chhaparia, Maria Voitovich, Pawan Dogra, Andrija Ražnatović, Zak Tsai, Chong You, Oleaser Johnson, George Tucker, Chenjie Gu, Jae Yoo, Maryam Majzoubi, Valentin Gabeur, Bahram Raad, Rocky Rhodes, Kashyap Kolipaka, Heidi Howard, Geta Sampemane, Benny Li, Chulayuth Asawaroengchai, Duy Nguyen, Chiyuan Zhang, Timothee Cour, Xinxin Yu, Zhao Fu, Joe Jiang, Po-Sen Huang, Gabriela Surita, Ifiaki Iturrate, Yael Karov, Michael Collins, Martin Baeuml, Fabian Fuchs, Shilpa Shetty, Swaroop Ramaswamy, Sayna Ebrahimi, Qiuchen Guo, Jeremy Shar, Gabe Barth-Maron, Sravanti Addepalli, Bryan Richter, Chin-Yi Cheng, Eugénie Rives, Fei Zheng, Johannes Griesser, Nishanth Dikkala, Yoel Zeldes, Ilkin Safarli, Dipanjan Das, Himanshu Srivastava, Sadh MNM Khan, Xin Li, Aditya Pandey, Larisa Markeeva, Dan Belov, Qiqi Yan, Mikołaj Rybiński, Tao Chen, Megha Nawhal, Michael Quinn, Vineetha Govindaraj, Sarah York, Reed Roberts, Roopal Garg, Namrata Godbole, Jake Abernethy, Anil Das, Lam Nguyen Thiet, Jonathan Tompson, John Nham, Neera Vats, Ben Caine, Wesley Helmholz, Francesco Pongetti, Yeongil Ko, James An, Clara Huiyi Hu, Yu-Cheng Ling, Julia Pawar, Robert Leland, Keisuke Kinoshita, Waleed Khawaja, Marco Selvi, Eugene Ie, Danila Sinopalnikov, Lev Proleev, Nilesh Tripuraneni, Michele Bevilacqua, Seungji Lee, Clayton Sanford, Dan Suh, Dustin Tran, Jeff Dean, Simon Baumgartner, Jens Heitkaemper, Sagar Gubbi, Kristina Toutanova, Yichong Xu, Chandu Thekkath, Keran Rong, Palak Jain, Annie Xie, Yan Virin, Yang Li, Lubo Litchev, Richard Powell, Tarun Bharti, Adam Kraft, Nan Hua, Marissa Ikonomidis, Ayal Hitron, Sanjiv Kumar, Loic Matthey, Sophie Bridgers, Lauren Lax, Ishaan Malhi, Ondrej Skopek, Ashish Gupta, Jiawei Cao, Michelle Rasquinha, Siim Põder, Wojciech Stokowiec, Nicholas Roth, Guowang Li, Michaël Sander, Joshua Kessinger, Vihan Jain, Edward Loper, Wonpyo Park, Michal Yarom, Lijun Cheng, Guru Guruganesh, Kanishka Rao, Yan Li, Catarina Barros, Mikhail Sushkov, Chun-Sung Ferng, Rohin Shah, Ophir Aharoni, Ravin Kumar, Tim McConnell, Peiran Li, Chen Wang, Fernando Pereira, Craig Swanson, Fayaz Jamil, Yan Xiong, Anitha Vijayakumar, Prakash Shroff, Kedar Soparkar, Jindong Gu, Livio Baldini Soares, Eric Wang, Kushal Majmundar, Aurora Wei, Kai Bailey, Nora Kassner, Chizu Kawamoto, Goran Žužić, Victor Gomes, Abhirut Gupta, Michael Guzman, Ishita Dasgupta, Xinyi Bai, Zhufeng Pan, Francesco Piccinno, Hadas Natalie Vogel, Octavio Ponce, Adrian Hutter, Paul Chang, Pan-Pan Jiang, Ionel Gog, Vlad Ionescu, James Manyika, Fabian Pedregosa, Harry Ragan, Zach Behrman, Ryan Mullins, Coline Devin, Aroonalok Pyne, Swapnil Gawde, Martin Chadwick, Yiming Gu, Sasan Tavakkol, Andy Twigg, Naman Goyal, Ndidi Elue, Anna Goldie, Srinivasan Venkatachary, Hongliang Fei, Ziqiang Feng, Marvin Ritter, Isabel Leal, Sudeep Dasari, Pei Sun, Alif Raditya Rochman, Brendan O'Donoghue, Yuchen Liu, Jim Sproch, Kai Chen, Natalie Clay, Slav Petrov, Sailesh Sidhwani, Ioana Mihailescu, Alex

918 Panagopoulos, A. J. Piergiovanni, Yunfei Bai, George Powell, Deep Karkhanis, Trevor Yacovone,
 919 Petr Mitrichev, Joe Kovac, Dave Uthus, Amir Yazdanbakhsh, David Amos, Steven Zheng, Bing
 920 Zhang, Jin Miao, Bhuvana Ramabhadran, Soroush Radpour, Shantanu Thakoor, Josh Newlan, Oran
 921 Lang, Orion Jankowski, Shikhar Bharadwaj, Jean-Michel Sarr, Shereen Ashraf, Sneha Mondal, Jun
 922 Yan, Ankit Singh Rawat, Sarmishta Velury, Greg Kochanski, Tom Eccles, Franz Och, Abhanshu
 923 Sharma, Ethan Mahintorabi, Alex Gurney, Carrie Muir, Vered Cohen, Saksham Thakur, Adam
 924 Bloniarz, Asier Mujika, Alexander Pritzel, Paul Caron, Altaf Rahman, Fiona Lang, Yasumasa Onoe,
 925 Petar Sirkovic, Jay Hoover, Ying Jian, Pablo Duque, Arun Narayanan, David Soergel, Alex Haig,
 926 Loren Maggiore, Shyamal Buch, Josef Dean, Ilya Figotin, Igor Karpov, Shaleen Gupta, Denny
 927 Zhou, Muhan Huang, Ashwin Vaswani, Christopher Semturs, Kaushik Shivakumar, Yu Watanabe,
 928 Vinodh Kumar Rajendran, Eva Lu, Yanhan Hou, Wenting Ye, Shikhar Vashishth, Nana Nti, Vytenis
 929 Sakenas, Darren Ni, Doug DeCarlo, Michael Bendersky, Sumit Bagri, Nacho Cano, Elijah Peake,
 930 Simon Tokumine, Varun Godbole, Carlos Guía, Tanya Lando, Vittorio Selo, Seher Ellis, Danny
 931 Tarlow, Daniel Gillick, Alessandro Epasto, Siddhartha Reddy Jonnalagadda, Meng Wei, Meiyang
 932 Xie, Ankur Taly, Michela Paganini, Mukund Sundararajan, Daniel Toyama, Ting Yu, Dessie
 933 Petrova, Aneesh Pappu, Rohan Agrawal, Senaka Buthpitiya, Justin Frye, Thomas Buschmann,
 934 Remi Crocker, Marco Tagliasacchi, Mengchao Wang, Da Huang, Sagi Perel, Brian Wieder, Hideto
 935 Kazawa, Weiyue Wang, Jeremy Cole, Himanshu Gupta, Ben Golan, Seojin Bang, Nitish Kulkarni,
 936 Ken Franko, Casper Liu, Doug Reid, Sid Dalmia, Jay Whang, Kevin Cen, Prasha Sundaram, Johan
 937 Ferret, Berivan Isik, Lucian Ionita, Guan Sun, Anna Shekhawat, Muqthar Mohammad, Philip
 938 Pham, Ronny Huang, Karthik Raman, Xingyi Zhou, Ross Mcilroy, Austin Myers, Sheng Peng,
 939 Jacob Scott, Paul Covington, Sofia Erell, Pratik Joshi, João Gabriel Oliveira, Natasha Noy, Tajwar
 940 Nasir, Jake Walker, Vera Axelrod, Tim Dozat, Pu Han, Chun-Te Chu, Eugene Weinstein, Anand
 941 Shukla, Shreyas Chandrakaladharan, Petra Poklukar, Bonnie Li, Ye Jin, Prem Erubetidine, Steven
 942 Hansen, Avigail Dabush, Alon Jacovi, Samrat Phatale, Chen Zhu, Steven Baker, Mo Shomrat, Yang
 943 Xiao, Jean Pouget-Abadie, Mingyang Zhang, Fanny Wei, Yang Song, Helen King, Yiling Huang,
 944 Yun Zhu, Ruoxi Sun, Juliana Vicente Franco, Chu-Cheng Lin, Sho Arora, Hui, Li, Vivian Xia,
 945 Luke Vilnis, Mariano Schain, Kaiz Alarakyia, Laurel Prince, Aaron Phillips, Caleb Habtegebriel,
 946 Luyao Xu, Huan Gui, Santiago Ontanon, Lora Aroyo, Karan Gill, Peggy Lu, Yash Katariya,
 947 Dhruv Madeka, Shankar Krishnan, Shubha Srinivas Raghvendra, James Freedman, Yi Tay, Gaurav
 948 Menghani, Peter Choy, Nishita Shetty, Dan Abolafia, Doron Kukliansky, Edward Chou, Jared
 949 Lichtarge, Ken Burke, Ben Coleman, Dee Guo, Larry Jin, Indro Bhattacharya, Victoria Langston,
 950 Yiming Li, Suyog Kotecha, Alex Yakubovich, Xinyun Chen, Petre Petrov, Tolly Powell, Yanzhang
 951 He, Corbin Quick, Kanav Garg, Dawsen Hwang, Yang Lu, Srinadh Bhojanapalli, Kristian Kjems,
 952 Ramin Mehran, Aaron Archer, Hado van Hasselt, Ashwin Balakrishna, J. K. Kearns, Meiqi Guo,
 953 Jason Riesa, Mikita Sazanovich, Xu Gao, Chris Sauer, Chengrun Yang, XiangHai Sheng, Thomas
 954 Jimma, Wouter Van Gansbeke, Vitaly Nikolaev, Wei Wei, Katie Millican, Ruizhe Zhao, Justin
 955 Snyder, Levent Bolelli, Maura O'Brien, Shawn Xu, Fei Xia, Wentao Yuan, Arvind Neelakantan,
 956 David Barker, Sachin Yadav, Hannah Kirkwood, Farooq Ahmad, Joel Wee, Jordan Grimstad, Boyu
 957 Wang, Matthew Wiethoff, Shane Settle, Miaosen Wang, Charles Blundell, Jingjing Chen, Chris
 958 Duvarney, Grace Hu, Olaf Ronneberger, Alex Lee, Yuanzhen Li, Abhishek Chakladar, Alena
 959 Butryna, Georgios Evangelopoulos, Guillaume Desjardins, Jonni Kanerva, Henry Wang, Averi
 960 Nowak, Nick Li, Alyssa Loo, Art Khurshudov, Laurent El Shafey, Nagabhushan Baddi, Karel Lenc,
 961 Yasaman Razeghi, Tom Lieber, Amer Sinha, Xiao Ma, Yao Su, James Huang, Asahi Ushio, Hanna
 962 Klimczak-Plucińska, Kareem Mohamed, J. D. Chen, Simon Osindero, Stav Ginzburg, Lampros
 963 Lamprou, Vasilisa Bashlovkina, Duc-Hieu Tran, Ali Khodaei, Ankit Anand, Yixian Di, Ramy
 964 Eskander, Manish Reddy Vuyyuru, Jasmine Liu, Aishwarya Kamath, Roman Goldenberg, Mathias
 965 Bellaiche, Juliette Pluto, Bill Rosgen, Hassan Mansoor, William Wong, Suhas Ganesh, Eric Bailey,
 966 Scott Baird, Dan Deutsch, Jinoo Baek, Xuhui Jia, Chansoo Lee, Abe Friesen, Nathaniel Braun, Kate
 967 Lee, Amayika Panda, Steven M. Hernandez, Duncan Williams, Jianqiao Liu, Ethan Liang, Arnaud
 968 Autef, Emily Pitler, Deepali Jain, Phoebe Kirk, Oskar Bunyan, Jaume Sanchez Elias, Tongxin Yin,
 969 Machel Reid, Aedan Pope, Nikita Putikhin, Bidisha Samanta, Sergio Guadarrama, Dahun Kim,
 970 Simon Rowe, Marcella Valentine, Geng Yan, Alex Salcianu, David Silver, Gan Song, Richa Singh,
 971 Shuai Ye, Hannah DeBalsi, Majd Al Merey, Eran Ofek, Albert Webson, Shibli Mourad, Ashwin
 972 Kakarla, Silvio Lattanzi, Nick Roy, Evgeny Sluzhaev, Christina Butterfield, Alessio Tonioni,
 973 Nathan Waters, Sudhindra Kopalle, Jason Chase, James Cohan, Girish Ramchandra Rao, Robert
 974 Berry, Michael Voznesensky, Shuguang Hu, Kristen Chiafullo, Sharat Chikkerur, George Scrivener,
 975 Ivy Zheng, Jeremy Wiesner, Wolfgang Macherey, Timothy Lillicrap, Fei Liu, Brian Walker, David
 976 Welling, Elinor Davies, Yangsibo Huang, Lijie Ren, Nir Shabat, Alessandro Agostini, Mariko

972 Iinuma, Dustin Zelle, Rohit Sathyanarayana, Andrea D'olimpio, Morgan Redshaw, Matt Ginsberg,
 973 Ashwin Murthy, Mark Geller, Tatiana Matejovicova, Ayan Chakrabarti, Ryan Julian, Christine
 974 Chan, Qiong Hu, Daniel Jarrett, Manu Agarwal, Jeshwanth Challagundla, Tao Li, Sandeep Tata,
 975 Wen Ding, Maya Meng, Zhuyun Dai, Giulia Vezzani, Shefali Garg, Jannis Bulian, Mary Jasarevic,
 976 Honglong Cai, Harish Rajamani, Adam Santoro, Florian Hartmann, Chen Liang, Bartek Perz,
 977 Apoorv Jindal, Fan Bu, Sungyong Seo, Ryan Poplin, Adrian Goedeckemeyer, Badih Ghazi, Nikhil
 978 Khadke, Leon Liu, Kevin Mather, Mingda Zhang, Ali Shah, Alex Chen, Jinliang Wei, Keshav
 979 Shivam, Yuan Cao, Donghyun Cho, Angelo Scorza Scarpati, Michael Moffitt, Clara Barbu, Ivan
 980 Jurin, Ming-Wei Chang, Hongbin Liu, Hao Zheng, Shachi Dave, Christine Kaeser-Chen, Xiaobin
 981 Yu, Alvin Abdagic, Lucas Gonzalez, Yanping Huang, Peilin Zhong, Cordelia Schmid, Bryce
 982 Petroni, Alex Wertheim, Jifan Zhu, Hoang Nguyen, Kaiyang Ji, Yanqi Zhou, Tao Zhou, Fangxiaoyu
 983 Feng, Regev Cohen, David Rim, Shubham Milind Phal, Petko Georgiev, Ariel Brand, Yue Ma,
 984 Wei Li, Somit Gupta, Chao Wang, Pavel Dubov, Jean Tarbouriech, Kingshuk Majumder, Huijian
 985 Li, Norman Rink, Apurv Suman, Yang Guo, Yinghao Sun, Arun Nair, Xiaowei Xu, Mohamed
 986 Elhawaty, Rodrigo Cabrera, Guangxing Han, Julian Eisenschlos, Junwen Bai, Yuqi Li, Yamini
 987 Bansal, Thibault Sellam, Mina Khan, Hung Nguyen, Justin Mao-Jones, Nikos Parotsidis, Jake
 988 Marcus, Cindy Fan, Roland Zimmermann, Yony Kochinski, Laura Graesser, Feryal Behbahani,
 989 Alvaro Caceres, Michael Riley, Patrick Kane, Sandra Lefdal, Rob Willoughby, Paul Vicol, Lun
 990 Wang, Shujian Zhang, Ashleah Gill, Yu Liang, Gautam Prasad, Soroosh Mariooryad, Mehran
 991 Kazemi, Zifeng Wang, Kritika Muralidharan, Paul Voigtlaender, Jeffrey Zhao, Huanjie Zhou,
 992 Nina D'Souza, Aditi Mavalankar, Séb Arnold, Nick Young, Obaid Sarvana, Chace Lee, Milad
 993 Nasr, Tingting Zou, Seokhwan Kim, Lukas Haas, Kaushal Patel, Neslihan Bulut, David Parkinson,
 994 Courtney Biles, Dmitry Kalashnikov, Chi Ming To, Aviral Kumar, Jessica Austin, Alex Greve,
 995 Lei Zhang, Megha Goel, Yeqing Li, Sergey Yaroshenko, Max Chang, Abhishek Jindal, Geoff
 996 Clark, Hagai Taitelbaum, Dale Johnson, Ofir Roval, Jeongwoo Ko, Anhad Mohananey, Christian
 997 Schuler, Shenil Dodhia, Ruichao Li, Kazuki Osawa, Claire Cui, Peng Xu, Rushin Shah, Tao Huang,
 998 Ela Gruzewska, Nathan Clement, Mudit Verma, Olcan Sercinoglu, Hai Qian, Viral Shah, Masa
 999 Yamaguchi, Abhinit Modi, Takahiro Kosakai, Thomas Strohmann, Junhao Zeng, Beliz Gunel, Jun
 1000 Qian, Austin Tarango, Krzysztof Jastrzębski, Robert David, Jyn Shan, Parker Schuh, Kunal Lad,
 1001 Willi Gierke, Mukundan Madhavan, Xinyi Chen, Mark Kurzeja, Rebeca Santamaria-Fernandez,
 1002 Dawn Chen, Alexandra Cordell, Yuri Chervonyi, Frankie Garcia, Nithish Kannen, Vincent Perot,
 1003 Nan Ding, Shlomi Cohen-Ganor, Victor Lavrenko, Junru Wu, Georgie Evans, Cicero Nogueira dos
 1004 Santos, Madhavi Sewak, Ashley Brown, Andrew Hard, Joan Puigcerver, Zeyu Zheng, Yizhong
 1005 Liang, Evgeny Gladchenko, Reeve Ingle, Uri First, Pierre Sermanet, Charlotte Magister, Mihajlo
 1006 Velimirović, Sashank Reddi, Susanna Ricco, Eirikur Agustsson, Hartwig Adam, Nir Levine, David
 1007 Gaddy, Dan Holtmann-Rice, Xuanhui Wang, Ashutosh Sathe, Abhijit Guha Roy, Blaž Bratanič,
 1008 Alen Carin, Harsh Mehta, Silvano Bonacina, Nicola De Cao, Mara Finkelstein, Verena Rieser,
 1009 Xinyi Wu, Florent Altché, Dylan Scandinaro, Li Li, Nino Vieillard, Nikhil Sethi, Garrett Tanzer,
 1010 Zhi Xing, Shibo Wang, Parul Bhatia, Gui Citovsky, Thomas Anthony, Sharon Lin, Tianze Shi,
 1011 Shoshana Jakobovits, Gena Gibson, Raj Apte, Lisa Lee, Mingqing Chen, Arunkumar Byravan,
 1012 Petros Maniatis, Kellie Webster, Andrew Dai, Pu-Chin Chen, Jiaqi Pan, Asya Fadeeva, Zach
 1013 Gleicher, Thang Luong, and Niket Kumar Bhumihar. Gemini 2.5: Pushing the Frontier with
 1014 Advanced Reasoning, Multimodality, Long Context, and Next Generation Agentic Capabilities,
 1015 July 2025. URL <http://arxiv.org/abs/2507.06261>. arXiv:2507.06261 [cs].
 1016
 1017 DeepSeek-AI, Daya Guo, Dejian Yang, Haowei Zhang, Junxiao Song, Ruoyu Zhang, Runxin Xu,
 1018 Qihao Zhu, Shirong Ma, Peiyi Wang, Xiao Bi, Xiaokang Zhang, Xingkai Yu, Yu Wu, Z. F. Wu,
 1019 Zhibin Gou, Zhihong Shao, Zhuoshu Li, Ziyi Gao, Aixin Liu, Bing Xue, Bingxuan Wang, Bochao
 1020 Wu, Bei Feng, Chengda Lu, Chenggang Zhao, Chengqi Deng, Chenyu Zhang, Chong Ruan,
 1021 Damai Dai, Deli Chen, Dongjie Ji, Erhang Li, Fangyun Lin, Fucong Dai, Fuli Luo, Guangbo Hao,
 1022 Guanting Chen, Guowei Li, H. Zhang, Han Bao, Hanwei Xu, Haocheng Wang, Honghui Ding,
 1023 Huajian Xin, Huazuo Gao, Hui Qu, Hui Li, Jianzhong Guo, Jiashi Li, Jiawei Wang, Jingchang
 1024 Chen, Jingyang Yuan, Junjie Qiu, Junlong Li, J. L. Cai, Jiaqi Ni, Jian Liang, Jin Chen, Kai Dong,
 1025 Kai Hu, Kaige Gao, Kang Guan, Kexin Huang, Kuai Yu, Lean Wang, Lecong Zhang, Liang Zhao,
 Litong Wang, Liyue Zhang, Lei Xu, Leyi Xia, Mingchuan Zhang, Minghua Zhang, Minghui Tang,
 Meng Li, Miaojun Wang, Mingming Li, Ning Tian, Panpan Huang, Peng Zhang, Qiancheng Wang,
 Qinyu Chen, Qiushi Du, Ruiqi Ge, Ruisong Zhang, Ruizhe Pan, Runji Wang, R. J. Chen, R. L.
 Jin, Ruyi Chen, Shanghao Lu, Shangyan Zhou, Shanhuang Chen, Shengfeng Ye, Shiyu Wang,
 Shuiping Yu, Shunfeng Zhou, Shuting Pan, S. S. Li, Shuang Zhou, Shaoqing Wu, Shengfeng

1026 Ye, Tao Yun, Tian Pei, Tianyu Sun, T. Wang, Wangding Zeng, Wanjia Zhao, Wen Liu, Wenfeng
 1027 Liang, Wenjun Gao, Wenqin Yu, Wentao Zhang, W. L. Xiao, Wei An, Xiaodong Liu, Xiaohan
 1028 Wang, Xiaokang Chen, Xiaotao Nie, Xin Cheng, Xin Liu, Xin Xie, Xingchao Liu, Xinyu Yang,
 1029 Xinyuan Li, Xuecheng Su, Xuheng Lin, X. Q. Li, Xiangyue Jin, Xiaoqin Shen, Xiaosha Chen,
 1030 Xiaowen Sun, Xiaoxiang Wang, Xinnan Song, Xinyi Zhou, Xianzu Wang, Xinxia Shan, Y. K. Li,
 1031 Y. Q. Wang, Y. X. Wei, Yang Zhang, Yanhong Xu, Yao Li, Yao Zhao, Yaofeng Sun, Yaohui Wang,
 1032 Yi Yu, Yichao Zhang, Yifan Shi, Yiliang Xiong, Ying He, Yishi Piao, Yisong Wang, Yixuan Tan,
 1033 Yiyang Ma, Yiyuan Liu, Yongqiang Guo, Yuan Ou, Yuduan Wang, Yue Gong, Yuheng Zou, Yujia
 1034 He, Yunfan Xiong, Yuxiang Luo, Yuxiang You, Yuxuan Liu, Yuyang Zhou, Y. X. Zhu, Yanhong
 1035 Xu, Yanping Huang, Yaohui Li, Yi Zheng, Yuchen Zhu, Yunxian Ma, Ying Tang, Yukun Zha,
 1036 Yuting Yan, Z. Z. Ren, Zehui Ren, Zhangli Sha, Zhe Fu, Zhean Xu, Zhenda Xie, Zhengyan Zhang,
 1037 Zhewen Hao, Zhicheng Ma, Zhigang Yan, Zhiyu Wu, Zihui Gu, Zijia Zhu, Zijun Liu, Zilin Li,
 1038 Ziwei Xie, Ziyang Song, Zizheng Pan, Zhen Huang, Zhipeng Xu, Zhongyu Zhang, and Zhen
 1039 Zhang. DeepSeek-R1: Incentivizing Reasoning Capability in LLMs via Reinforcement Learning,
 1040 January 2025. URL <http://arxiv.org/abs/2501.12948>. arXiv:2501.12948 [cs].

1041 Oliver Groth, Fabian B. Fuchs, Ingmar Posner, and Andrea Vedaldi. ShapeStacks: Learning Vision-
 1042 Based Physical Intuition for Generalised Object Stacking, July 2018. URL <http://arxiv.org/abs/1804.08018>. arXiv:1804.08018 [cs].

1043 Justin Johnson, Bharath Hariharan, Laurens van der Maaten, Li Fei-Fei, C. Lawrence Zitnick,
 1044 and Ross Girshick. CLEVR: A Diagnostic Dataset for Compositional Language and Elemen-
 1045 tary Visual Reasoning, December 2016. URL <http://arxiv.org/abs/1612.06890>.
 1046 arXiv:1612.06890 [cs].

1047 Panagiotis Michalatos and Sawako Kaijima. Millipede Plugin Grasshopper 3D, 2024. URL <https://www.creativemutation.com/millipede>.

1048 OpenAI, Josh Achiam, Steven Adler, Sandhini Agarwal, Lama Ahmad, Ilge Akkaya, Florencia Leoni
 1049 Aleman, Diogo Almeida, Janko Altenschmidt, Sam Altman, Shyamal Anadkat, Red Avila, Igor
 1050 Babuschkin, Suchir Balaji, Valerie Balcom, Paul Baltescu, Haiming Bao, Mohammad Bavarian,
 1051 Jeff Belgum, Irwan Bello, Jake Berdine, Gabriel Bernadett-Shapiro, Christopher Berner, Lenny
 1052 Bogdonoff, Oleg Boiko, Madelaine Boyd, Anna-Luisa Brakman, Greg Brockman, Tim Brooks,
 1053 Miles Brundage, Kevin Button, Trevor Cai, Rosie Campbell, Andrew Cann, Brittany Carey, Chelsea
 1054 Carlson, Rory Carmichael, Brooke Chan, Che Chang, Fotis Chantzis, Derek Chen, Sully Chen,
 1055 Ruby Chen, Jason Chen, Mark Chen, Ben Chess, Chester Cho, Casey Chu, Hyung Won Chung,
 1056 Dave Cummings, Jeremiah Currier, Yunxing Dai, Cory Decareaux, Thomas Degry, Noah Deutsch,
 1057 Damien Deville, Arka Dhar, David Dohan, Steve Dowling, Sheila Dunning, Adrien Ecoffet, Atty
 1058 Eleti, Tyna Eloundou, David Farhi, Liam Fedus, Niko Felix, Simón Posada Fishman, Juston Forte,
 1059 Isabella Fulford, Leo Gao, Elie Georges, Christian Gibson, Vik Goel, Tarun Gogineni, Gabriel
 1060 Goh, Rapha Gontijo-Lopes, Jonathan Gordon, Morgan Grafstein, Scott Gray, Ryan Greene, Joshua
 1061 Gross, Shixiang Shane Gu, Yufei Guo, Chris Hallacy, Jesse Han, Jeff Harris, Yuchen He, Mike
 1062 Heaton, Johannes Heidecke, Chris Hesse, Alan Hickey, Wade Hickey, Peter Hoeschele, Brandon
 1063 Houghton, Kenny Hsu, Shengli Hu, Xin Hu, Joost Huizinga, Shantanu Jain, Shawn Jain, Joanne
 1064 Jang, Angela Jiang, Roger Jiang, Haozhun Jin, Denny Jin, Shino Jomoto, Billie Jonn, Heewoo
 1065 Jun, Tomer Kaftan, Łukasz Kaiser, Ali Kamali, Ingmar Kanitscheider, Nitish Shirish Keskar,
 1066 Tabarak Khan, Logan Kilpatrick, Jong Wook Kim, Christina Kim, Yongjik Kim, Jan Hendrik
 1067 Kirchner, Jamie Kiro, Matt Knight, Daniel Kokotajlo, Łukasz Kondraciuk, Andrew Kondrich,
 1068 Aris Konstantinidis, Kyle Koscic, Gretchen Krueger, Vishal Kuo, Michael Lampe, Ikai Lan, Teddy
 1069 Lee, Jan Leike, Jade Leung, Daniel Levy, Chak Ming Li, Rachel Lim, Molly Lin, Stephanie
 1070 Lin, Mateusz Litwin, Theresa Lopez, Ryan Lowe, Patricia Lue, Anna Makanju, Kim Malfacini,
 1071 Sam Manning, Todor Markov, Yaniv Markovski, Bianca Martin, Katie Mayer, Andrew Mayne,
 1072 Bob McGrew, Scott Mayer McKinney, Christine McLeavey, Paul McMillan, Jake McNeil, David
 1073 Medina, Aalok Mehta, Jacob Menick, Luke Metz, Andrey Mishchenko, Pamela Mishkin, Vinnie
 1074 Monaco, Evan Morikawa, Daniel Mossing, Tong Mu, Mira Murati, Oleg Murk, David Mély,
 1075 Ashvin Nair, Reiichiro Nakano, Rajeev Nayak, Arvind Neelakantan, Richard Ngo, Hyeonwoo
 1076 Noh, Long Ouyang, Cullen O’Keefe, Jakub Pachocki, Alex Paino, Joe Palermo, Ashley Pantuliano,
 1077 Giambattista Parascandolo, Joel Parish, Emry Parparita, Alex Passos, Mikhail Pavlov, Andrew
 1078 Peng, Adam Perelman, Filipe de Avila Belbute Peres, Michael Petrov, Henrique Ponde de Oliveira
 1079 Pinto, Michael, Pokorny, Michelle Pokrass, Vitchyr H. Pong, Tolly Powell, Alethea Power, Boris

1080 Power, Elizabeth Proehl, Raul Puri, Alec Radford, Jack Rae, Aditya Ramesh, Cameron Raymond,
 1081 Francis Real, Kendra Rimbach, Carl Ross, Bob Rotsted, Henri Roussez, Nick Ryder, Mario
 1082 Saltarelli, Ted Sanders, Shibani Santurkar, Girish Sastry, Heather Schmidt, David Schnurr, John
 1083 Schulman, Daniel Selsam, Kyla Sheppard, Toki Sherbakov, Jessica Shieh, Sarah Shoker, Pranav
 1084 Shyam, Szymon Sidor, Eric Sigler, Maddie Simens, Jordan Sitkin, Katarina Slama, Ian Sohl,
 1085 Benjamin Sokolowsky, Yang Song, Natalie Staudacher, Felipe Petroski Such, Natalie Summers,
 1086 Ilya Sutskever, Jie Tang, Nikolas Tezak, Madeleine B. Thompson, Phil Tillet, Amin Tootoonchian,
 1087 Elizabeth Tseng, Preston Tuggle, Nick Turley, Jerry Tworek, Juan Felipe Cerón Uribe, Andrea
 1088 Vallone, Arun Vijayvergiya, Chelsea Voss, Carroll Wainwright, Justin Jay Wang, Alvin Wang, Ben
 1089 Wang, Jonathan Ward, Jason Wei, C. J. Weinmann, Akila Welihinda, Peter Welinder, Jiayi Weng,
 1090 Lilian Weng, Matt Wiethoff, Dave Willner, Clemens Winter, Samuel Wolrich, Hannah Wong,
 1091 Lauren Workman, Sherwin Wu, Jeff Wu, Michael Wu, Kai Xiao, Tao Xu, Sarah Yoo, Kevin Yu,
 1092 Qiming Yuan, Wojciech Zaremba, Rowan Zellers, Chong Zhang, Marvin Zhang, Shengjia Zhao,
 1093 Tianhao Zheng, Juntang Zhuang, William Zhuk, and Barret Zoph. GPT-4 Technical Report, March
 2024a. URL <http://arxiv.org/abs/2303.08774>. arXiv:2303.08774 [cs].
 1094

1095 OpenAI, Aaron Hurst, Adam Lerer, Adam P. Goucher, Adam Perelman, Aditya Ramesh, Aidan
 1096 Clark, A. J. Ostrow, Akila Welihinda, Alan Hayes, Alec Radford, Aleksander Mądry, Alex
 1097 Baker-Whitcomb, Alex Beutel, Alex Borzunov, Alex Carney, Alex Chow, Alex Kirillov, Alex
 1098 Nichol, Alex Paino, Alex Renzin, Alex Tachard Passos, Alexander Kirillov, Alexi Christakis,
 1099 Alexis Conneau, Ali Kamali, Allan Jabri, Allison Moyer, Allison Tam, Amadou Crookes, Amin
 1100 Tootoonchian, Amin Tootoonchian, Ananya Kumar, Andrea Vallone, Andrej Karpathy, Andrew
 1101 Braunstein, Andrew Cann, Andrew Codispoti, Andrew Galu, Andrew Kondrich, Andrew Tulloch,
 1102 Andrey Mishchenko, Angela Baek, Angela Jiang, Antoine Pelisse, Antonia Woodford, Anuj
 1103 Gosalia, Arka Dhar, Ashley Pantuliano, Avi Nayak, Avital Oliver, Barret Zoph, Behrooz Ghorbani,
 1104 Ben Leimberger, Ben Rossen, Ben Sokolowsky, Ben Wang, Benjamin Zweig, Beth Hoover, Blake
 1105 Samic, Bob McGrew, Bobby Spero, Bogo Giertler, Bowen Cheng, Brad Lightcap, Brandon Walkin,
 1106 Brendan Quinn, Brian Guaraci, Brian Hsu, Bright Kellogg, Brydon Eastman, Camillo Lugaressi,
 1107 Carroll Wainwright, Cary Bassin, Cary Hudson, Casey Chu, Chad Nelson, Chak Li, Chan Jun
 1108 Shern, Channing Conger, Charlotte Barette, Chelsea Voss, Chen Ding, Cheng Lu, Chong Zhang,
 1109 Chris Beaumont, Chris Hallacy, Chris Koch, Christian Gibson, Christina Kim, Christine Choi,
 1110 Christine McLeavey, Christopher Hesse, Claudia Fischer, Clemens Winter, Coley Czarnecki,
 1111 Colin Jarvis, Colin Wei, Constantin Koumouzelis, Dane Sherburn, Daniel Kappler, Daniel Levin,
 1112 Daniel Levy, David Carr, David Farhi, David Mely, David Robinson, David Sasaki, Denny Jin,
 1113 Dev Valladares, Dimitris Tsipras, Doug Li, Duc Phong Nguyen, Duncan Findlay, Edede Oiwoh,
 1114 Edmund Wong, Ehsan Asdar, Elizabeth Proehl, Elizabeth Yang, Eric Antonow, Eric Kramer, Eric
 1115 Peterson, Eric Sigler, Eric Wallace, Eugene Brevdo, Evan Mays, Farzad Khorasani, Felipe Petroski
 1116 Such, Filippo Raso, Francis Zhang, Fred von Lohmann, Freddie Sulit, Gabriel Goh, Gene Oden,
 1117 Geoff Salmon, Giulio Starace, Greg Brockman, Hadi Salman, Haiming Bao, Haitang Hu, Hannah
 1118 Wong, Haoyu Wang, Heather Schmidt, Heather Whitney, Heewoo Jun, Hendrik Kirchner, Henrique
 1119 Ponde de Oliveira Pinto, Hongyu Ren, Huiwen Chang, Hyung Won Chung, Ian Kivlichan, Ian
 1120 O'Connell, Ian O'Connell, Ian Osband, Ian Silber, Ian Sohl, Ibrahim Okuyucu, Ikai Lan, Ilya
 1121 Kostrikov, Ilya Sutskever, Ingmar Kanitscheider, Ishaan Gulrajani, Jacob Coxon, Jacob Menick,
 1122 Jakub Pachocki, James Aung, James Betker, James Crooks, James Lennon, Jamie Kiros, Jan
 1123 Leike, Jane Park, Jason Kwon, Jason Phang, Jason Teplitz, Jason Wei, Jason Wolfe, Jay Chen,
 1124 Jeff Harris, Jenia Varavva, Jessica Gan Lee, Jessica Shieh, Ji Lin, Jiahui Yu, Jiayi Weng, Jie
 1125 Tang, Jieqi Yu, Joanne Jang, Joaquin Quinonero Candela, Joe Beutler, Joe Landers, Joel Parish,
 1126 Johannes Heidecke, John Schulman, Jonathan Lachman, Jonathan McKay, Jonathan Uesato,
 1127 Jonathan Ward, Jong Wook Kim, Joost Huizinga, Jordan Sitkin, Jos Kraaijeveld, Josh Gross, Josh
 1128 Kaplan, Josh Snyder, Joshua Achiam, Joy Jiao, Joyce Lee, Juntang Zhuang, Justyn Harriman, Kai
 1129 Fricke, Kai Hayashi, Karan Singhal, Katy Shi, Kavin Karthik, Kayla Wood, Kendra Rimbach,
 1130 Kenny Hsu, Kenny Nguyen, Keren Gu-Lemberg, Kevin Button, Kevin Liu, Kiel Howe, Krithika
 1131 Muthukumar, Kyle Luther, Lama Ahmad, Larry Kai, Lauren Itow, Lauren Workman, Leher Pathak,
 1132 Leo Chen, Li Jing, Lia Guy, Liam Fedus, Liang Zhou, Lien Mamitsuka, Lilian Weng, Lindsay
 1133 McCallum, Lindsey Held, Long Ouyang, Louis Feuvrier, Lu Zhang, Lukas Kondraciuk, Lukasz
 Kaiser, Luke Hewitt, Luke Metz, Lyric Doshi, Mada Aflak, Maddie Simens, Madelaine Boyd,
 Madeleine Thompson, Marat Dukhan, Mark Chen, Mark Gray, Mark Hudnall, Marvin Zhang,
 Marwan Aljubeh, Mateusz Litwin, Matthew Zeng, Max Johnson, Maya Shetty, Mayank Gupta,
 Meghan Shah, Mehmet Yatbaz, Meng Jia Yang, Mengchao Zhong, Mia Glaese, Mianna Chen,

1134 Michael Janner, Michael Lampe, Michael Petrov, Michael Wu, Michele Wang, Michelle Fradin,
 1135 Michelle Pokrass, Miguel Castro, Miguel Oom Temudo de Castro, Mikhail Pavlov, Miles Brundage,
 1136 Miles Wang, Minal Khan, Mira Murati, Mo Bavarian, Molly Lin, Murat Yesildal, Nacho Soto,
 1137 Natalia Gimelshein, Natalie Cone, Natalie Staudacher, Natalie Summers, Natan LaFontaine, Neil
 1138 Chowdhury, Nick Ryder, Nick Stathas, Nick Turley, Nik Tezak, Niko Felix, Nithanth Kudige,
 1139 Nitish Keskar, Noah Deutsch, Noel Bundick, Nora Puckett, Ofir Nachum, Ola Okelola, Oleg Boiko,
 1140 Oleg Murk, Oliver Jaffe, Olivia Watkins, Olivier Godement, Owen Campbell-Moore, Patrick Chao,
 1141 Paul McMillan, Pavel Belov, Peng Su, Peter Bak, Peter Bakkum, Peter Deng, Peter Dolan, Peter
 1142 Hoeschele, Peter Welinder, Phil Tillet, Philip Pronin, Philippe Tillet, Prafulla Dhariwal, Qiming
 1143 Yuan, Rachel Dias, Rachel Lim, Rahul Arora, Rajan Troll, Randall Lin, Rapha Gontijo Lopes, Raul
 1144 Puri, Reah Miyara, Reimar Leike, Renaud Gaubert, Reza Zamani, Ricky Wang, Rob Donnelly, Rob
 1145 Honsby, Rocky Smith, Rohan Sahai, Rohit Ramchandani, Romain Huet, Rory Carmichael, Rowan
 1146 Zellers, Roy Chen, Ruby Chen, Ruslan Nigmatullin, Ryan Cheu, Saachi Jain, Sam Altman, Sam
 1147 Schoenholz, Sam Toizer, Samuel Miserendino, Sandhini Agarwal, Sara Culver, Scott Ethersmith,
 1148 Scott Gray, Sean Grove, Sean Metzger, Shamez Hermani, Shantanu Jain, Shengjia Zhao, Sherwin
 1149 Wu, Shino Jomoto, Shirong Wu, Shuaiqi, Xia, Sonia Phene, Spencer Papay, Srinivas Narayanan,
 1150 Steve Coffey, Steve Lee, Stewart Hall, Suchir Balaji, Tal Broda, Tal Stramer, Tao Xu, Tarun
 1151 Gogineni, Taya Christianson, Ted Sanders, Tejal Patwardhan, Thomas Cunninghamman, Thomas
 1152 Degry, Thomas Dimson, Thomas Raoux, Thomas Shadwell, Tianhao Zheng, Todd Underwood,
 1153 Todor Markov, Toki Sherbakov, Tom Rubin, Tom Stasi, Tomer Kaftan, Tristan Heywood, Troy
 1154 Peterson, Tyce Walters, Tyna Eloundou, Valerie Qi, Veit Moeller, Vinnie Monaco, Vishal Kuo,
 1155 Vlad Fomenko, Wayne Chang, Weiyi Zheng, Wenda Zhou, Wesam Manassra, Will Sheu, Wojciech
 1156 Zaremba, Yash Patil, Yilei Qian, Yongjik Kim, Youlong Cheng, Yu Zhang, Yuchen He, Yuchen
 1157 Zhang, Yujia Jin, Yunxing Dai, and Yury Malkov. GPT-4o System Card, October 2024b. URL
 1158 <http://arxiv.org/abs/2410.21276>. arXiv:2410.21276 [cs].

1159 Sharad Rawat and M.-H. Herman Shen. A Novel Topology Optimization Approach using Con-
 1160 ditional Deep Learning, January 2019. URL <http://arxiv.org/abs/1901.04859>.
 1161 arXiv:1901.04859 [cs].

1162 Ronan Riochet, Mario Ynocente Castro, Mathieu Bernard, Adam Lerer, Rob Fergus, Véronique Izard,
 1163 and Emmanuel Dupoux. IntPhys: A Framework and Benchmark for Visual Intuitive Physics Rea-
 1164 soning, February 2020. URL <http://arxiv.org/abs/1803.07616>. arXiv:1803.07616
 1165 [cs].

1166 Gemini Team, Petko Georgiev, Ving Ian Lei, Ryan Burnell, Libin Bai, Anmol Gulati, Garrett Tanzer,
 1167 Damien Vincent, Zhufeng Pan, Shibo Wang, Soroosh Mariooryad, Yifan Ding, Xinyang Geng, Fred
 1168 Alcober, Roy Frostig, Mark Omernick, Lexi Walker, Cosmin Paduraru, Christina Sorokin, Andrea
 1169 Tacchetti, Colin Gaffney, Samira Daruki, Olcan Sercinoglu, Zach Gleicher, Juliette Love, Paul
 1170 Voigtlaender, Rohan Jain, Gabriela Surita, Kareem Mohamed, Rory Blevins, Junwhan Ahn, Tao
 1171 Zhu, Kornraphop Kawintiranon, Orhan Firat, Yiming Gu, Yujing Zhang, Matthew Rahtz, Manaal
 1172 Faruqui, Natalie Clay, Justin Gilmer, J. D. Co-Reyes, Ivo Penchev, Rui Zhu, Nobuyuki Morioka,
 1173 Kevin Hui, Krishna Haridasan, Victor Campos, Mahdis Mahdieh, Mandy Guo, Samer Hassan,
 1174 Kevin Kilgour, Arpi Vezer, Heng-Tze Cheng, Raoul de Liedekerke, Siddharth Goyal, Paul Barham,
 1175 D. J. Strouse, Seb Noury, Jonas Adler, Mukund Sundararajan, Sharad Vikram, Dmitry Lepikhin,
 1176 Michela Paganini, Xavier Garcia, Fan Yang, Dasha Valter, Maja Trebacz, Kiran Vodrahalli,
 1177 Chulayuth Asawaroengchai, Roman Ring, Norbert Kalb, Livio Baldini Soares, Siddhartha Brahma,
 1178 David Steiner, Tianhe Yu, Fabian Mentzer, Antoine He, Lucas Gonzalez, Bibo Xu, Raphael Lopez
 1179 Kaufman, Laurent El Shafey, Junhyuk Oh, Tom Hennigan, George van den Driessche, Seth Odoom,
 1180 Mario Lucic, Becca Roelofs, Sid Lall, Amit Marathe, Betty Chan, Santiago Ontanon, Luheng He,
 1181 Denis Teplyashin, Jonathan Lai, Phil Crone, Bogdan Damoc, Lewis Ho, Sebastian Riedel, Karel
 1182 Lenc, Chih-Kuan Yeh, Aakanksha Chowdhery, Yang Xu, Mehran Kazemi, Ehsan Amid, Anastasia
 1183 Petrushkina, Kevin Swersky, Ali Khodaei, Gwoon Chen, Chris Larkin, Mario Pinto, Geng Yan,
 1184 Adria Puigdomenech Badia, Piyush Patil, Steven Hansen, Dave Orr, Sebastien M. R. Arnold,
 1185 Jordan Grimstad, Andrew Dai, Sholto Douglas, Rishika Sinha, Vikas Yadav, Xi Chen, Elena
 1186 Gribovskaya, Jacob Austin, Jeffrey Zhao, Kaushal Patel, Paul Komarek, Sophia Austin, Sebastian
 1187 Borgeaud, Linda Friso, Abhimanyu Goyal, Ben Caine, Kris Cao, Da-Woon Chung, Matthew
 1188 Lamm, Gabe Barth-Maron, Thais Kagohara, Kate Olszewska, Mia Chen, Kaushik Shivakumar,
 1189 Rishabh Agarwal, Harshal Godhia, Ravi Rajwar, Javier Snaider, Xerxes Dotiwalla, Yuan Liu,
 1190 Aditya Barua, Victor Ungureanu, Yuan Zhang, Bat-Orgil Batsaikhan, Mateo Wirth, James Qin, Ivo

1188 Danihelka, Tulsee Doshi, Martin Chadwick, Jilin Chen, Sanil Jain, Quoc Le, Arjun Kar, Madhu
 1189 Gurumurthy, Cheng Li, Ruoxin Sang, Fangyu Liu, Lampros Lamprou, Rich Munoz, Nathan Lintz,
 1190 Harsh Mehta, Heidi Howard, Malcolm Reynolds, Lora Aroyo, Quan Wang, Lorenzo Blanco, Albin
 1191 Cassirer, Jordan Griffith, Dipanjan Das, Stephan Lee, Jakub Sygnowski, Zach Fisher, James Besley,
 1192 Richard Powell, Zafarali Ahmed, Dominik Paulus, David Reitter, Zalan Borsos, Rishabh Joshi,
 1193 Aedan Pope, Steven Hand, Vittorio Selo, Vihan Jain, Nikhil Sethi, Megha Goel, Takaki Makino,
 1194 Rhys May, Zhen Yang, Johan Schalkwyk, Christina Butterfield, Anja Hauth, Alex Goldin, Will
 1195 Hawkins, Evan Senter, Sergey Brin, Oliver Woodman, Marvin Ritter, Eric Noland, Minh Giang,
 1196 Vijay Bolina, Lisa Lee, Tim Blyth, Ian Mackinnon, Machel Reid, Obaid Sarvana, David Silver,
 1197 Alexander Chen, Lily Wang, Loren Maggiore, Oscar Chang, Nithya Attaluri, Gregory Thornton,
 1198 Chung-Cheng Chiu, Oskar Bunyan, Nir Levine, Timothy Chung, Evgenii Eltyshev, Xianc Si,
 1199 Timothy Lillicrap, Demetra Brady, Vaibhav Aggarwal, Boxi Wu, Yuanzhong Xu, Ross McIlroy,
 1200 Kartikeya Badola, Paramjit Sandhu, Erica Moreira, Wojciech Stokowiec, Ross Hemsley, Dong Li,
 1201 Alex Tudor, Pranav Shyam, Elahe Rahimtoroghi, Salem Haykal, Pablo Sprechmann, Xiang Zhou,
 1202 Diana Mincu, Yujia Li, Ravi Addanki, Kalpesh Krishna, Xiao Wu, Alexandre Frechette, Matan
 1203 Eyal, Allan Dafoe, Dave Lacey, Jay Whang, Thi Avrahami, Ye Zhang, Emanuel Taropa, Hanzhao
 1204 Lin, Daniel Toyama, Eliza Rutherford, Motoki Sano, HyunJeong Choe, Alex Tomala, Chalence
 1205 Safranek-Shrader, Nora Kassner, Mantas Pajarskas, Matt Harvey, Sean Sechrist, Meire Fortunato,
 1206 Christina Lyu, Gamaleldin Elsayed, Chenkai Kuang, James Lottes, Eric Chu, Chao Jia, Chih-Wei
 1207 Chen, Peter Humphreys, Kate Baumli, Connie Tao, Rajkumar Samuel, Cicero Nogueira dos
 1208 Santos, Anders Andreassen, Nemanja Rakićević, Dominik Grewe, Aviral Kumar, Stephanie
 1209 Winkler, Jonathan Caton, Andrew Brock, Sid Dalmia, Hannah Sheahan, Iain Barr, Yingjie Miao,
 1210 Paul Natsev, Jacob Devlin, Feryal Behbahani, Flavien Prost, Yanhua Sun, Artiom Myaskovsky,
 1211 Thanumalayan Sankaranarayana Pillai, Dan Hurt, Angeliki Lazaridou, Xi Xiong, Ce Zheng, Fabio
 1212 Pardo, Xiaowei Li, Dan Horgan, Joe Stanton, Moran Ambar, Fei Xia, Alejandro Lince, Mingqiu
 1213 Wang, Basil Mustafa, Albert Webson, Hyo Lee, Rohan Anil, Martin Wicke, Timothy Dozat,
 1214 Abhishek Sinha, Enrique Piqueras, Elahe Dabir, Shyam Upadhyay, Anudhyan Boral, Lisa Anne
 1215 Hendricks, Corey Fry, Josip Djolonga, Yi Su, Jake Walker, Jane Labanowski, Ronny Huang, Vedant
 1216 Misra, Jeremy Chen, R. J. Skerry-Ryan, Avi Singh, Shruti Rijhwani, Dian Yu, Alex Castro-Ros,
 1217 Beer Changpinyo, Romina Datta, Sumit Bagri, Arnar Mar Hrafnkelsson, Marcello Maggioni,
 1218 Daniel Zheng, Yury Sulsky, Shaobo Hou, Tom Le Paine, Antoine Yang, Jason Riesa, Dominika
 1219 Rogozinska, Dror Marcus, Dalia El Badawy, Qiao Zhang, Luyu Wang, Helen Miller, Jeremy
 1220 Greer, Lars Lowe Sjos, Azade Nova, Heiga Zen, Rahma Chaabouni, Mihaela Rosca, Jiepu Jiang,
 1221 Charlie Chen, Ruibo Liu, Tara Sainath, Maxim Krikun, Alex Polozov, Jean-Baptiste Lespiau,
 1222 Josh Newlan, Zeyncep Cankara, Soo Kwak, Yunhan Xu, Phil Chen, Andy Coenen, Clemens
 1223 Meyer, Katerina Tsihlas, Ada Ma, Juraj Gottweis, Jinwei Xing, Chenjie Gu, Jin Miao, Christian
 1224 Frank, Zeynep Cankara, Sanjay Ganapathy, Ishita Dasgupta, Steph Hughes-Fitt, Heng Chen,
 1225 David Reid, Keran Rong, Hongmin Fan, Joost van Amersfoort, Vincent Zhuang, Aaron Cohen,
 1226 Shixiang Shane Gu, Anhad Mohananey, Anastasija Ilic, Taylor Tobin, John Wieting, Anna Bortsova,
 1227 Phoebe Thacker, Emma Wang, Emily Caveness, Justin Chiu, Eren Sezener, Alex Kaskasoli,
 1228 Steven Baker, Katie Millican, Mohamed Elhawaty, Kostas Aisopos, Carl Lebsack, Nathan Byrd,
 1229 Hanjun Dai, Wenhao Jia, Matthew Wiethoff, Elnaz Davoodi, Albert Weston, Lakshman Yagati,
 1230 Arun Ahuja, Isabel Gao, Golan Pundak, Susan Zhang, Michael Azzam, Khe Chai Sim, Sergi
 1231 Caelles, James Keeling, Abhanshu Sharma, Andy Swing, YaGuang Li, Chenxi Liu, Carrie Grimes
 1232 Bostock, Yamini Bansal, Zachary Nado, Ankesh Anand, Josh Lipschultz, Abhijit Karmarkar,
 1233 Lev Proleev, Abe Ittycheriah, Soheil Hassas Yeganeh, George Polovets, Aleksandra Faust, Jiao
 1234 Sun, Alban Rrustemi, Pen Li, Rakesh Shivanna, Jeremiah Liu, Chris Welty, Federico Lebron,
 1235 Anirudh Baddepudi, Sebastian Krause, Emilio Parisotto, Radu Soricut, Zheng Xu, Dawn Bloxwich,
 1236 Melvin Johnson, Behnam Neyshabur, Justin Mao-Jones, Renshen Wang, Vinay Ramasesh, Zaheer
 1237 Abbas, Arthur Guez, Constant Segal, Duc Dung Nguyen, James Svensson, Le Hou, Sarah York,
 1238 Kieran Milan, Sophie Bridgers, Wiktor Gworek, Marco Tagliasacchi, James Lee-Thorp, Michael
 1239 Chang, Alexey Guseynov, Ale Jakse Hartman, Michael Kwong, Ruizhe Zhao, Sheleem Kashem,
 1240 Elizabeth Cole, Antoine Miech, Richard Tanburn, Mary Phuong, Filip Pavetic, Sebastien Cevey,
 1241 Ramona Comanescu, Richard Ives, Sherry Yang, Cosmo Du, Bo Li, Zizhao Zhang, Mariko Iinuma,
 Clara Huiyi Hu, Aurko Roy, Shaan Bijwadia, Zhenkai Zhu, Danilo Martins, Rachel Saputro, Anita
 Gergely, Steven Zheng, Dawei Jia, Ioannis Antonoglou, Adam Sadovsky, Shane Gu, Yingying
 Bi, Alek Andreev, Sina Samangooei, Mina Khan, Tomas Kociský, Angelos Filos, Chintu Kumar,
 Colton Bishop, Adams Yu, Sarah Hodkinson, Sid Mittal, Premal Shah, Alexandre Moufarek, Yong
 Cheng, Adam Bloniarz, Jaehoon Lee, Pedram Pejman, Paul Michel, Stephen Spencer, Vladimir

1242 Feinberg, Xuehan Xiong, Nikolay Savinov, Charlotte Smith, Siamak Shakeri, Dustin Tran, Mary
 1243 Chesus, Bernd Bohnet, George Tucker, Tamara von Glehn, Carrie Muir, Yiran Mao, Hideto Kazawa,
 1244 Ambrose Slone, Kedar Soparkar, Disha Shrivastava, James Cobon-Kerr, Michael Sharman, Jay
 1245 Pavagadhi, Carlos Araya, Karolis Misiunas, Nimesh Ghelani, Michael Laskin, David Barker,
 1246 Qiuji Li, Anton Briukhov, Neil Housby, Mia Glaese, Balaji Lakshminarayanan, Nathan Schucher,
 1247 Yunhao Tang, Eli Collins, Hyeontaek Lim, Fangxiaoyu Feng, Adria Recasens, Guangda Lai,
 1248 Alberto Magni, Nicola De Cao, Aditya Siddhant, Zoe Ashwood, Jordi Orbay, Mostafa Dehghani,
 1249 Jenny Brennan, Yifan He, Kelvin Xu, Yang Gao, Carl Saroufim, James Molloy, Xinyi Wu, Seb
 1250 Arnold, Solomon Chang, Julian Schrittwieser, Elena Buchatskaya, Soroush Radpour, Martin
 1251 Polacek, Skye Giordano, Ankur Bapna, Simon Tokumine, Vincent Hellendoorn, Thibault Sottiaux,
 1252 Sarah Cogan, Aliaksei Severyn, Mohammad Saleh, Shantanu Thakoor, Laurent Shefey, Siyuan
 1253 Qiao, Meenu Gaba, Shuo-yiin Chang, Craig Swanson, Biao Zhang, Benjamin Lee, Paul Kishan
 1254 Rubenstein, Gan Song, Tom Kwiatkowski, Anna Koop, Ajay Kannan, David Kao, Parker Schuh,
 1255 Axel Stjerngren, Golnaz Ghiasi, Gena Gibson, Luke Vilnis, Ye Yuan, Felipe Tiengo Ferreira,
 1256 Aishwarya Kamath, Ted Klimenko, Ken Franko, Kefan Xiao, Indro Bhattacharya, Miteyan Patel,
 1257 Rui Wang, Alex Morris, Robin Strudel, Vivek Sharma, Peter Choy, Sayed Hadi Hashemi, Jessica
 1258 Landon, Mara Finkelstein, Priya Jhakra, Justin Frye, Megan Barnes, Matthew Mauger, Dennis
 1259 Daun, Khuslen Baatarsukh, Matthew Tung, Wael Farhan, Henryk Michalewski, Fabio Viola, Felix
 1260 de Chaumont Quity, Charline Le Lan, Tom Hudson, Qingze Wang, Felix Fischer, Ivy Zheng,
 1261 Elspeth White, Anca Dragan, Jean-baptiste Alayrac, Eric Ni, Alexander Pritzel, Adam Iwanicki,
 1262 Michael Isard, Anna Bulanova, Lukas Zilka, Ethan Dyer, Devendra Sachan, Srivatsan Srinivasan,
 1263 Hannah Muckenheim, Honglong Cai, Amol Mandhane, Mukarram Tariq, Jack W. Rae, Gary Wang,
 1264 Kareem Ayoub, Nicholas FitzGerald, Yao Zhao, Woohyun Han, Chris Alberti, Dan Garrette,
 1265 Kashyap Krishnakumar, Mai Gimenez, Anselm Levskaya, Daniel Sohn, Josip Matak, Inaki Iturrate,
 1266 Michael B. Chang, Jackie Xiang, Yuan Cao, Nishant Ranka, Geoff Brown, Adrian Hutter, Vahab
 1267 Mirrokni, Nanxin Chen, Kaisheng Yao, Zoltan Egyed, Francois Galilee, Tyler Liechty, Praveen
 1268 Kallakuri, Evan Palmer, Sanjay Ghemawat, Jasmine Liu, David Tao, Chloe Thornton, Tim Green,
 1269 Mimi Jasarevic, Sharon Lin, Victor Cotruta, Yi-Xuan Tan, Noah Fiedel, Hongkun Yu, Ed Chi,
 1270 Alexander Neitz, Jens Heitkaemper, Anu Sinha, Denny Zhou, Yi Sun, Charbel Kaed, Brice Hulse,
 1271 Swaroop Mishra, Maria Georgaki, Sneha Kudugunta, Clement Farabet, Izhak Shafran, Daniel
 1272 Vlasic, Anton Tsitsulin, Rajagopal Ananthanarayanan, Alen Carin, Guolong Su, Pei Sun, Shashank
 1273 V, Gabriel Carvajal, Josef Broder, Iulia Comsa, Alena Repina, William Wong, Warren Weilun Chen,
 1274 Peter Hawkins, Egor Filonov, Lucia Loher, Christoph Hirnschall, Weiyi Wang, Jingchen Ye, Andrea
 1275 Burns, Hardie Cate, Diana Gage Wright, Federico Piccinini, Lei Zhang, Chu-Cheng Lin, Ionel
 1276 Gog, Yana Kulizhskaya, Ashwin Sreevatsa, Shuang Song, Luis C. Cobo, Anand Iyer, Chetan Tekur,
 1277 Guillermo Garrido, Zhuyun Xiao, Rupert Kemp, Huaixiu Steven Zheng, Hui Li, Ananth Agarwal,
 1278 Christel Ngani, Kati Goshvadi, Rebeca Santamaria-Fernandez, Wojciech Fica, Xinyun Chen,
 1279 Chris Gorgolewski, Sean Sun, Roopal Garg, Xinyu Ye, S. M. Ali Eslami, Nan Hua, Jon Simon,
 1280 Pratik Joshi, Yelin Kim, Ian Tenney, Sahitya Potluri, Lam Nguyen Thiet, Quan Yuan, Florian
 1281 Luisier, Alexandra Chronopoulou, Salvatore Scellato, Praveen Srinivasan, Minmin Chen, Vinod
 1282 Koverkathu, Valentin Dalibard, Yaming Xu, Brennan Saeta, Keith Anderson, Thibault Sellam,
 1283 Nick Fernando, Fantine Huot, Junehyuk Jung, Mani Varadarajan, Michael Quinn, Amit Raul,
 1284 Maigo Le, Ruslan Habalov, Jon Clark, Komal Jalan, Kalesha Bullard, Achintya Singhal, Thang
 1285 Luong, Boyu Wang, Sujeevan Rajayogam, Julian Eisenschlos, Johnson Jia, Daniel Finchelstein,
 1286 Alex Yakubovich, Daniel Balle, Michael Fink, Sameer Agarwal, Jing Li, Dj Dvijotham, Shalini
 1287 Pal, Kai Kang, Jaclyn Konzelmann, Jennifer Beattie, Olivier Dousse, Diane Wu, Remi Crocker,
 1288 Chen Elkind, Siddhartha Reddy Jonnalagadda, Jong Lee, Dan Holtmann-Rice, Krystal Kallarackal,
 1289 Rosanne Liu, Denis Vnukov, Neera Vats, Luca Invernizzi, Mohsen Jafari, Huanjie Zhou, Lilly
 1290 Taylor, Jennifer Prendki, Marcus Wu, Tom Eccles, Tianqi Liu, Kavya Kopparapu, Francoise
 1291 Beaufays, Christof Angermueller, Andreea Marzoca, Shourya Sarker, Hilal Dib, Jeff Stanway,
 1292 Frank Perbet, Nejc Trdin, Rachel Sterneck, Andrey Khorlin, Dinghua Li, Xihui Wu, Sonam Goenka,
 1293 David Madras, Sasha Goldshtain, Willi Gierke, Tong Zhou, Yaxin Liu, Yannie Liang, Anais White,
 1294 Yunjie Li, Shreya Singh, Sanaz Bahargam, Mark Epstein, Sujoy Basu, Li Lao, Adnan Ozturel, Carl
 1295 Crous, Alex Zhai, Han Lu, Zora Tung, Neeraj Gaur, Alanna Walton, Lucas Dixon, Ming Zhang,
 Amir Globerson, Grant Uy, Andrew Bolt, Olivia Wiles, Milad Nasr, Ilia Shumailov, Marco Selvi,
 Francesco Piccinno, Ricardo Aguilar, Sara McCarthy, Misha Khalman, Mrinal Shukla, Vlado Galic,
 John Carpenter, Kevin Villela, Haibin Zhang, Harry Richardson, James Martens, Matko Bosnjak,
 Shreyas Rammohan Belle, Jeff Seibert, Mahmoud Alnahlawi, Brian McWilliams, Sankalp Singh,
 Annie Louis, Wen Ding, Dan Popovici, Lenin Simicich, Laura Knight, Pulkit Mehta, Nishesh

1296 Gupta, Chongyang Shi, Saaber Fatehi, Jovana Mitrovic, Alex Grills, Joseph Pagadora, Tsendsuren
 1297 Munkhdalai, Dessie Petrova, Danielle Eisenbud, Zhishuai Zhang, Damion Yates, Bhavishya
 1298 Mittal, Nilesh Tripuraneni, Yannis Assael, Thomas Brovelli, Prateek Jain, Mihajlo Velimirovic,
 1299 Canfer Akbulut, Jiaqi Mu, Wolfgang Macherey, Ravin Kumar, Jun Xu, Haroon Qureshi, Gheorghe
 1300 Comanici, Jeremy Wiesner, Zhitao Gong, Anton Ruddock, Matthias Bauer, Nick Felt, Anirudh
 1301 GP, Anurag Arnab, Dustin Zelle, Jonas Rothfuss, Bill Rosgen, Ashish Shenoy, Bryan Seybold,
 1302 Xinjian Li, Jayaram Mudigonda, Goker Erdogan, Jiawei Xia, Jiri Simsa, Andrea Michi, Yi Yao,
 1303 Christopher Yew, Steven Kan, Isaac Caswell, Carey Radabaugh, Andre Elisseeff, Pedro Valenzuela,
 1304 Kay McKinney, Kim Paterson, Albert Cui, Eri Latorre-Chimoto, Solomon Kim, William Zeng, Ken
 1305 Durden, Priya Ponnappalli, Tiberiu Sosea, Christopher A. Choquette-Choo, James Manyika, Brona
 1306 Robenek, Harsha Vashisht, Sebastien Pereira, Hoi Lam, Marko Velic, Denese Owusu-Afriyie,
 1307 Katherine Lee, Tolga Bolukbasi, Alicia Parrish, Shawn Lu, Jane Park, Balaji Venkatraman, Alice
 1308 Talbert, Lambert Rosique, Yuchung Cheng, Andrei Sozanschi, Adam Paszke, Praveen Kumar,
 1309 Jessica Austin, Lu Li, Khalid Salama, Bartek Perz, Wooyeon Kim, Nandita Dukkipati, Anthony
 1310 Baryshnikov, Christos Kaplanis, XiangHai Sheng, Yuri Chervonyi, Caglar Unlu, Diego de Las
 1311 Casas, Harry Askham, Kathryn Tunyasuvunakool, Felix Gimeno, Siim Poder, Chester Kwak,
 1312 Matt Miecnikowski, Vahab Mirrokni, Alek Dimitriev, Aaron Parisi, Dangyi Liu, Tomy Tsai, Toby
 1313 Shevlane, Christina Kouridi, Drew Garmon, Adrian Goedeckemeyer, Adam R. Brown, Anitha
 1314 Vijayakumar, Ali Elqursh, Sadegh Jazayeri, Jin Huang, Sara Mc Carthy, Jay Hoover, Lucy Kim,
 1315 Sandeep Kumar, Wei Chen, Courtney Biles, Garrett Bingham, Evan Rosen, Lisa Wang, Qijun Tan,
 1316 David Engel, Francesco Pongetti, Dario de Cesare, Dongseong Hwang, Lily Yu, Jennifer Pullman,
 1317 Sriniv Narayanan, Kyle Levin, Siddharth Gopal, Megan Li, Asaf Aharoni, Trieu Trinh, Jessica Lo,
 1318 Norman Casagrande, Roopali Vij, Loic Matthey, Bramandia Ramadhana, Austin Matthews, C. J.
 1319 Carey, Matthew Johnson, Kremena Goranova, Rohin Shah, Shereen Ashraf, Kingshuk Dasgupta,
 1320 Rasmus Larsen, Yicheng Wang, Manish Reddy Vuyyuru, Chong Jiang, Joana Ijazi, Kazuki Osawa,
 1321 Celine Smith, Ramya Sree Boppana, Taylan Bilal, Yuma Koizumi, Ying Xu, Yasemin Altun, Nir
 1322 Shabat, Ben Bariach, Alex Korchemniy, Kiam Choo, Olaf Ronneberger, Chimezie Iwuanyanwu,
 1323 Shubin Zhao, David Soergel, Cho-Jui Hsieh, Irene Cai, Shariq Iqbal, Martin Sundermeyer, Zhe
 1324 Chen, Elie Bursztein, Chaitanya Malaviya, Fadi Biadsy, Prakash Shroff, Inderjit Dhillon, Tejas
 1325 Latkar, Chris Dyer, Hannah Forbes, Massimo Nicosia, Vitaly Nikolaev, Somer Greene, Marin
 1326 Georgiev, Pidong Wang, Nina Martin, Hanie Sedghi, John Zhang, Praseem Banzal, Doug Fritz,
 1327 Vikram Rao, Xuezhi Wang, Jiageng Zhang, Viorica Patraucean, Dayou Du, Igor Mordatch, Ivan
 1328 Jurin, Lewis Liu, Ayush Dubey, Abhi Mohan, Janek Nowakowski, Vlad-Doru Ion, Nan Wei, Reiko
 1329 Tojo, Maria Abi Raad, Drew A. Hudson, Vaishakh Keshava, Shubham Agrawal, Kevin Ramirez,
 1330 Zhichun Wu, Hoang Nguyen, Ji Liu, Madhavi Sewak, Bryce Petri, DongHyun Choi, Ivan Philips,
 1331 Ziyue Wang, Ioana Bica, Ankush Garg, Jarek Wilkiewicz, Priyanka Agrawal, Xiaowei Li, Danhao
 1332 Guo, Emily Xue, Naseer Shaik, Andrew Leach, Sadh MNM Khan, Julia Wiesinger, Sammy Jerome,
 1333 Abhishek Chakladar, Alek Wenjiao Wang, Tina Ornduff, Folake Abu, Alireza Ghaffarkhah, Marcus
 1334 Wainwright, Mario Cortes, Frederick Liu, Joshua Maynez, Andreas Terzis, Pouya Samangouei,
 1335 Riham Mansour, Tomasz Kępa, François-Xavier Aubet, Anton Algymr, Dan Banica, Agoston
 1336 Weisz, Andras Orban, Alexandre Senges, Ewa Andrejczuk, Mark Geller, Niccolo Dal Santo,
 1337 Valentin Anklin, Majd Al Merey, Martin Baeuml, Trevor Strohman, Junwen Bai, Slav Petrov,
 1338 Yonghui Wu, Demis Hassabis, Koray Kavukcuoglu, Jeff Dean, and Oriol Vinyals. Gemini 1.5:
 1339 Unlocking multimodal understanding across millions of tokens of context, December 2024. URL
 1340 <http://arxiv.org/abs/2403.05530>. arXiv:2403.05530 [cs].

1341 Perplexity Team. Meet new Sonar: A Blazing Fast Model Optimized for Perplexity Search, February
 1342 2025a. URL <https://www.perplexity.ai/hub>.

1343 Perplexity Team. RL Training For Math Reasoning, May 2025b. URL <https://www.perplexity.ai/hub>.

1344 Kexin Yi, Chuang Gan, Yunzhu Li, Pushmeet Kohli, Jiajun Wu, Antonio Torralba, and Joshua B.
 1345 Tenenbaum. CLEVRER: CoLlision Events for Video REpresentation and Reasoning, March 2020.
 1346 URL <http://arxiv.org/abs/1910.01442>. arXiv:1910.01442 [cs].

1347 Xinyu Zhang, Yuxuan Dong, Yanrui Wu, Jiaxing Huang, Chengyou Jia, Basura Fernando, Mike Zheng
 1348 Shou, Lingling Zhang, and Jun Liu. PhysReason: A Comprehensive Benchmark towards
 1349 Physics-Based Reasoning, February 2025. URL <http://arxiv.org/abs/2502.12054>.
 arXiv:2502.12054 [cs].

1350 Yiquan Zhang, Bo Peng, Xiaoyi Zhou, Cheng Xiang, and Dalei Wang. A deep Convolutional
1351 Neural Network for topology optimization with strong generalization ability, March 2020. URL
1352 <http://arxiv.org/abs/1901.07761>. arXiv:1901.07761 [cs].
1353
1354
1355
1356
1357
1358
1359
1360
1361
1362
1363
1364
1365
1366
1367
1368
1369
1370
1371
1372
1373
1374
1375
1376
1377
1378
1379
1380
1381
1382
1383
1384
1385
1386
1387
1388
1389
1390
1391
1392
1393
1394
1395
1396
1397
1398
1399
1400
1401
1402
1403

1404
1405

A APPENDIX

1406
1407

B TOPOLOGY OPTIMIZATION SOLVER PARAMETERS: GRASSHOPPER MILLIPEDE

1408
1409

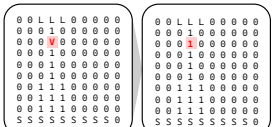
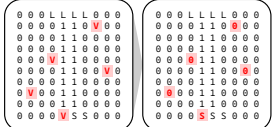
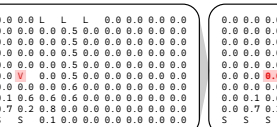
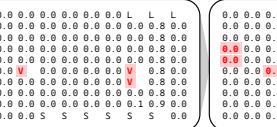
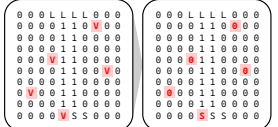
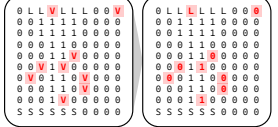
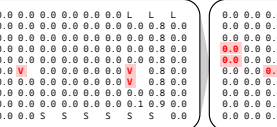
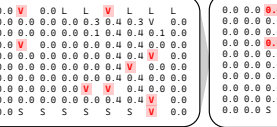
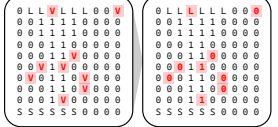
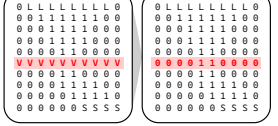
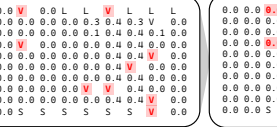
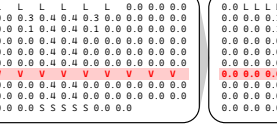
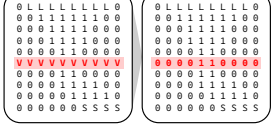
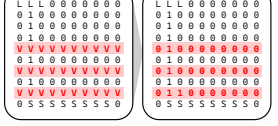
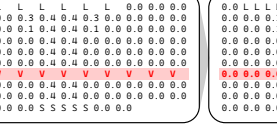
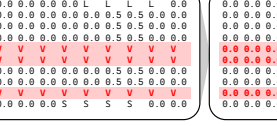
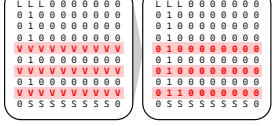
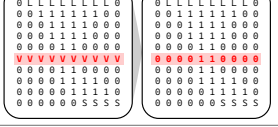
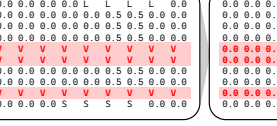
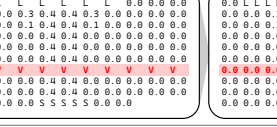
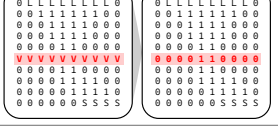
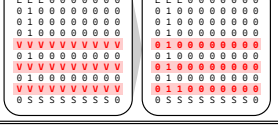
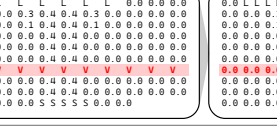
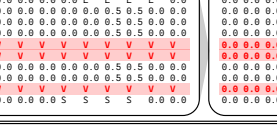
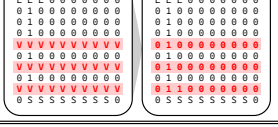
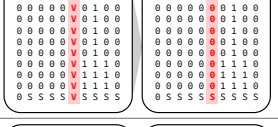
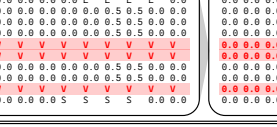
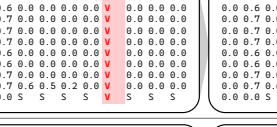
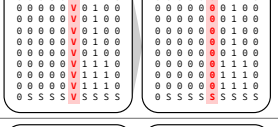
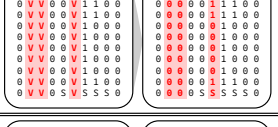
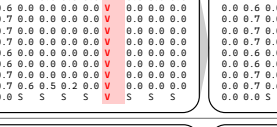
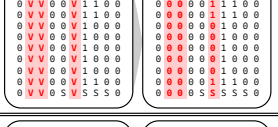
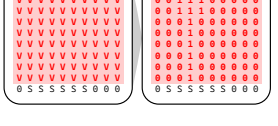
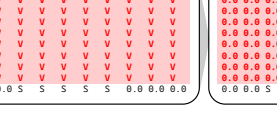
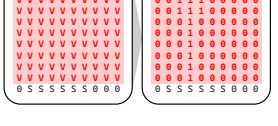
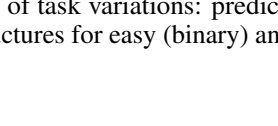
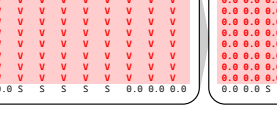
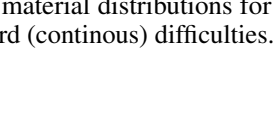
Solver parameters are:

1410
1411

target density = 0.1
self-weight = 0
iterations = 10
smoothing = 0.1
penalization = 3.0
minimum density = 0.001
delete threshold = 0.5
compliant mechanism disabled

1412
14131414
14151416
14171418
14191420
14211422
14231424
14251426
14271428
14291430
14311432
14331434
14351436
14371438
14391439
14401441
14421443
14441444
14451445
14461446
14471447
14481448
14491449
14501450
14511451
14521452
14531453
14541454
14551455
14561456
1457

1458 C VISUAL TASK VARIATIONS OVERVIEW
1459

	Difficulty: Easy Prompt {GRID}	Ground Truth	Difficulty: Hard Prompt {GRID}	Ground Truth
1 Random Cell				
5 Random Cell				
10 Random Cell				
1 Random Row				
3 Random Row				
1 Random Row				
3 Random Row				
1 Random Column				
3 Random Column				
Full				

1508 Figure 3: Overview of task variations: predicting material distributions for N random cells, rows,
1509 columns, or full structures for easy (binary) and hard (continuous) difficulties.
1510

1511

1512 **D ADDITIONAL EVALUATION METRICS COMPUTATION AND PROMPT AND
1513 COMPLETION EXAMPLES**
1514

1515 **D.1 FORCE-PATH COST COMPUTATION**
1516

1517 To approximate the physical efficiency of load transmission through the predicted topology, we define
1518 a gravity-aligned cost metric that measures the minimum traversal effort for any load cell to reach a
1519 support cell through contiguous solid material.

1520 Each grid cell g_{ij} can take values in $\{L, S\} \cup [0, 1]$, where L and S denote applied load and support,
1521 respectively, and real-valued entries represent material density. We assume a fixed gravity direction
1522 $\mathbf{g} = (d_r, d_c) \in \{(1, 0), (0, 1), (-1, 0), (0, -1)\}$.
1523

1524 **Directional neighborhood.** We consider all 8-connected neighbors of (i, j) ,

$$1525 \quad \mathcal{N}(i, j) = \{(i', j') \mid (i' - i, j' - j) \in \{(\pm 1, 0), (0, \pm 1), (\pm 1, \pm 1)\}\},$$

1527 with direction vector $\mathbf{d} = (i' - i, j' - j)$. Each neighbor is assigned a traversal cost $w_{\mathbf{d}}$ based on its
1528 angular deviation from gravity:

$$1529 \quad w_{\mathbf{d}} = \begin{cases} 1.0, & \angle(\mathbf{g}, \mathbf{d}) < 15^\circ, \\ 1.2, & 15^\circ \leq \angle < 45^\circ, \\ 1.5, & 45^\circ \leq \angle < 100^\circ, \\ 3.0, & \text{otherwise.} \end{cases}$$

1535 Upward (against-gravity) moves are disallowed whenever $\mathbf{d} \cdot \mathbf{g} < -0.5$, ensuring that load flow occurs
1536 only downward or laterally.
1537

1538 **Shortest-path computation.** For each load cell $\ell = (i_\ell, j_\ell)$, we compute the minimal cost to any
1539 support $s \in S$ using Dijkstra's algorithm over the graph of solid nodes $\{(i, j) \mid g_{ij} > 0\}$. The
1540 cumulative path cost is defined as

$$1542 \quad C(\ell) = \min_{p \in P_{\ell \rightarrow s}} \sum_{((i, j), (i', j')) \in p} w_{(i'-i), (j'-j)} (1 + 0.05 |i' - i_\ell|),$$

1544 where the multiplicative term $1 + 0.05 |i' - i_\ell|$ imposes a mild depth penalty to discourage long
1545 vertical travel from the load origin. If no valid support is reachable, a finite penalty C_{\max} is assigned.
1546

1547 The mean force-path cost for a grid G is

$$1548 \quad \bar{C}(G) = \frac{1}{N_L} \sum_{\ell \in L} C(\ell), \quad C(\ell) = C_{\max} \text{ if unsupported.}$$

1552 **Force-Path Cost Average Efficiency Ratio.** We define the final metric as

$$1553 \quad \text{FPCEff} = \text{clip}_{[0, 1]} \left(\frac{\bar{C}(G^*)}{\bar{C}(\hat{G})} \right),$$

1556 where G^* and \hat{G} denote the ground-truth and predicted grids, respectively. Higher values indicate
1557 that the predicted structure achieves comparable or better load-support transmission efficiency than
1558 the reference.
1559

1560
1561
1562
1563
1564
1565

1566 D.2 RECONSTRUCTION METRIC TESTS

1567

1568 D.2.1 EXACT MATCH EXAMPLES

1569

1570 **Exact Match Examples**1571 This test validates the `get_exact_match` function, which returns True
1572 if the predicted grid \hat{G} exactly matches the ground truth G^*
1573 cell-by-cell.1574 **1. Perfect match (True)**1575 Ground truth: [0 , **L** , 0],
1576 [0 , 1 , 0],
1577 [0 , **S** , 0]
1578 Prediction: [0 , **L** , 0],
1579 [0 , 1 , 0],
[0 , **S** , 0]

1580 Expected output: True

1581 **2. Slight difference (False)**1582 Ground truth: [0 , **L** , 0],
1583 [0 , 1 , 0],
[0 , **S** , 0]
1584 Prediction: [1 , **L** , 0],
1585 [1 , 1 , 0],
[0 , **S** , 0]

1586 Expected output: False

1587

1588 D.2.2 DIFFERENCE RATIO EXAMPLES

1589

1590 **Difference Ratio Examples**

1591

1592 This test validates `get_difference_ratio`, which measures similarity
1593 between \hat{G} and G^* .1594 A value of 1.0 means perfect reconstruction, while lower values
indicate greater deviation.1595 **1. Perfect match (1.000)**1596 Ground truth: [0 , **L** , 0],
1597 [0 , 1 , 0],
1598 [0 , **S** , 0]
1599 Prediction: [0 , **L** , 0],
1600 [0 , 1 , 0],
[0 , **S** , 0]

1601 Expected output: 1.000

1602 **2. One altered column (0.000)**1603 Ground truth: [0 , **L** , 0],
1604 [0 , 1 , 0],
1605 [0 , **S** , 0]
1606 Prediction: [1 , **L** , 0],
1607 [1 , 1 , 0],
[0 , **S** , 0]

1608 Expected output: 0.000

1609 **3. Half correct (0.500)**1610 Ground truth: [0 , **L** , 0],
1611 [1 , 1 , 0],
1612 [0 , **S** , 0]
1613 Prediction: [0 , **L** , 0],
1614 [0 , 1 , 0],
[0 , **S** , 0]

1615 Expected output: 0.500

1616

1617

1618

1619

1620 D.2.3 RELATIVE AND PENALIZED DIFFERENCE RATIO EXAMPLES
16211622 **Relative and Penalized Difference Ratio Examples**1623
1624 These tests validate `get_relative_difference_ratio` and
1625 `get_penalized_difference_ratio`, which account for numeric
1626 cell differences and penalize fixed-cell deviations respectively.1627 **1. Perfect alignment (1.000)**1628 Ground truth: [0 , **L** , 0],
1629 [0 , 1 , 0],
1630 [0 , **S** , 0]
1631 Prediction: [0 , **L** , 0],
1632 [0 , 1 , 0],
1633 [0 , **S** , 0]

1634 Expected output: 1.000

1635 **2. Gradual deviation (0.333)**1636 Ground truth: [0 , **L** , 0],
1637 [1 , 1 , **1**],
1638 [0 , **S** , 0]
1639 Prediction: [0 , **L** , 0],
1640 [0 , 1 , 0],
1641 [0 , **S** , 0]

1642 Expected output: 0.333

1643 **3. Continuous values (0.500)**1644 Ground truth: [0 , **L** , 0],
1645 [**0.8** , 1 , **0.8**],
1646 [0 , **S** , 0]
1647 Prediction: [0 , **L** , 0],
1648 [**0.4** , **0.5** , **0.4**],
1649 [0 , **S** , 0]

1650 Expected output: 0.500

1651 **4. Over-extrapolation (0.308)**1652 Ground truth: [0 , **L** , 0],
1653 [**0.8** , 1 , **0.8**],
1654 [0 , **S** , 0]
1655 Prediction: [0 , **L** , 0],
1656 [**0.4** , **2.0** , **0.4**],
1657 [0 , **S** , 0]

1658 Expected output: 0.308

1659 **5. Negative ratio (-1.000 or -2.000)**1660 Ground truth: [0 , **L** , 0],
1661 [0 , 1 , 0],
1662 [0 , **S** , 0]
1663 Prediction: [0 , 1 , 0],
1664 [**1** , **1** , **1**],
1665 [0 , **S** , 0]

1666 Expected output: -1.000 (unpenalized), -2.000 (penalized)

1667 **Interpretation:**1668 The ratios decrease as predictions deviate numerically from the ground
1669 truth,
1670 and penalized variants further reduce the score when fixed regions
1671 (load or support)
1672 are incorrectly modified. Scores near or below 0 reflect large or
1673 structurally
meaningful errors.1674
1675
1676
1677
1678
1679
1680
1681
1682
1683
1684
1685
1686
1687
1688
1689
1690
1691
1692
1693
1694
1695
1696
1697
1698
1699
1700
1701
1702
1703

1674 D.3 TOPOLOGY METRIC
 1675
 1676 D.3.1 GRID VALIDITY EXAMPLES
 1677
 1678 **Grid Validity Examples**

1679 This test validates the `get_grid_shape_and_value_validity` function,
 1680 which ensures that a generated grid has valid symbols and a consistent
 1681 rectangular shape.
 1682 A valid grid:
 1683 • Uses only the symbols {0, 1, L, S};
 1684 • Contains values within allowed numeric bounds;
 1685 • Has equal row lengths (rectangular shape).
 1686 **1. Valid grid**
 1687 Completion: [0 , **L** , 0],
 1688 [0 , 1 , 0],
 1689 [0 , **S** , 0]
 1690 Expected: True
 1691 (All symbols valid, shape consistent.)
 1692 **2. Invalid character (X)**
 1693 Completion: [0 , **X** , 0],
 1694 [0 , 1 , 0],
 1695 [0 , **S** , 0]
 1696 Expected: False
 1697 (Unrecognized symbol X.)
 1698 **3. Invalid character (P)**
 1699 Completion: [0 , **L** , 0],
 1700 [0 , 1 , 0],
 1701 [0 , **P** , 0]
 1702 Expected: False
 1703 (Unrecognized symbol P.)
 1704 **4. Out-of-range value (-1)**
 1705 Completion: [0 , **L** , 0],
 1706 [0 , -1 , 0],
 1707 [0 , **S** , 0]
 1708 Expected: False
 1709 (Negative numeric value not allowed.)
 1710 **5. Out-of-range value (2)**
 1711 Completion: [0 , **L** , 0],
 1712 [0 , 2 , 0],
 1713 [0 , **S** , 0]
 1714 Expected: False
 1715 (Value exceeds permitted range.)
 1716 **6. Non-rectangular grid**
 1717 Completion: [0 , **L** , 0],
 1718 [0 , 1],
 1719 [0 , **S** , 0]
 1720 Expected: False
 1721 (Inconsistent row lengths.)
 1722 **Interpretation:**
 1723 This check ensures that downstream metrics operate on well-formed
 1724 grids only.
 1725 Any invalid symbol, numeric range violation, or non-rectangular
 1726 structure
 1727 results in a False validity flag.

1728 D.3.2 LOAD-SUPPORT CONNECTIVITY EXAMPLES
17291730 **Load-Support Connectivity Examples**

1731 These tests validate `is_load_supported` and
1732 `is_load_supported_force_directional`, which determine whether
1733 loads (L) are connected to supports (S) through solid
1734 cells (1, L, S). The directional variant allows
1735 only gravity-aligned or lateral connections.

1736 **1. Perfect vertical connection**

1737 Completion: [0 , L , 0],
1738 [0 , 1 , 0],
1739 [0 , S , 0]

1739 Expected: True (both directional & non-directional)

1740 **2. Diagonal bridge**

1741 Completion: [0 , L , 0],
1742 [1 , 1 , 0],
1743 [0 , S , S]

1743 Expected: True (connected diagonally)

1744 **3. Horizontal load alignment**

1745 Completion: [0 , L , L],
1746 [0 , 1 , 0],
1747 [0 , S , 0]

1747 Expected: True (non-directional)

1748 **4. Incomplete bridge**

1749 Completion: [0 , L , L],
1750 [1 , 0 , 0],
1751 [0 , S , 0]

1752 Expected: True (non-directional), False (directional)

1753 **5. Disconnected load**

1754 Completion: [0 , 0 , L],
1755 [1 , 0 , 0],
1756 [0 , S , 0]

1756 Expected: False (no path)

1757 **6. Complex multi-load structure**

1758 Completion: [1 , 1 , 1 , 0 , 1 , L],
1759 [1 , 0 , 1 , 0 , 1 , 0],
1760 [1 , 0 , 1 , 1 , 1 , 0],
1761 [1 , 0 , 0 , 0 , 0 , 0],
1762 [S , 0 , 0 , 0 , 0 , 0]

1762 Expected: True (non-directional), False (directional)

1763 **Interpretation:**

1764 The directional test approximates gravity-aligned force flow, while
1765 the
1766 non-directional variant checks only geometric reachability.
1766 Disconnected or upward-only paths yield False.

1767
1768
1769
1770
1771
1772
1773
1774
1775
1776
1777
1778
1779
1780
1781

1782 D.3.3 ISOLATED CLUSTER COUNT EXAMPLES
17831784 **Isolated Cluster Count Examples**1785 This test validates `get_isolated_clusters_count`, which counts
1786 solid regions (1) disconnected from any load (L) or
1787 support (S). A higher count indicates fragmented or non-functional
1788 material regions.1789 **1. Single isolated column (1)**1790 Completion: [L , 0 , 0 , 0 , 0 , 0 , 0],
1791 [1 , 0 , 0 , 0 , 0 , 0 , 0],
1792 [1 , 0 , 1 , 0 , 0 , 0 , 0],
1793 [1 , 0 , 0 , 0 , 0 , 0 , 0],
1794 [1 , 0 , 0 , 0 , 0 , 0 , 0],
1795 [S , 0 , 0 , 0 , 0 , 0 , 0]

1796 Expected: 1

1797 **2. Slightly connected cluster (1)**1798 Completion: [L , 0 , 0 , 0 , 0 , 0 , 0],
1799 [1 , 0 , 0 , 0 , 0 , 0 , 0],
1800 [1 , 0 , 1 , 1 , 0 , 0 , 0],
1801 [1 , 0 , 0 , 1 , 0 , 0 , 0],
1802 [1 , 0 , 0 , 0 , 0 , 0 , 0],
1803 [S , 0 , 0 , 0 , 0 , 0 , 0]

1804 Expected: 1

1805 **3. Two isolated clusters (2)**1806 Completion: [L , 0 , 0 , 0 , 0 , 1 , 0],
1807 [1 , 0 , 0 , 0 , 0 , 0 , 1],
1808 [1 , 0 , 1 , 1 , 0 , 0 , 1],
1809 [1 , 0 , 0 , 1 , 0 , 0 , 0],
1810 [1 , 0 , 0 , 0 , 0 , 0 , 0],
1811 [S , 0 , 0 , 0 , 0 , 0 , 0]

1812 Expected: 2

1813 **4. Multiple detached clusters (3)**1814 Completion: [L , 0 , 0 , 1 , 0 , 0 , 0],
1815 [1 , 0 , 0 , 0 , 0 , 0 , 0],
1816 [1 , 0 , 1 , 1 , 0 , 0 , 0],
1817 [1 , 0 , 0 , 1 , 0 , 0 , 1],
1818 [1 , 0 , 0 , 0 , 0 , 0 , 0],
1819 [S , 0 , 0 , 0 , 0 , 0 , 0]

1820 Expected: 3

1821 **Interpretation:**1822 Isolated clusters represent solid “islands” that do not participate in
1823 load-support transfer. Lower counts indicate more integrated and
1824 structurally valid predictions.

1825

1826

1827

1828

1829

1830

1831

1832

1833

1834

1835

1836 D.3.4 DIFFICULTY SCORE (DWCS) EXAMPLES
18371838 **Difficulty Score (DWCS) Examples**
18391840 This test validates `get_difficulty_score`, which computes the
1841 average difficulty of masked (V) cells in the *input grid*
1842 based on their ground-truth neighborhood configuration in the *GT grid*.
1843 The *completion grid* is used to confirm the reconstruction context.
1844 Higher scores correspond to more complex masked regions.1844 **1. Simple vertical case (2.0)**1845 *Input:* [0 , L , 0],
1846 [0 , V , 0],
1847 [0 , S , 0]
1848 *Ground truth:* [0 , L , 0],
1849 [0 , 1 , 0],
1850 [0 , S , 0]
1851 *Completion:* [0 , L , 0],
1852 [0 , 1 , 0],
[0 , S , 0]

1852 Expected output: 2.000

1853 **2. Mixed neighborhood (3.0)**1854 *Input:* [0 , L , 0],
1855 [V , 1 , 0],
1856 [0 , S , 0]
1857 *Ground truth:* [0 , L , 0],
1858 [0 , 1 , 0],
1859 [0 , S , 0]
1860 *Completion:* [0 , L , 0],
1861 [1 , 1 , 0],
[0 , S , 0]

1862 Expected output: 3.000

1863 **3. Large structure (1.0)**1864 *Input:* [0 , L , 0],
1865 [0 , 1 , 0],
1866 [0 , 1 , V],
1867 [0 , 1 , 0],
1868 [0 , S , 0]
1869 *Ground truth:* [0 , L , 0],
1870 [0 , 1 , 0],
1871 [0 , 1 , 0],
1872 [0 , 1 , 0],
1873 [0 , 1 , 0],
1874 [0 , 1 , 0],
1875 [0 , S , 0]

1876 Expected output: 1.000

1877 **4. Dense structure with boundary void (3.0)**1878 *Input:* [0 , L , L , L , 0],
1879 [0 , 1 , 1 , 1 , 0],
1880 [0 , 1 , V , 1 , 0],
1881 [0 , 1 , 1 , 1 , 0],
[0 , S , S , S , 0]
1882 *Ground truth:* [0 , L , L , L , 0],
1883 [0 , 1 , 1 , 0 , 0],
1884 [0 , 1 , 0 , 1 , 0],
1885 [0 , 1 , 1 , 0 , 0],
[0 , S , S , S , 0]
1886 *Completion:* [0 , L , L , L , 0],
1887 [0 , 1 , 1 , 0 , 0],
1888 [0 , 1 , 0 , 1 , 0],
1889 [0 , S , S , S , 0]

1890

Expected output: 3.000

Interpretation:

The score increases when masked cells (V) occur in ambiguous or mixed regions, particularly around structural boundaries. Uniform neighborhoods yield lower scores, reflecting easier reconstruction.

1896

1897

1898

1899

1900

1901

1902

1903

1904

1905

1906

1907

1908

1909

1910

1911

1912

1913

1914

1915

1916

1917

1918

1919

1920

1921

1922

1923

1924

1925

1926

1927

1928

1929

1930

1931

1932

1933

1934

1935

1936

1937

1938

1939

1940

1941

1942

1943

1944 D.4 PHYSICS APPROXIMATION METRIC

1945

1946 D.4.1 FORCE PATH COST EXAMPLES

1947

1948 **Force Path Cost Examples**

1949 This test validates the
 1950 `get_total_force_path_cost_average_efficiency_ratio` function, which
 1951 computes the Force Path Cost Average Efficiency Ratio (FPCEff).
 1952 Higher ratios indicate more efficient and physically plausible
 1953 load-support paths aligned with gravity.
 1954 Gravity direction: (1, 0) downward
 1955 Test cases:
 1956 **1. Perfect vertical alignment**
 1957 Ground truth: [0 , **L** , 0],
 [0 , 1 , 0],
 [0 , **S** , 0]
 1958 Prediction: [0 , **L** , 0],
 [0 , 1 , 0],
 [0 , **S** , 0]
 1959 Expected output: 1.000
 1960 **2. Slightly wider vertical column (still efficient)**
 1961 Ground truth: [0 , **L** , 0],
 [0 , 1 , 0],
 [0 , **S** , 0]
 1962 Prediction: [0 , **L** , 0],
 [1 , 1 , 0],
 [0 , **S** , 0]
 1963 Expected output: 1.000
 1964 **3. Offset load-support connection (less efficient)**
 1965 Ground truth: [0 , **L** , 0],
 [0 , 1 , 0],
 [**S** , 0 , 0]
 1966 Prediction: [0 , **L** , 0],
 [1 , 1 , 0],
 [**S** , 0 , 0]
 1967 Expected output: 0.8037
 1968 **4. Broken vertical link (similar inefficiency)**
 1969 Ground truth: [0 , **L** , 0],
 [0 , 1 , 0],
 [**S** , 0 , 0]
 1970 Prediction: [0 , **L** , 0],
 [1 , 0 , 0],
 [**S** , 0 , 0]
 1971 Expected output: 0.8037
 1972 **5. Horizontally displaced load (least efficient)**
 1973 Ground truth: [0 , 0 , **L**],
 [0 , 1 , 0],
 [**S** , 0 , 0]
 1974 Prediction: [0 , 1 , **L**],
 [1 , 0 , 0],
 [**S** , 0 , 0]
 1975 Expected output: 0.7724
 1976 Interpretation:
 1977 As load-support paths deviate from the gravity direction or become
 1978 discontinuous,
 1979 FPCEff decreases from 1.0 toward 0, reflecting reduced
 1980 physical plausibility of the structure.

1993

1994

1995

1996

1997

1998
1999
2000
2001
2002

E TOPOLOGY OPTIMIZATION SAMPLE PLOTS

2003
2004
2005
2006
2007

E.1 2D SAMPLES

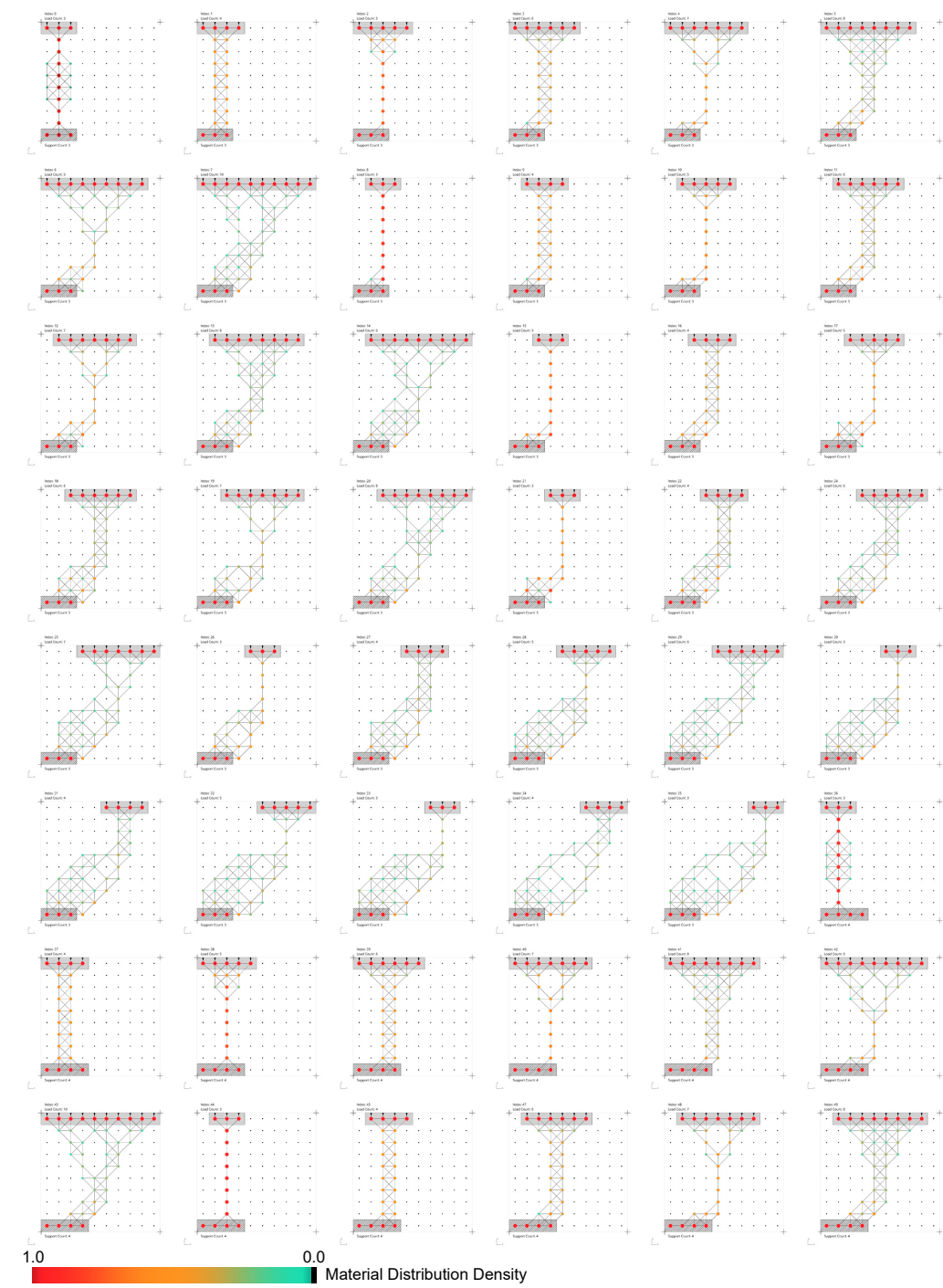
2008
2009
2010
2011
20122047
2048
2049
2050
2051

Figure 4: Example 2D topology optimization samples from the SPhyR dataset.

2052
2053

E.2 3D SAMPLES

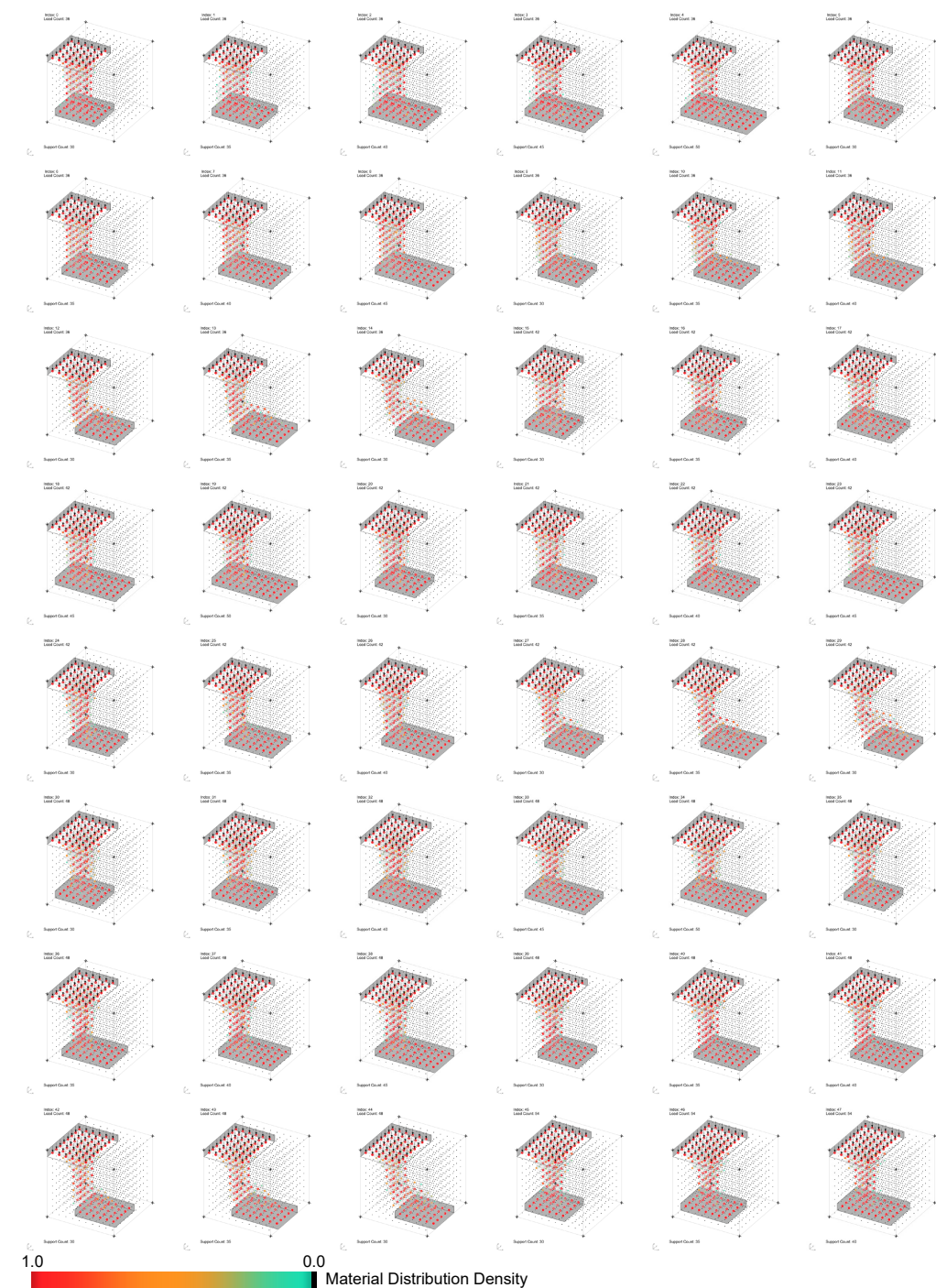
2054
2055
2056
2057
2058
2059
2060
2061
2062
2063
2064
2065
2066
2067
2068
2069
2070
2071
2072
2073
2074
2075
2076
2077
2078
2079
2080
2081
2082
2083
2084
2085
2086
2087
2088
2089
2090
2091
2092
2093
2094
2095
2096
20972099
2100
2101
2102
2103
2104
2105

Figure 5: Example 3D topology optimization samples included for future benchmark extensions.

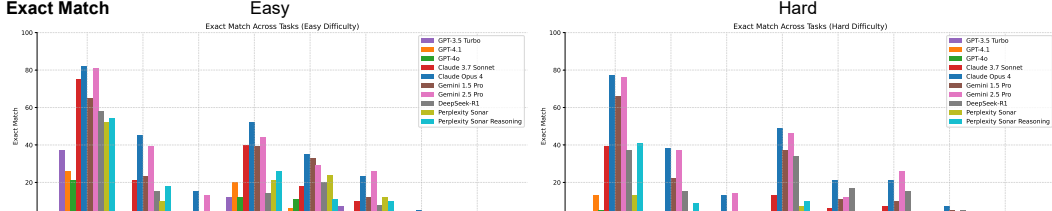
2106 F ADDITIONAL MAIN RUN RESULTS

2108 F.1 RESULTS FOR ALL MODELS AND TASKS

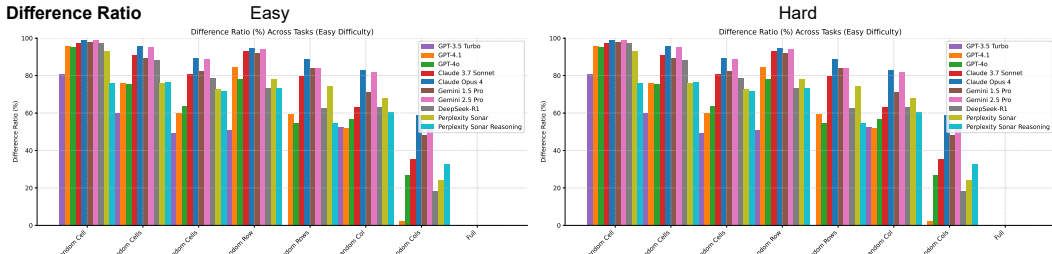
2110 Main Evaluation Results

2111 Reconstruction Accuracy Metrics 1/2

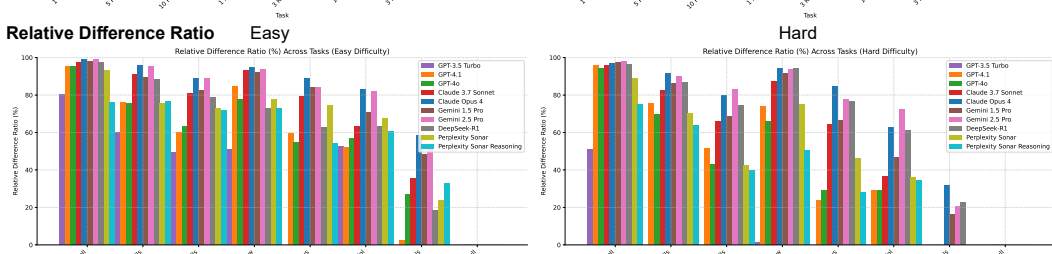
2113 Exact Match



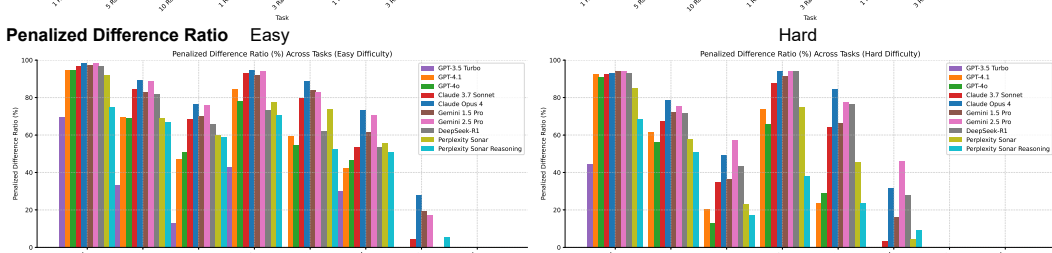
2121 Difference Ratio



2130 Relative Difference Ratio

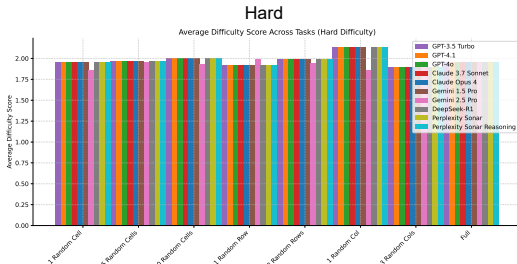
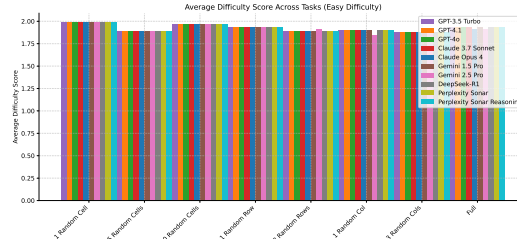
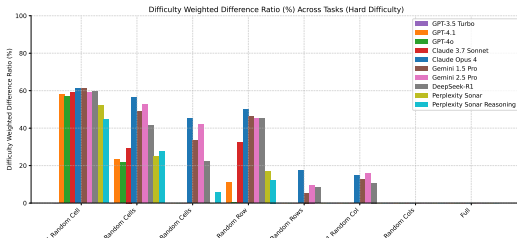
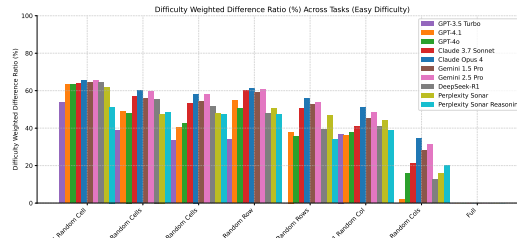
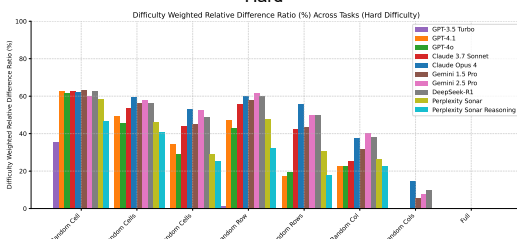
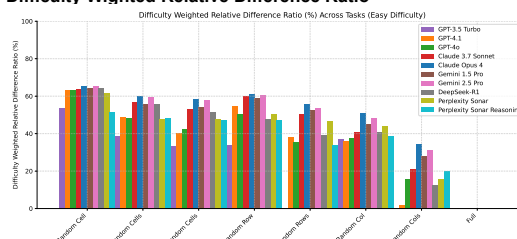
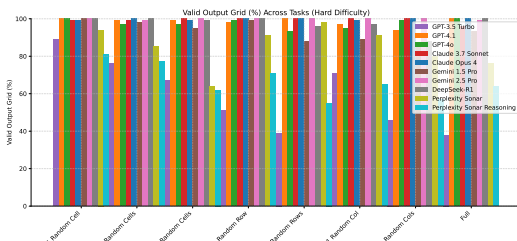
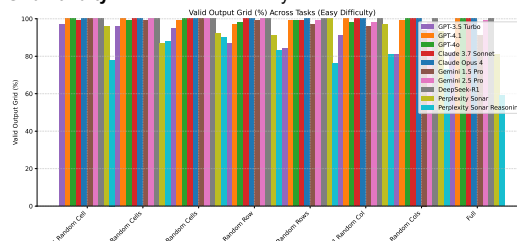


2139 Penalized Difference Ratio

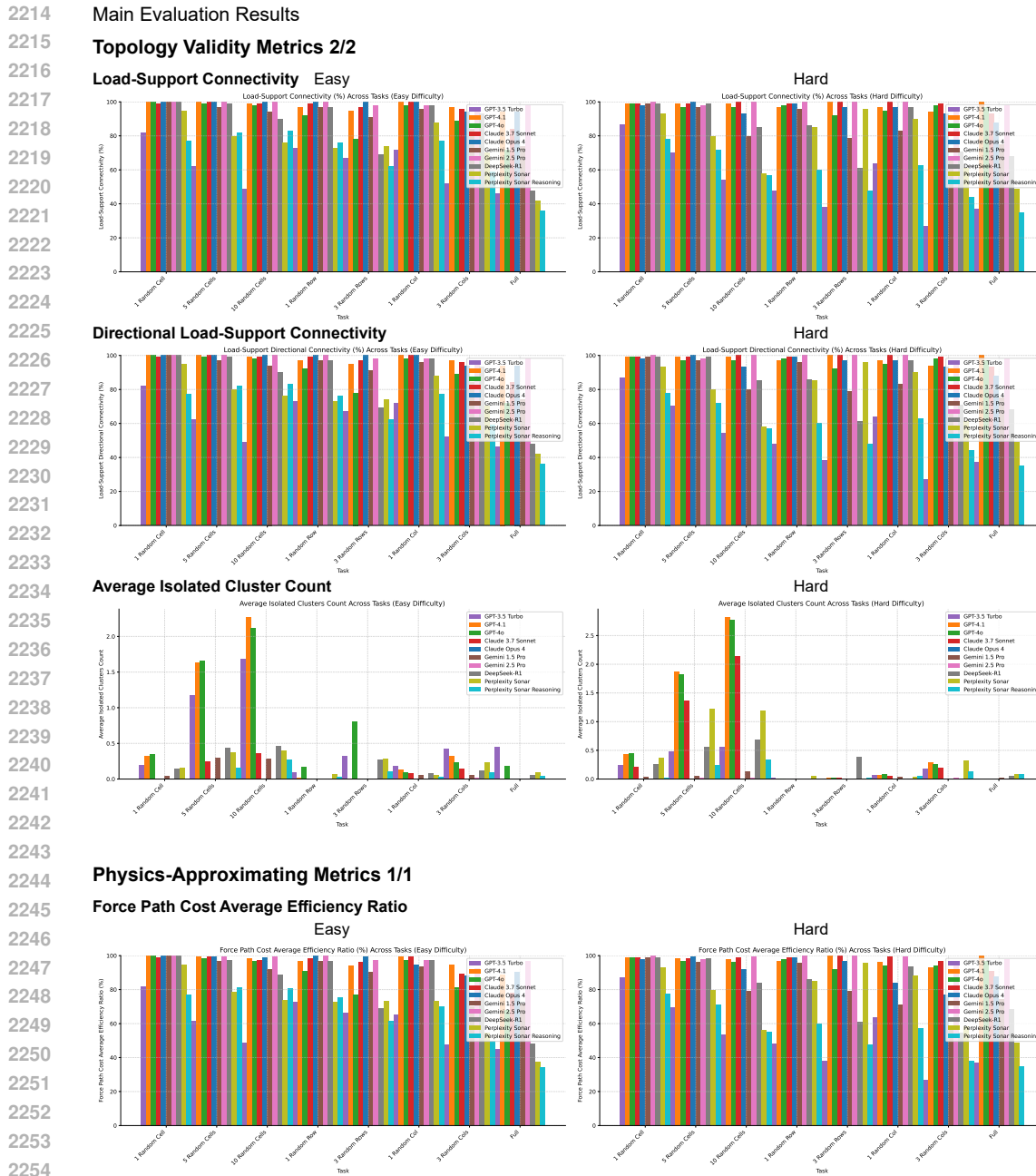


2153 Figure 6: Main evaluation run results: Exact Match, Difference Ratio, Relative Difference Ratio and
2154 Penalized Difference Ratio for all models, across all tasks and difficulties.

2160 Main Evaluation Results

2161 **Reconstruction Accuracy Metrics 2/2**2162 **Average Difficulty Score**2163 **Difficulty Weighted Difference Ratio**2164 **Difficulty Weighted Relative Difference Ratio**2165 **Topology Validity Metrics 1/2**2166 **Grid Validity**

2167 **Figure 7: Main evaluation run results: Average Difficulty Score, Difficulty Weighted Difference Ratio, Difficulty Weighted Relative Difference Ratio and Grid Validity for all models, across all tasks and difficulties.**



2226 **Figure 8: Main evaluation run results: Load-Support Connectivity, Directional Load-Support Connectivity, Average Isolated Cluster Count and Force Path Cost Average Efficiency Ratio for all models, across all tasks and difficulties.**

2268
2269

G ADDITIONAL ROTATION EXPERIMENT RESULTS

2270
2271

G.1 PROMPT AND COMPLETION - 1 RANDOM CELL EASY: ROTATED X 3

2272
2273

Prompt and Completion - 1 Random Cell Easy: Rotated x 3

2274

Prompt:

You are given a structural material distribution represented as a grid. Each cell can

2275

have one of the following states:

2276

- 'L' indicates applied load.

2277

- 'V' indicates void.

2278

- 'S' indicates support.

2279
2280

The goal is to predict the correct material distribution by filling in all 'V' cells with either '1' (solid) or '0' (empty), based on the surrounding structure and implicit physical reasoning (such as load paths, supports, and forces).

2281
2282

Important: The completed structure should use as little material as possible while remaining stable and plausible for carrying the applied forces. Minimize material usage unless necessary for structural support.

2283
2284

Below is the input grid with masked regions:

2285

```
0 0 0 0 0 0 0 0 0 0  
0 0 0 0 0 0 0 0 0 S  
0 0 0 0 0 0 0 0 0 S  
0 0 0 0 0 0 0 0 0 S  
0 0 0 0 0 0 0 0 0 S  
L 0 0 0 0 0 1 1 1 S  
L 1 V 1 1 1 1 1 1 S  
L 0 0 0 0 0 1 1 1 S  
0 0 0 0 0 0 0 0 0 S  
0 0 0 0 0 0 0 0 0 S
```

2292
2293

Please output the completed grid by replacing all 'V' cells with either '1' (solid) or '0' (empty).

2294
2295

Maintain the same format as the input: one row per line, cells separated by spaces, and the total number of rows and columns unchanged.

Return only the completed grid without any additional explanation.

2296

Model Completion (differences in red):

2297

```
0 0 0 0 0 0 0 0 0 0  
0 0 0 0 0 0 0 0 0 S  
0 0 0 0 0 0 0 0 0 S  
0 0 0 0 0 0 0 0 0 S  
0 0 0 0 0 0 0 0 0 S  
L 0 0 0 0 0 1 1 1 S  
L 1 1 1 1 1 1 1 1 S  
L 0 0 0 0 0 1 1 1 S  
0 0 0 0 0 0 0 0 0 S  
0 0 0 0 0 0 0 0 0 S
```

2304

Ground Truth:

2305

```
0 0 0 0 0 0 0 0 0 0  
0 0 0 0 0 0 0 0 0 S  
0 0 0 0 0 0 0 0 0 S  
0 0 0 0 0 0 0 0 0 S  
0 0 0 0 0 0 0 0 0 S  
L 0 0 0 0 0 1 1 1 S  
L 1 1 1 1 1 1 1 1 S  
L 0 0 0 0 0 1 1 1 S  
0 0 0 0 0 0 0 0 0 S  
0 0 0 0 0 0 0 0 0 S
```

2312

2313

2314

2315

2316

2317

2318

2319

2320

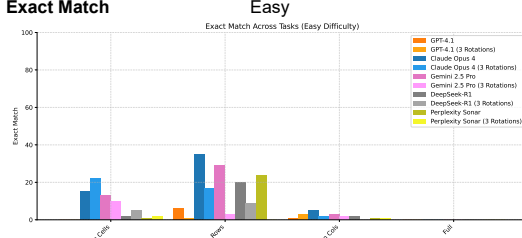
2321

2322 G.2 RESULTS FOR MODEL SUB-SET AND TASK SUB-SET

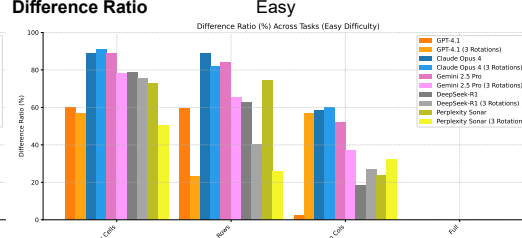
2324 Grid Rotation on All Models and Selected Tasks Evaluation Results: Easy

2325 Reconstruction Accuracy Metrics 1/1

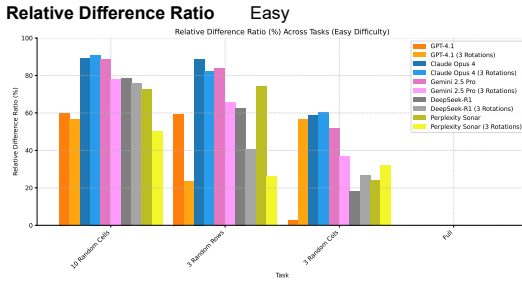
2326 Exact Match



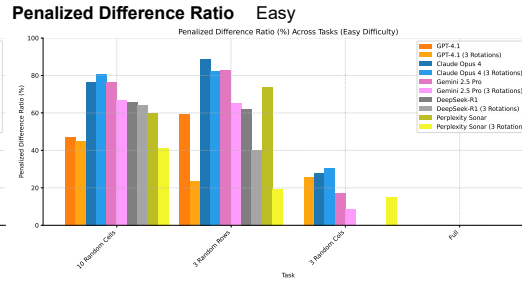
2328 Difference Ratio



2330 Relative Difference Ratio

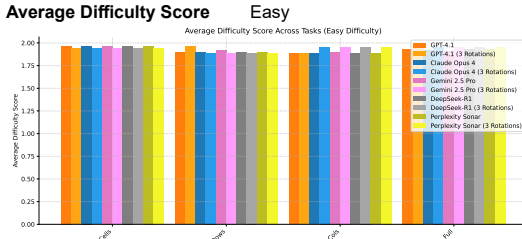


2332 Penalized Difference Ratio

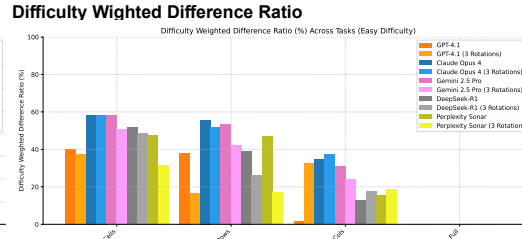


2334 Reconstruction Accuracy Metrics 1/2

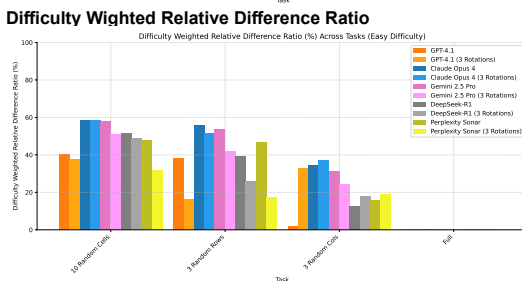
2335 Average Difficulty Score



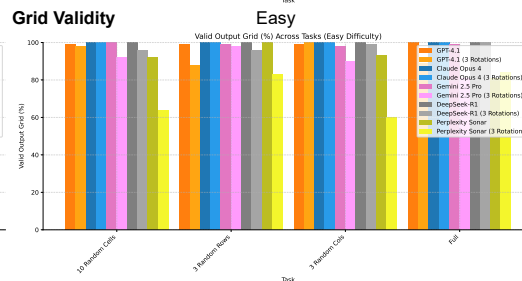
2337 Difficulty Weighted Difference Ratio



2339 Difficulty Weighted Relative Difference Ratio

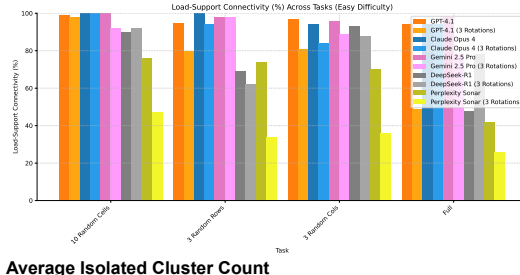
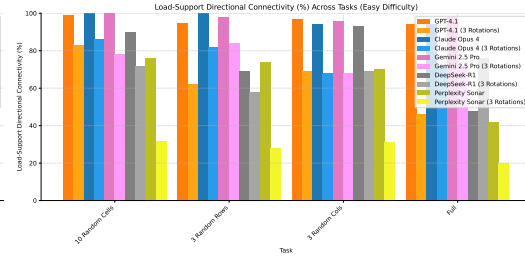
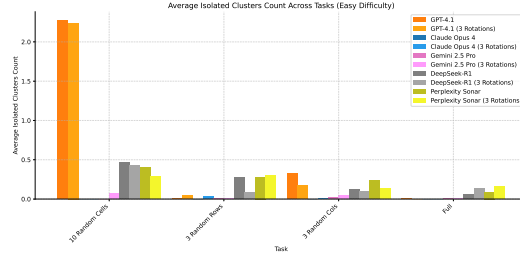
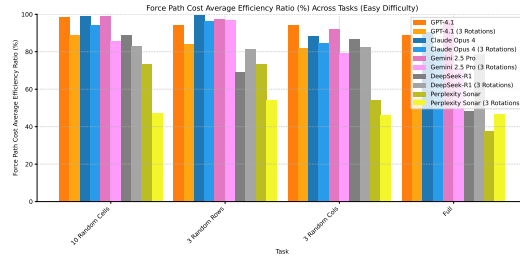


2341 Grid Validity



2343 Figure 9: Grid rotation evaluation results: Exact Match, Difference Ratio, Relative Difference Ratio, Penalized Difference Ratio, Average Difficulty Score, Difficulty Weighted Difference Ratio, Difficulty Weighted Relative Difference Ratio and Grid Validity for GPT-4.1, Claude Opus 4, Gemini 2.5 Pro, DeepSeek-R1 and Perplexity, for 10 Random Cells, 3 Random Rows, 3 Random Cells and Full tasks and easy difficulty.

2376 Grid Rotation on All Models and Selected Tasks Evaluation Results: Easy

2377 **Topology Validity Metrics 2/2**2378 **Load-Support Connectivity** Easy2379 **Directional Load-Support Connectivity**2380 **Average Isolated Cluster Count**2381 **Physics-Approximating Metrics 1/1**2382 **Force Path Cost Average Efficiency Ratio**

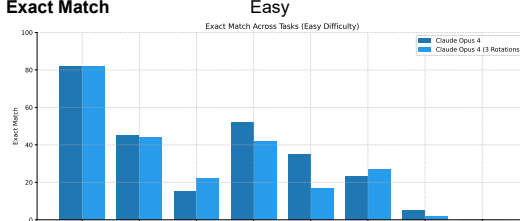
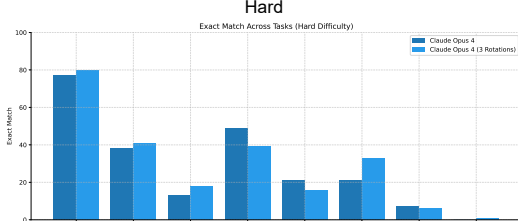
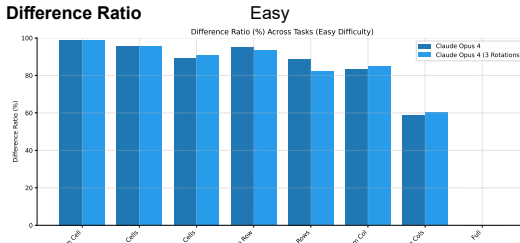
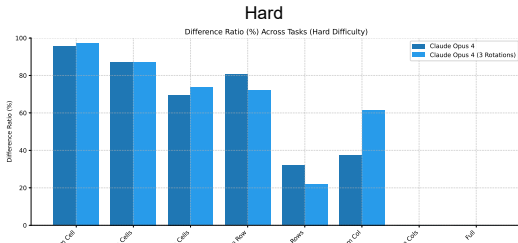
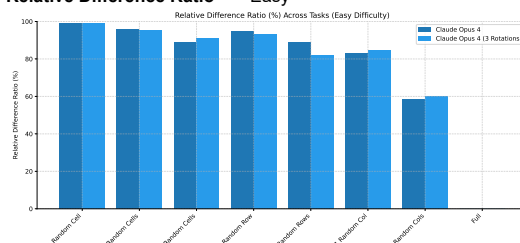
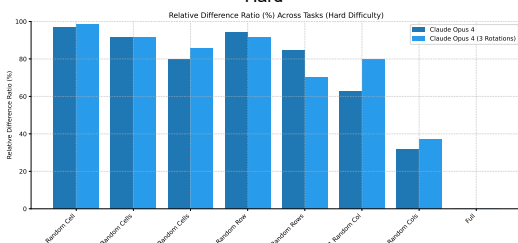
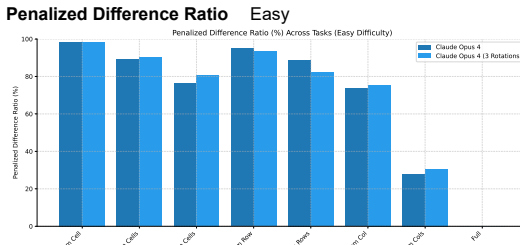
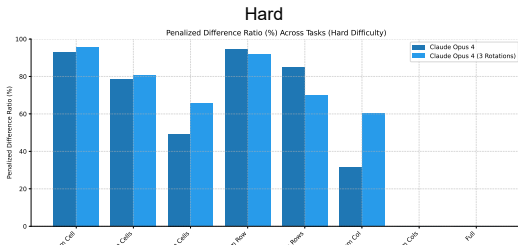
2383 Figure 10: Grid rotation evaluation results: Load-Support Connectivity, Directional Load-Support Connectivity, Average Isolated Cluster Count and Force Path Cost Average Efficiency Ratio for GPT-4.1, Claude Opus 4, Gemini 2.5 Pro, DeepSeek-R1 and Perplexity, for 10 Random Cells, 3 Random Rows, 3 Random Cells and Full tasks and easy difficulty.

2430

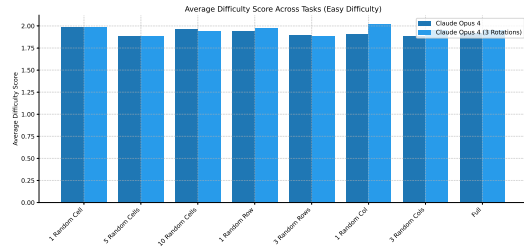
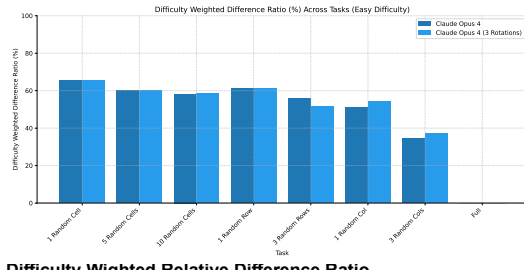
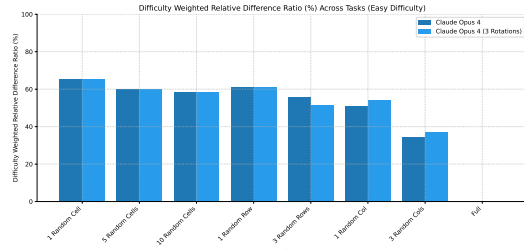
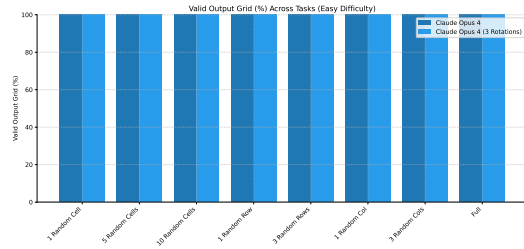
2431 Table 4: Grid rotation evaluation results for all metrics, for GPT-4.1, Claude Opus 4, Gemini 2.5 Pro,
2432 DeepSeek-R1 and Perplexity, for 10 Random Cells, 3 Random Rows, 3 Random Cells and Full tasks
2433 and easy difficulty.

Tech	Metric	GPT-4.1	GPT-4.1 (3 Rotations)	Claude Opus 4	Claude Opus 4 (3 Rotations)	Gemini 2.5 Pro	Gemini 2.5 Pro (3 Rotations)	DeepSeek-R1	DeepSeek-R1 (3 Rotations)	Perplexity Sonar	Perplexity Sonar (3 Rotations)
Difficulty: Easy											
10 Random Cells	Exact Match \downarrow	0	0	15	22	13	10	2	5	1	2
	Difference Ratio (%) \uparrow	59.82	56.85	89.08	91.02	88.88	78.26	78.78	75.62	72.68	50.19
	Relative Difference Ratio (%) \uparrow	59.82	56.85	89.08	91.02	88.88	78.26	78.78	75.62	72.68	50.19
	Penalized Difference Ratio (%) \uparrow	47.03	44.09	88.79	76.21	88.98	84.27	84.27	84.27	59.45	41.15
	Average Difficulty Score	1.97	1.94	1.94	1.97	1.94	1.94	1.97	1.94	1.97	1.94
	Average Weighted Difference Ratio (%) \uparrow	40.24	37.62	58.23	58.52	58.06	50.94	51.72	48.69	47.81	31.74
	Difficulty Weighted Relative Difference Ratio (%) \uparrow	37.93	37.62	58.23	58.52	58.06	50.94	51.72	48.69	47.81	31.74
	Valid Output Grid \uparrow	99.00	98.00	100.00	100.00	99.00	92.00	100.00	96.00	92.00	64.00
	Load-Support Connectivity (%) \uparrow	99.00	98.00	100.00	100.00	99.00	92.00	100.00	96.00	92.00	64.00
	Load-Support Directional Connectivity (%) \uparrow	99.00	98.00	100.00	100.00	99.00	92.00	100.00	96.00	92.00	64.00
	Average Isolated Clusters Count \downarrow	2.27	2.24	0.00	0.00	0.00	0.00	0.46	0.43	0.40	0.29
	Force Path Cost Average Efficiency Ratio (%) \uparrow	98.28	88.93	99.06	94.41	99.31	88.72	82.77	73.62	27.18	
3 Random Rows	Exact Match \downarrow	6	1	17	29	3	2	3	24	0	
	Difference Ratio (%) \uparrow	59.31	23.28	88.64	82.19	84.09	65.52	62.64	40.38	74.23	26.11
	Relative Difference Ratio (%) \uparrow	59.31	23.28	88.64	82.19	84.09	65.52	62.64	40.38	74.23	26.11
	Penalized Difference Ratio (%) \uparrow	59.31	23.28	88.64	82.19	82.84	65.08	62.04	40.21	73.99	19.33
	Average Difficulty Score	1.89	1.96	1.89	1.94	1.89	1.89	1.89	1.89	1.89	1.89
	Average Weighted Difference Ratio (%) \uparrow	37.91	16.47	55.81	51.60	53.52	42.02	39.27	36.05	46.97	17.17
	Difficulty Weighted Relative Difference Ratio (%) \uparrow	37.91	16.47	55.81	51.60	53.52	42.02	39.27	36.05	46.97	17.17
	Valid Output Grid \uparrow	99.00	88.00	100.00	100.00	99.00	98.00	100.00	96.00	100.00	83.00
	Load-Support Connectivity (%) \uparrow	99.00	88.00	100.00	100.00	99.00	98.00	100.00	96.00	100.00	83.00
	Load-Support Directional Connectivity (%) \uparrow	99.00	88.00	100.00	100.00	99.00	98.00	100.00	96.00	100.00	83.00
	Average Isolated Clusters Count \downarrow	2.27	2.24	0.00	0.00	0.00	0.00	0.46	0.43	0.40	0.29
	Force Path Cost Average Efficiency Ratio (%) \uparrow	94.09	83.83	93.68	90.30	97.54	86.68	82.32	41.37	73.47	14.16
3 Random Columns	Exact Match \downarrow	1	3	5	2	2	1	1	1	1	
	Difference Ratio (%) \uparrow	2.46	56.64	68.16	52.03	37.06	33.34	26.74	24.01	22.05	
	Relative Difference Ratio (%) \uparrow	2.46	56.64	68.16	52.03	37.06	33.34	26.74	24.01	22.05	
	Penalized Difference Ratio (%) \uparrow	25.47	25.76	27.96	30.59	17.06	8.67	12.54	4.77	9.25	15.25
	Average Difficulty Score	1.88	1.88	1.88	1.96	1.90	1.88	1.88	1.88	1.88	1.96
	Average Weighted Difference Ratio (%) \uparrow	1.88	32.76	32.76	37.29	11.14	1.82	12.74	11.90	15.59	15.59
	Difficulty Weighted Relative Difference Ratio (%) \uparrow	1.88	32.76	32.76	37.29	11.14	1.82	12.74	11.90	15.59	15.59
	Valid Output Grid \uparrow	97.00	69.00	94.00	100.00	100.00	98.00	99.00	99.00	93.00	60.00
	Load-Support Connectivity (%) \uparrow	97.00	69.00	94.00	100.00	100.00	98.00	99.00	99.00	93.00	60.00
	Load-Support Directional Connectivity (%) \uparrow	97.00	69.00	94.00	100.00	100.00	98.00	99.00	99.00	93.00	60.00
	Average Isolated Clusters Count \downarrow	0.01	0.01	0.01	0.01	0.01	0.01	0.01	0.01	0.01	0.01
	Force Path Cost Average Efficiency Ratio (%) \uparrow	94.43	82.06	88.28	84.62	92.30	79.45	65.51	82.60	54.44	46.29
Full	Exact Match \downarrow	0	0	0	0	0	0	0	0	0	0
	Difference Ratio (%) \uparrow	40.00	32.96	35.78	32.88	25.03	30.85	126.02	84.98	49.16	34.84
	Relative Difference Ratio (%) \uparrow	40.00	32.96	35.78	32.88	25.03	32.85	126.02	84.98	49.16	34.84
	Penalized Difference Ratio (%) \uparrow	40.00	32.96	35.78	32.88	25.06	38.93	142.73	104.95	49.86	45.60
	Average Difficulty Score	1.93	1.93	1.93	1.93	1.93	1.93	1.93	1.93	1.93	1.93
	Average Weighted Difference Ratio (%) \uparrow	37.69	20.14	21.79	20.08	14.61	19.98	79.62	54.42	29.78	21.20
	Difficulty Weighted Relative Difference Ratio (%) \uparrow	37.69	20.14	21.79	20.08	14.61	19.98	79.62	54.42	29.78	21.20
	Valid Output Grid \uparrow	94.00	49.00	94.00	94.00	98.00	78.00	48.00	78.00	42.00	26.00
	Load-Support Connectivity (%) \uparrow	94.00	46.00	94.00	94.00	72.00	98.00	48.00	76.00	42.00	26.00
	Load-Support Directional Connectivity (%) \uparrow	94.00	46.00	94.00	94.00	72.00	98.00	48.00	76.00	42.00	26.00
	Average Isolated Clusters Count \downarrow	0.01	0.01	0.01	0.01	0.01	0.01	0.13	0.09	0.09	0.16
	Force Path Cost Average Efficiency Ratio (%) \uparrow	88.87	55.53	90.33	81.69	96.85	70.68	48.31	79.00	37.61	46.55
Average	Exact Match \downarrow	1	1	13	10	11	3	5	3	6	0
	Difference Ratio (%) \uparrow	14.88	25.98	50.16	50.13	49.99	37.00	8.43	14.44	30.44	18.38
	Relative Difference Ratio (%) \uparrow	14.88	25.98	50.16	50.13	49.99	37.00	8.43	14.44	30.44	18.38
	Penalized Difference Ratio (%) \uparrow	3.95	15.26	39.31	40.15	37.54	25.45	6.82	1.31	18.68	7.53
	Average Difficulty Score	1.92	1.93	1.92	1.93	1.92	1.93	1.92	1.93	1.92	1.93
	Average Weighted Difference Ratio (%) \uparrow	10.54	16.68	31.69	31.83	32.03	24.33	6.03	13.55	20.15	11.68
	Difficulty Weighted Relative Difference Ratio (%) \uparrow	10.54	16.68	31.69	31.83	32.03	24.33	6.03	13.55	20.15	11.68
	Valid Output Grid \uparrow	99.25	93.75	100.00	100.00	99.00	90.25	100.00	97.75	91.50	72.75
	Load-Support Connectivity (%) \uparrow	99.25	93.75	100.00	100.00	99.00	90.25	100.00	97.75	91.50	72.75
	Load-Support Directional Connectivity (%) \uparrow	99.25	93.75	100.00	100.00	99.00	90.25	100.00	97.75	91.50	72.75
	Average Isolated Clusters Count \downarrow	0.45	0.61	0.00	0.01	0.01	0.04	0.23	0.18	0.25	0.22
	Force Path Cost Average Efficiency Ratio (%) \uparrow	93.92	77.59	94.34	89.28	96.50	83.11	78.19	84.43	58.79	48.85

2483

2484 **G.3 RESULTS FOR CLAUDE OPUS 4 ON ALL TASKS**
24852486 **Grid Rotation on Claude Opus 4 Evaluation Results**
24872488 **Reconstruction Accuracy Metrics 1/2**
24892490 **Exact Match**
24912495 **Hard**
24962499 **Difference Ratio**
25002504 **Hard**
25052508 **Relative Difference Ratio**
25092513 **Hard**
25142517 **Penalized Difference Ratio**
25182522 **Hard**
25232526 **Figure 11: Grid rotation evaluation results: Exact Match, Difference Ratio, Relative Difference Ratio and Penalized Difference Ratio for Claude Opus 4, for all tasks, easy and hard difficulty.**
25272528
2529
2530
2531
2532
2533
2534
2535
2536
2537

2538 Grid Rotation on Claude Opus 4 Evaluation Results

2539 **Reconstruction Accuracy Metrics 2/2**2540 **Average Difficulty Score**2541 **Difficulty Weighted Difference Ratio**2542 **Difficulty Weighted Relative Difference Ratio**2543 **Topology Validity Metrics 1/2**2544 **Grid Validity**

2545 **Figure 12: Grid rotation evaluation results: Average Difficulty Score, Difficulty Weighted Difference**
 2546 **Ratio, Difficulty Weighted Relative Difference Ratio and Grid Validity for Claude Opus 4, for all**
 2547 **tasks, easy and hard difficulty.**

2548

2549

2550

2551

2552

2553

2554

2555

2556

2557

2558

2559

2560

2561

2562

2563

2564

2565

2566

2567

2568

2569

2570

2571

2572

2573

2574

2575

2576

2577

2578

2579

2580

2581

2582

2583

2584

2585

2586

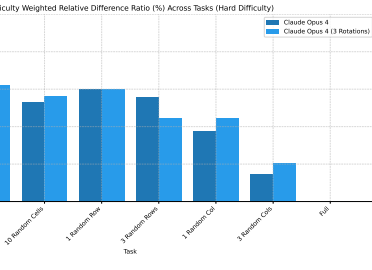
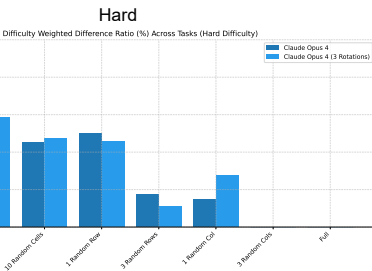
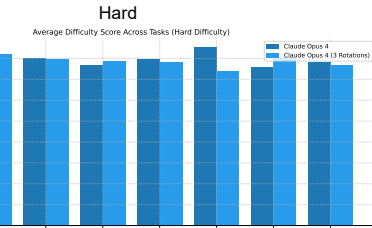
2587

2588

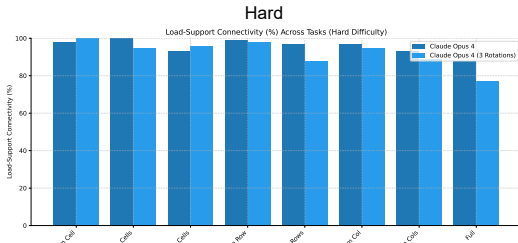
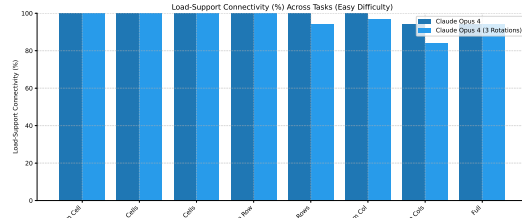
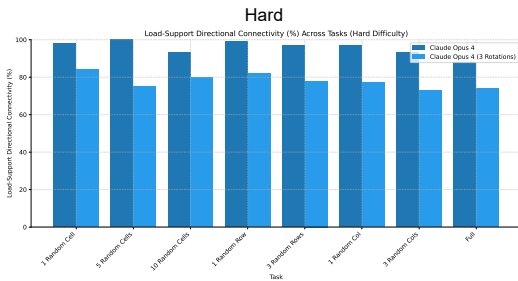
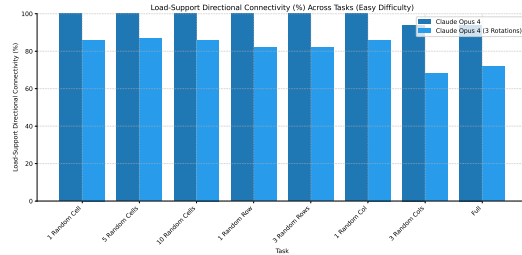
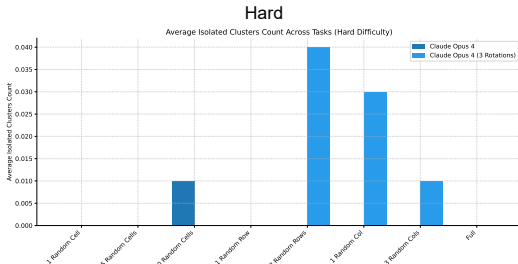
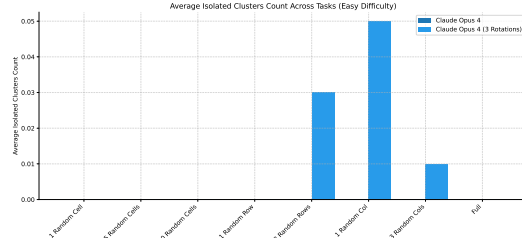
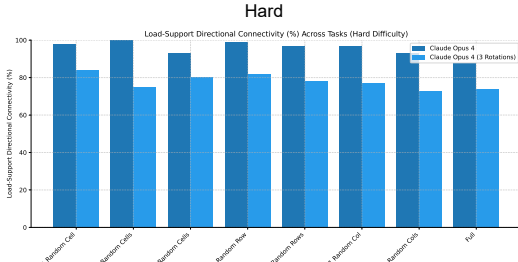
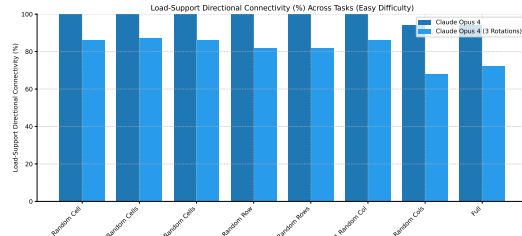
2589

2590

2591



2592 Grid Rotation on Claude Opus 4 Evaluation Results

2593 **Topology Validity Metrics 2/2**2594 **Load-Support Connectivity** **Easy**2603 **Directional Load-Support Connectivity**2612 **Average Isolated Cluster Count**2622 **Physics-Approximating Metrics 1/1**2623 **Force Path Cost Average Efficiency Ratio**2624 **Easy**

2635 Figure 13: Grid rotation evaluation results: Load-Support Connectivity, Directional Load-Support Connectivity, Average Isolated Cluster Count and Force Path Cost Average Efficiency Ratio for Claude Opus 4, for all tasks, easy and hard difficulty.

2646
2647
2648

Table 5: Grid rotation evaluation run results for all metrics for Claude Opus 4, for all tasks, easy and hard difficulty.

2649 2650 2651 2652 2653 2654 2655 2656 2657 2658 2659 2660 2661 2662 2663 2664 2665 2666 2667 2668 2669 2670 2671 2672 2673 2674 2675 2676 2677 2678 2679 2680 2681 2682 2683 2684 2685 2686 2687 2688 2689 2690 2691 2692 2693 2694 2695 2696 2697 2698 2699	Task	Metric	Easy		Hard	
			Claude Opus 4	Claude Opus 4 (3 Rotations)	Claude Opus 4	Claude Opus 4 (3 Rotations)
1 Random Cell	Exact Match \uparrow	82	82	77	80	
	Difference Ratio (%) \uparrow	99.05	99.02	95.45	97.24	
	Relative Difference Ratio (%) \uparrow	99.05	99.02	96.72	98.32	
	Penalized Difference Ratio (%) \uparrow	98.50	98.47	97.11	98.32	
	Average Difficulty Score	1.99	1.99	1.96	1.87	
	Difficulty Weighted Difference Ratio (%) \uparrow	65.51	65.40	60.97	59.80	
	Difficulty Weighted Relative Difference Ratio (%) \uparrow	65.51	65.40	62.25	60.88	
	Valid Output Grid \uparrow	100.00	100.00	99.00	100.00	
	Load-Support Connectivity (%) \uparrow	100.00	100.00	98.00	100.00	
	Load-Support Directional Connectivity (%) \uparrow	100.00	86.00	98.00	84.00	
	Average Isolated Clusters Count \downarrow	0.00	0.00	0.00	0.00	
	Force Path Cost Average Efficiency Ratio (%) \uparrow	99.94	99.72	97.91	100.00	
5 Random Cells	Exact Match \uparrow	45	44	38	41	
	Difference Ratio (%) \uparrow	95.76	95.54	87.27	87.23	
	Relative Difference Ratio (%) \uparrow	95.76	95.54	91.58	91.71	
	Penalized Difference Ratio (%) \uparrow	89.26	90.06	78.42	80.79	
	Average Difficulty Score	1.89	1.89	1.97	2.05	
	Difficulty Weighted Difference Ratio (%) \uparrow	59.89	59.91	56.17	58.59	
	Difficulty Weighted Relative Difference Ratio (%) \uparrow	59.89	59.91	59.65	62.07	
	Valid Output Grid \uparrow	100.00	100.00	100.00	99.00	
	Load-Support Connectivity (%) \uparrow	100.00	100.00	100.00	95.00	
	Load-Support Directional Connectivity (%) \uparrow	100.00	87.00	100.00	75.00	
	Average Isolated Clusters Count \downarrow	0.00	0.00	0.00	0.00	
	Force Path Cost Average Efficiency Ratio (%) \uparrow	99.70	98.20	99.49	95.37	
10 Random Cells	Exact Match \uparrow	15	22	13	18	
	Difference Ratio (%) \uparrow	89.08	91.02	69.70	73.57	
	Relative Difference Ratio (%) \uparrow	89.08	91.02	79.91	85.93	
	Penalized Difference Ratio (%) \uparrow	76.41	80.78	49.33	65.62	
	Average Difficulty Score	1.97	1.94	2.01	2.00	
	Difficulty Weighted Difference Ratio (%) \uparrow	58.23	58.52	45.17	47.31	
	Difficulty Weighted Relative Difference Ratio (%) \uparrow	58.23	58.52	52.88	56.59	
	Valid Output Grid \uparrow	100.00	100.00	99.00	100.00	
	Load-Support Connectivity (%) \uparrow	100.00	100.00	93.00	96.00	
	Load-Support Directional Connectivity (%) \uparrow	100.00	86.00	93.00	80.00	
	Average Isolated Clusters Count \downarrow	0.00	0.00	0.01	0.00	
	Force Path Cost Average Efficiency Ratio (%) \uparrow	99.06	94.41	91.98	95.00	
1 Random Row	Exact Match \uparrow	52	42	49	39	
	Difference Ratio (%) \uparrow	94.92	93.30	80.55	71.92	
	Relative Difference Ratio (%) \uparrow	94.92	93.30	94.39	91.71	
	Penalized Difference Ratio (%) \uparrow	94.92	93.30	94.39	91.71	
	Average Difficulty Score	1.94	1.98	1.92	1.97	
	Difficulty Weighted Difference Ratio (%) \uparrow	61.04	61.36	59.98	61.12	
	Difficulty Weighted Relative Difference Ratio (%) \uparrow	61.04	61.36	60.02	60.12	
	Valid Output Grid \uparrow	100.00	100.00	100.00	100.00	
	Load-Support Connectivity (%) \uparrow	100.00	100.00	99.00	98.00	
	Load-Support Directional Connectivity (%) \uparrow	100.00	82.00	99.00	82.00	
	Average Isolated Clusters Count \downarrow	0.00	0.00	0.00	0.00	
	Force Path Cost Average Efficiency Ratio (%) \uparrow	99.88	100.00	98.92	98.85	
3 Random Rows	Exact Match \uparrow	35	17	21	16	
	Difference Ratio (%) \uparrow	88.64	82.19	82.01	79.88	
	Relative Difference Ratio (%) \uparrow	88.64	82.19	84.70	70.12	
	Penalized Difference Ratio (%) \uparrow	88.64	82.19	84.70	70.12	
	Average Difficulty Score	1.89	1.89	1.99	1.96	
	Difficulty Weighted Difference Ratio (%) \uparrow	55.81	51.60	17.50	11.08	
	Difficulty Weighted Relative Difference Ratio (%) \uparrow	55.81	51.60	55.67	44.35	
	Valid Output Grid \uparrow	100.00	100.00	100.00	100.00	
	Load-Support Connectivity (%) \uparrow	100.00	94.00	97.00	88.00	
	Load-Support Directional Connectivity (%) \uparrow	100.00	82.00	97.00	78.00	
	Average Isolated Clusters Count \downarrow	0.00	0.03	0.00	0.04	
	Force Path Cost Average Efficiency Ratio (%) \uparrow	99.68	96.39	84.17	93.51	
1 Random Column	Exact Match \uparrow	23	27	21	33	
	Difference Ratio (%) \uparrow	83.09	84.86	37.46	61.54	
	Relative Difference Ratio (%) \uparrow	83.09	84.86	62.68	79.72	
	Penalized Difference Ratio (%) \uparrow	73.51	75.48	31.65	60.26	
	Average Difficulty Score	1.90	2.02	2.13	1.85	
	Difficulty Weighted Difference Ratio (%) \uparrow	50.85	54.04	14.68	27.37	
	Difficulty Weighted Relative Difference Ratio (%) \uparrow	50.85	54.04	37.62	44.46	
	Valid Output Grid \uparrow	100.00	100.00	99.00	100.00	
	Load-Support Connectivity (%) \uparrow	100.00	94.00	97.00	88.00	
	Load-Support Directional Connectivity (%) \uparrow	100.00	86.00	97.00	77.00	
	Average Isolated Clusters Count \downarrow	0.00	0.05	0.00	0.03	
	Force Path Cost Average Efficiency Ratio (%) \uparrow	94.90	92.78	84.17	93.51	
3 Random Columns	Exact Match \uparrow	5	2	7	6	
	Difference Ratio (%) \uparrow	58.69	60.16	17.63	-18.77	
	Relative Difference Ratio (%) \uparrow	58.69	60.16	31.78	36.93	
	Penalized Difference Ratio (%) \uparrow	27.96	30.59	43.98	-38.28	
	Average Difficulty Score	1.88	1.96	1.90	2.01	
	Difficulty Weighted Difference Ratio (%) \uparrow	34.52	37.29	22.99	-21.91	
	Difficulty Weighted Relative Difference Ratio (%) \uparrow	34.52	37.29	14.44	20.53	
	Valid Output Grid \uparrow	100.00	100.00	100.00	100.00	
	Load-Support Connectivity (%) \uparrow	100.00	84.00	93.00	89.00	
	Load-Support Directional Connectivity (%) \uparrow	94.00	68.00	93.00	73.00	
	Average Isolated Clusters Count \downarrow	0.00	0.01	0.00	0.01	
	Force Path Cost Average Efficiency Ratio (%) \uparrow	88.28	84.62	77.05	82.98	
Full	Exact Match \uparrow	0	0	0	1	
	Difference Ratio (%) \uparrow	-35.78	-32.88	-466.42	-403.39	
	Relative Difference Ratio (%) \uparrow	-35.78	-32.88	-177.48	-136.14	
	Penalized Difference Ratio (%) \uparrow	-33.76	-32.95	-177.48	-138.43	
	Average Difficulty Score	1.92	1.95	1.96	1.93	
	Difficulty Weighted Difference Ratio (%) \uparrow	-21.79	-20.08	-310.26	-266.48	
	Difficulty Weighted Relative Difference Ratio (%) \uparrow	-21.79	-20.08	-117.17	-98.28	
	Valid Output Grid \uparrow	100.00	100.00	100.00	100.00	
	Load-Support Connectivity (%) \uparrow	94.00	94.00	88.00	77.00	
	Load-Support Directional Connectivity (%) \uparrow	94.00	72.00	88.00	74.00	
	Average Isolated Clusters Count \downarrow	0.00	0.00	0.00	0.00	
	Force Path Cost Average Efficiency Ratio (%) \uparrow	90.33	81.69	87.83	86.43	
Average	Exact Match \uparrow	32.12	29.50	28.25	29.25	
	Difference Ratio (%) \uparrow	71.68	71.65	10.20	-1.08	
	Relative Difference Ratio (%) \uparrow	71.68	71.65	45.53	52.29	
	Penalized Difference Ratio (%) \uparrow	64.16	64.74	26.27	35.92	
	Average Difficulty Score	1.92	1.95	1.98	1.95	
	Difficulty Weighted Difference Ratio (%) \uparrow	45.51	46.01	-11.10	-4.81	
	Difficulty Weighted Relative Difference Ratio (%) \uparrow	45.51	46.01	28.17	32.34	
	Valid Output Grid \uparrow	100.00	100.00	99.62	99.88	
	Load-Support Connectivity (%) \uparrow	98.50	96.12	95.62	92.25	
	Load-Support Directional Connectivity (%) \uparrow	98.50	81.12	95.62	77.88	
	Average Isolated Clusters Count \downarrow	0.00	0.01	0.00	0.01	
	Force Path Cost Average Efficiency Ratio (%) \uparrow	96.47	93.48	91.79	93.44	

2700 H ADDITIONAL FEW-SHOT EXPERIMENT RESULTS

2702 H.1 PROMPT AND COMPLETION - 1 RANDOM CELL EASY: 1-SHOT

2704 Prompt and Completion - 1 Random Cell Easy: 1-Shot

2705 **Prompt:**

2706 You are given a structural material distribution represented as a grid. Each cell can
2707 have one of the following states:

- 2708 - 'L' indicates applied load.
- 2709 - 'V' indicates void.
- 2710 - 'S' indicates support.

2711 The goal is to predict the correct material distribution by filling in all 'V' cells
2712 with either '1' (solid) or '0' (empty), based on the surrounding structure and implicit
2713 physical reasoning (such as load paths, supports, and forces).

2714 Example input grid with masked regions:

```
2713 0 0 0 L L L L 0 0 0
2714 0 0 0 0 1 1 0 0 0 0 0
2715 0 0 0 0 1 1 0 V 0 0 0
2716 0 0 0 0 1 1 0 0 0 0 0
2717 0 0 0 0 1 1 0 0 0 0 0
2718 0 0 0 0 1 1 0 0 0 0 0
2719 0 0 0 0 S S S S S 0
```

2720 Corresponding completed output grid:

```
2721 0 0 0 L L L L 0 0 0
2722 0 0 0 0 1 1 0 0 0 0 0
2723 0 0 0 0 1 1 0 0 0 0 0
2724 0 0 0 0 1 1 0 0 0 0 0
2725 0 0 0 0 1 1 0 0 0 0 0
2726 0 0 0 0 S S S S S 0
```

2727 Important: The completed structure should use as little material as possible while
2728 remaining stable and plausible for carrying the applied forces. Minimize material usage
unless necessary for structural support.

2728 Below is the input grid with masked regions:

```
2729 0 0 L L L 0 0 0 0 0 0
2730 0 0 0 1 0 0 0 0 0 0 0
2731 0 0 0 V 0 0 0 0 0 0 0
2732 0 0 0 1 0 0 0 0 0 0 0
2733 0 0 0 1 1 1 0 0 0 0 0
2734 0 0 1 1 1 0 0 0 0 0 0
2735 0 0 1 1 1 0 0 0 0 0 0
2736 S S S S S S S S S 0
```

2737 Please output the completed grid by replacing all 'V' cells with either '1' (solid) or '0'
(empty).

2738 Maintain the same format as the input: one row per line, cells separated by spaces, and
the total number of rows and columns unchanged.

2739 Return only the completed grid without any additional explanation.

2739 **Model Completion (differences in red):**

```
2740 0 0 L L L 0 0 0 0 0 0
2741 0 0 0 1 0 0 0 0 0 0 0
2742 0 0 0 V 0 0 0 0 0 0 0
2743 0 0 0 1 0 0 0 0 0 0 0
2744 0 0 0 1 1 1 0 0 0 0 0
2745 0 0 1 1 1 0 0 0 0 0 0
2746 S S S S S S S S S 0
```

2746 **Ground Truth:**

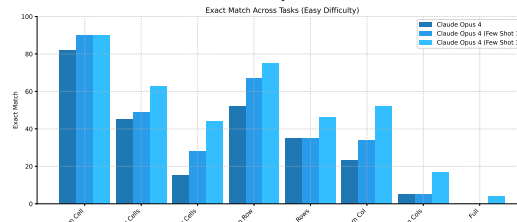
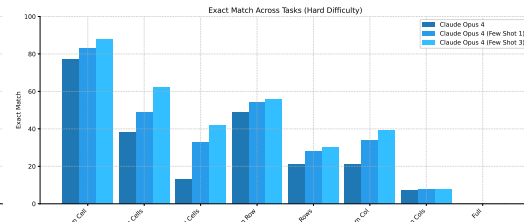
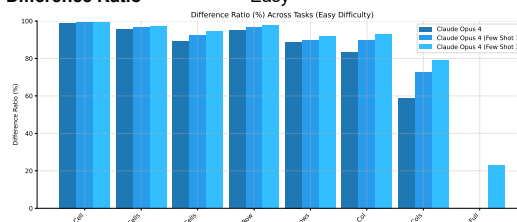
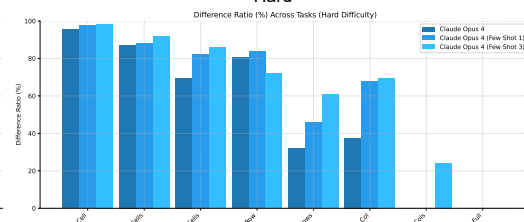
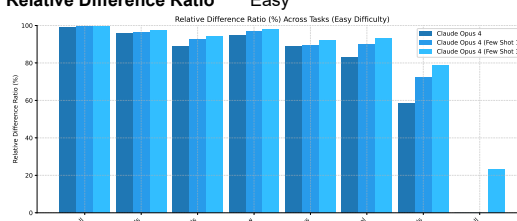
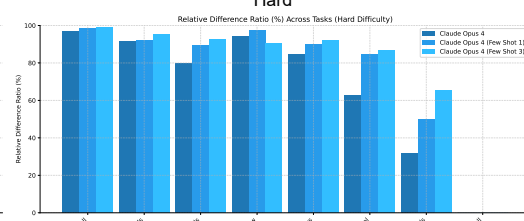
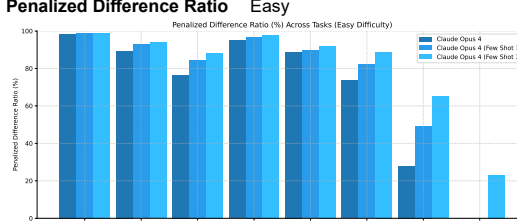
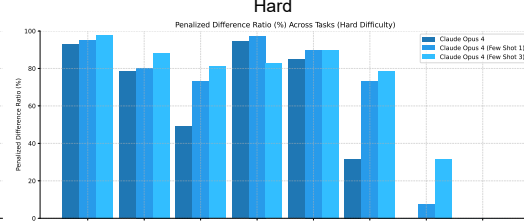
```
2747 0 0 L L L 0 0 0 0 0 0
2748 0 0 0 1 0 0 0 0 0 0 0
2749 0 0 0 V 0 0 0 0 0 0 0
2750 0 0 0 1 0 0 0 0 0 0 0
2751 0 0 0 1 1 1 0 0 0 0 0
2752 0 0 1 1 1 0 0 0 0 0 0
2753 S S S S S S S S S 0
```

2754 H.2 PROMPT AND COMPLETION - 1 RANDOM CELL EASY: 3-SHOT
 2755

Prompt and Completion - 1 Random Cell Easy: 3-Shot

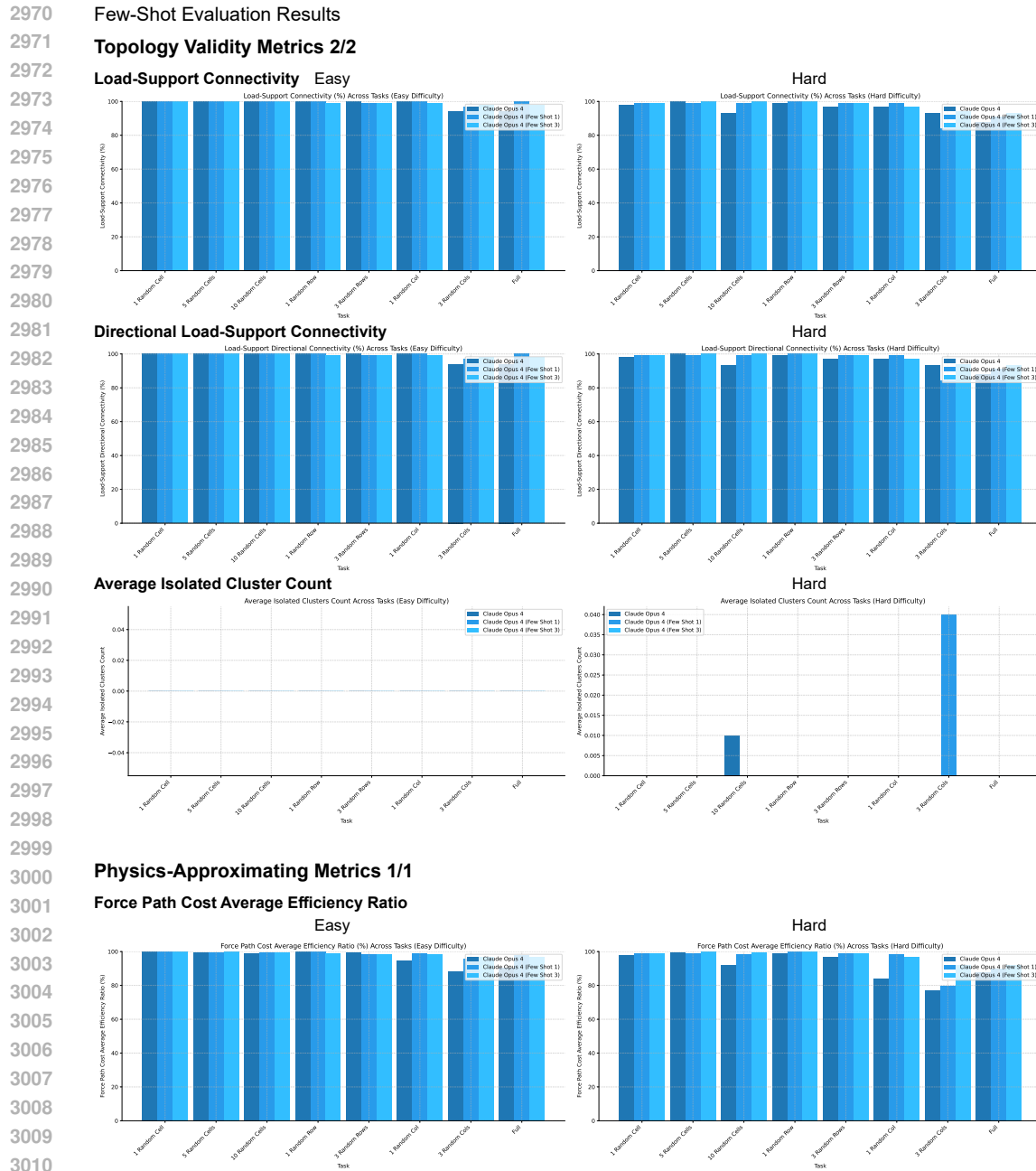
2756 **Prompt:**
 2757 You are given a structural material distribution represented as a grid. Each cell can
 2759 have one of the following states:
 2760 - 'L' indicates applied load.
 2761 - 'V' indicates void.
 2762 - 'S' indicates support.
 2763 The goal is to predict the correct material distribution by filling in all 'V' cells
 2764 with either '1' (solid) or '0' (empty), based on the surrounding structure and implicit
 2765 physical reasoning (such as load paths, supports, and forces).
 2766 Example input grid with masked regions:
 2767 0 0 0 L L L 0 0 0
 2768 0 0 0 0 1 1 0 0 0 0
 2769 0 0 0 0 1 1 0 V 0 0
 2770 0 0 0 0 1 1 0 0 0 0
 2771 0 0 0 0 1 1 0 0 0 0
 2772 0 0 0 0 1 1 0 0 0 0
 2773 0 0 0 0 1 1 0 0 0 0
 2774 0 0 0 0 1 1 0 0 0 0
 2775 0 0 0 0 1 1 0 0 0 0
 2776 0 0 0 0 1 1 0 0 0 0
 2777 0 0 0 0 1 1 0 0 0 0
 2778 0 0 0 0 S S S S S 0
 2779 Corresponding completed output grid:
 2780 0 0 0 L L L L 0 0 0
 2781 0 0 0 0 1 1 0 0 0 0
 2782 0 0 0 0 1 1 0 0 0 0
 2783 0 0 0 0 1 1 0 0 0 0
 2784 0 0 0 0 1 1 1 1 0 0
 2785 0 0 0 0 0 1 S S S 0
 2786 Example input grid with masked regions:
 2787 0 0 0 L L L 0 0 0 0
 2788 0 0 0 0 1 0 0 0 0 0 0
 2789 0 0 0 0 1 0 0 0 0 0 0
 2790 0 0 0 0 1 0 0 0 0 0 0
 2791 0 0 0 0 1 1 1 1 0 0
 2792 0 0 0 0 0 1 1 1 0 0
 2793 0 0 0 0 0 1 S S S 0
 2794 Corresponding completed output grid:
 2795 0 0 0 L L L L L 0 0 0
 2796 0 0 0 0 1 1 1 0 0 0 0
 2797 0 0 0 0 1 1 1 V 0 0 0 0
 2798 0 0 0 0 1 1 1 0 0 0 0
 2799 0 0 0 0 1 1 1 0 0 0 0
 2800 0 S S S S S S S 0 0 0
 2801 Corresponding completed output grid:
 2802 0 0 0 L L L L L 0 0 0
 2803 0 0 0 0 1 1 1 0 0 0 0
 2804 0 0 0 0 1 1 1 0 0 0 0
 2805 0 0 0 0 1 1 1 0 0 0 0
 2806 0 0 0 0 1 1 1 0 0 0 0
 2807 0 S S S S S S S 0 0 0

2808
 2809 Important: The completed structure should use as little material as possible while
 2810 remaining stable and plausible for carrying the applied forces. Minimize material usage
 2811 unless necessary for structural support.
 2812 Below is the input grid with masked regions:
 2813 0 0 L L L 0 0 0 0 0
 2814 0 0 0 1 0 0 0 0 0 0
 2815 0 0 0 V 0 0 0 0 0 0
 2816 0 0 0 1 0 0 0 0 0 0
 2817 0 0 0 1 0 0 0 0 0 0
 2818 0 0 0 1 0 0 0 0 0 0
 2819 0 0 1 1 1 0 0 0 0 0
 2820 0 0 1 1 1 0 0 0 0 0
 2821 0 0 1 1 1 0 0 0 0 0
 2822 S S S S S S S S S S
 2823 Please output the completed grid by replacing all 'V' cells with either '1' (solid) or '0'
 2824 (empty).
 2825 Maintain the same format as the input: one row per line, cells separated by spaces, and
 2826 the total number of rows and columns unchanged.
 2827 Return only the completed grid without any additional explanation.
 2828 **Model Completion (differences in red):**
 2829 0 0 L L L 0 0 0 0 0
 2830 0 0 0 1 0 0 0 0 0 0
 2831 0 0 0 1 0 0 0 0 0 0
 2832 0 0 0 1 0 0 0 0 0 0
 2833 0 0 0 1 0 0 0 0 0 0
 2834 0 0 1 1 1 0 0 0 0 0
 2835 0 0 1 1 1 0 0 0 0 0
 2836 0 0 1 1 1 0 0 0 0 0
 2837 S S S S S S S S S S
 2838
 2839
 2840
 2841
 2842
 2843
 2844
 2845
 2846
 2847
 2848
 2849
 2850
 2851
 2852
 2853
 2854
 2855
 2856
 2857
 2858
 2859
 2860
 2861

2862 H.3 RESULTS FOR CLAUDE OPUS 4 ON ALL TASKS
28632864 Few-Shot Evaluation Results
28652866 Reconstruction Accuracy Metrics 1/2
28672868 Exact Match
28692870 Hard
28712872 Difference Ratio
28732874 Hard
28752876 Relative Difference Ratio
28772878 Hard
28792880 Penalized Difference Ratio
28812882 Hard
28832902
2903
2904
2905
2906
2907 Figure 14: Few-shot (1, 3) evaluation results: Exact Match, Difference Ratio, Relative Difference
2908 Ratio and Penalized Difference Ratio for Claude Opus 4, for all tasks, easy and hard difficulty.
2909
2910
2911
2912
2913
2914
2915



2931 **Figure 15: Few-shot (1, 3) evaluation results: Average Difficulty Score, Difficulty Weighted Difference Ratio, Difficulty Weighted Relative Difference Ratio and Grid Validity for Claude Opus 4, for all tasks, easy and hard difficulty.**



3013 Figure 16: Few-shot (1, 3) evaluation results: Load-Support Connectivity, Directional Load-Support
3014 Connectivity, Average Isolated Cluster Count and Force Path Cost Average Efficiency Ratio for
3015 Claude Opus 4, for all tasks, easy and hard difficulty.

3024
3025
3026

Table 6: Few-shot (1, 3) evaluation results for all metrics, for Claude Opus 4, for all tasks, easy and hard difficulty.

3027

Task	Metric	Easy			Hard		
		Claude Opus 4 (Zero-Shot)	Claude Opus 4 (1-Shot)	Claude Opus 4 (3-Shot)	Claude Opus 4 (Zero-Shot)	Claude Opus 4 (1-Shot)	Claude Opus 4 (3-Shot)
1 Random Cell	Exact Match \uparrow	92	99	99	92	98	98.33
	Difference Ratio (%) \uparrow	99.05	99.51	99.50	95.45	97.64	98.33
	Relative Difference Ratio (%) \uparrow	99.05	99.51	99.50	96.72	98.28	99.13
	Penalized Difference Ratio (%) \uparrow	98.40	98.93	99.03	93.11	95.20	97.72
	Average Difficulty Score	1.99	1.99	1.99	1.96	2.09	1.89
	Difficulty Weighted Difference Ratio (%) \uparrow	65.51	65.92	65.88	60.97	67.45	61.43
	Difficulty Weighted Relative Difference Ratio (%) \uparrow	65.51	65.92	65.88	62.25	66.09	62.22
	Valid Output Grid \uparrow	100.00	100.00	100.00	99.00	100.00	100.00
	Load-Support Connectivity (%) \uparrow	100.00	100.00	100.00	98.00	99.00	99.00
	Load-Support Directional Connectivity (%) \uparrow	100.00	100.00	100.00	98.00	99.00	99.00
	Average Isolated Clusters Count \downarrow	0.00	0.00	0.00	0.00	0.00	0.00
	Force Path Cost Average Efficiency Ratio (%) \uparrow	99.94	99.94	99.95	97.91	95.96	99.00
5 Random Cells	Exact Match \uparrow	45	49	63	38	49	62
	Difference Ratio (%) \uparrow	95.76	96.53	97.25	87.27	88.28	91.85
	Relative Difference Ratio (%) \uparrow	95.76	96.53	97.25	91.58	92.10	95.31
	Penalized Difference Ratio (%) \uparrow	89.26	92.90	93.93	76.42	80.15	88.27
	Average Difficulty Score	1.89	1.92	1.88	1.97	2.01	2.04
	Difficulty Weighted Difference Ratio (%) \uparrow	59.89	61.73	60.69	56.17	58.62	61.94
	Difficulty Weighted Relative Difference Ratio (%) \uparrow	59.89	61.73	60.69	59.65	61.59	64.85
	Valid Output Grid \uparrow	100.00	100.00	100.00	100.00	99.00	100.00
	Load-Support Connectivity (%) \uparrow	100.00	100.00	100.00	100.00	99.00	100.00
	Load-Support Directional Connectivity (%) \uparrow	100.00	100.00	100.00	100.00	99.00	100.00
	Average Isolated Clusters Count \downarrow	0.00	0.00	0.00	0.00	0.00	0.00
	Force Path Cost Average Efficiency Ratio (%) \uparrow	99.70	99.66	99.87	99.49	98.89	99.90
10 Random Cells	Exact Match \uparrow	15	28	44	13	33	42
	Difference Ratio (%) \uparrow	89.08	92.63	94.31	69.70	82.11	85.88
	Relative Difference Ratio (%) \uparrow	89.08	92.63	94.31	79.91	89.57	92.63
	Penalized Difference Ratio (%) \uparrow	76.41	84.37	88.11	49.33	73.32	81.11
	Average Difficulty Score	1.97	1.98	1.98	2.01	1.97	1.97
	Difficulty Weighted Difference Ratio (%) \uparrow	52.23	60.24	60.77	45.17	53.92	56.05
	Difficulty Weighted Relative Difference Ratio (%) \uparrow	58.23	60.24	60.77	52.88	58.43	61.07
	Valid Output Grid \uparrow	100.00	100.00	100.00	99.00	100.00	100.00
	Load-Support Connectivity (%) \uparrow	100.00	100.00	100.00	93.00	99.00	100.00
	Load-Support Directional Connectivity (%) \uparrow	100.00	100.00	100.00	93.00	99.00	100.00
	Average Isolated Clusters Count \downarrow	0.00	0.00	0.00	0.01	0.00	0.00
	Force Path Cost Average Efficiency Ratio (%) \uparrow	99.06	99.32	99.37	91.98	98.41	99.55
1 Random Row	Exact Match \uparrow	52	67	75	49	54	56
	Difference Ratio (%) \uparrow	94.92	96.86	97.72	80.65	82.25	72.00
	Relative Difference Ratio (%) \uparrow	94.92	96.86	97.72	94.39	97.25	92.99
	Penalized Difference Ratio (%) \uparrow	94.92	96.86	97.72	84.70	89.71	82.61
	Average Difficulty Score	1.94	1.91	1.90	1.92	1.98	1.98
	Difficulty Weighted Difference Ratio (%) \uparrow	61.04	61.29	61.66	49.95	53.53	45.64
	Difficulty Weighted Relative Difference Ratio (%) \uparrow	61.04	61.29	61.66	60.02	63.78	59.35
	Valid Output Grid \uparrow	100.00	100.00	100.00	100.00	100.00	100.00
	Load-Support Connectivity (%) \uparrow	100.00	100.00	100.00	99.00	100.00	100.00
	Load-Support Directional Connectivity (%) \uparrow	100.00	100.00	100.00	97.00	100.00	100.00
	Average Isolated Clusters Count \downarrow	0.00	0.00	0.00	0.00	0.00	0.00
	Force Path Cost Average Efficiency Ratio (%) \uparrow	99.88	99.96	98.85	98.92	99.99	99.84
3 Random Rows	Exact Match \uparrow	35	35	46	21	28	30
	Difference Ratio (%) \uparrow	88.64	89.67	91.83	32.01	45.88	60.79
	Relative Difference Ratio (%) \uparrow	88.64	89.67	91.83	84.70	89.71	92.24
	Penalized Difference Ratio (%) \uparrow	88.64	89.67	91.83	84.70	89.71	89.97
	Average Difficulty Score	1.94	1.91	1.90	1.92	1.98	1.98
	Difficulty Weighted Difference Ratio (%) \uparrow	61.04	61.29	61.66	49.95	53.53	45.64
	Difficulty Weighted Relative Difference Ratio (%) \uparrow	61.04	61.29	61.66	60.02	63.78	59.35
	Valid Output Grid \uparrow	100.00	100.00	100.00	100.00	100.00	100.00
	Load-Support Connectivity (%) \uparrow	100.00	100.00	100.00	99.00	100.00	100.00
	Load-Support Directional Connectivity (%) \uparrow	100.00	100.00	100.00	97.00	99.00	99.00
	Average Isolated Clusters Count \downarrow	0.00	0.00	0.00	0.00	0.00	0.00
	Force Path Cost Average Efficiency Ratio (%) \uparrow	99.68	98.49	98.62	96.97	98.75	98.73
1 Random Column	Exact Match \uparrow	25	34	52	21	34	35
	Difference Ratio (%) \uparrow	83.09	89.98	93.14	37.46	67.96	69.20
	Relative Difference Ratio (%) \uparrow	83.09	89.98	93.14	62.68	84.74	86.73
	Penalized Difference Ratio (%) \uparrow	73.51	82.16	88.94	31.65	73.11	78.56
	Average Difficulty Score	1.90	1.95	1.86	2.13	1.98	2.07
	Difficulty Weighted Difference Ratio (%) \uparrow	50.85	56.22	56.20	14.68	37.66	41.22
	Difficulty Weighted Relative Difference Ratio (%) \uparrow	50.85	56.22	56.20	37.62	53.13	57.79
	Valid Output Grid \uparrow	100.00	100.00	99.00	99.00	100.00	100.00
	Load-Support Connectivity (%) \uparrow	100.00	100.00	99.00	97.00	99.00	97.00
	Load-Support Directional Connectivity (%) \uparrow	100.00	100.00	99.00	97.00	99.00	97.00
	Average Isolated Clusters Count \downarrow	0.00	0.00	0.00	0.00	0.00	0.00
	Force Path Cost Average Efficiency Ratio (%) \uparrow	94.90	98.74	98.65	84.17	98.62	96.66
3 Random Columns	Exact Match \uparrow	5	5	17	7	8	8
	Difference Ratio (%) \uparrow	58.69	72.50	78.86	-17.63	-0.45	24.33
	Relative Difference Ratio (%) \uparrow	58.69	72.50	78.86	49.90	65.66	65.66
	Penalized Difference Ratio (%) \uparrow	27.06	49.17	65.12	-43.98	7.30	37.72
	Average Difficulty Score	1.88	1.93	1.96	1.94	1.96	1.88
	Difficulty Weighted Difference Ratio (%) \uparrow	34.52	45.21	50.03	-23.99	-10.19	7.45
	Difficulty Weighted Relative Difference Ratio (%) \uparrow	34.52	45.21	50.03	14.44	28.98	38.82
	Valid Output Grid \uparrow	100.00	100.00	100.00	100.00	100.00	100.00
	Load-Support Connectivity (%) \uparrow	100.00	100.00	100.00	97.00	99.00	99.00
	Load-Support Directional Connectivity (%) \uparrow	100.00	100.00	100.00	97.00	99.00	99.00
	Average Isolated Clusters Count \downarrow	0.00	0.00	0.00	0.00	0.04	0.00
	Force Path Cost Average Efficiency Ratio (%) \uparrow	88.28	95.82	96.94	77.05	79.48	92.20
Full	Exact Match \uparrow	0	0	4	0	0	0
	Difference Ratio (%) \uparrow	35.78	-14.18	23.06	-66.42	-392.37	-240.02
	Relative Difference Ratio (%) \uparrow	35.78	-14.18	23.06	-177.48	-27.72	-4.41
	Penalized Difference Ratio (%) \uparrow	35.78	-14.18	23.06	-177.48	-27.72	-4.41
	Average Difficulty Score	1.92	1.94	1.91	1.96	2.00	1.96
	Difficulty Weighted Difference Ratio (%) \uparrow	-27.79	-8.72	14.96	-31.26	-19.92	-154.54
	Difficulty Weighted Relative Difference Ratio (%) \uparrow	-27.79	-8.72	14.96	-17.17	-19.24	-5.04
	Valid Output Grid \uparrow	100.00	100.00	100.00	100.00	99.00	100.00
	Load-Support Connectivity (%) \uparrow	94.00	100.00	98.00	88.00	91.00	93.00
	Load-Support Directional Connectivity (%) \uparrow	94.00	100.00	98.00	88.00	91.00	93.00
	Average Isolated Clusters Count \downarrow	0.00	0.00	0.00	0.00	0.00	0.00
	Force Path Cost Average Efficiency Ratio (%) \uparrow	90.33	97.86	96.77	87.83	90.10	91.89
Average	Exact Match \uparrow	32.12	38.50	48.88	28.25	36.12	40.62
	Difference Ratio (%) \uparrow	71.68	77.94	84.46	-10.20	21.60	32.79
	Relative Difference Ratio (%) \uparrow	71.68	77.94	84.46	45.53	71.73	72.22
	Penalized Difference Ratio (%) \uparrow	64.16	72.52	80.97	26.27	61.05	63.19
	Average Difficulty Score	1.92	1.94	1.92	1.93	1.99	1.98
	Difficulty Weighted Difference Ratio (%) \uparrow	45.51	49.95	53.56	-11.10	11.42	17.78
	Difficulty Weighted Relative Difference Ratio (%) \uparrow	45.51	49.95	53.56	28.17	46.75	49.93
	Valid Output Grid \uparrow	100.00	100.00	99.88	99.62	99.75	100.00
	Load-Support Connectivity (%) \uparrow	98.50	99.50	99.12	95.62	96.25	97.75
	Load-Support Directional Connectivity (%) \uparrow	98.50	99.50	99.12	95.62	96.25	97.75
	Average Isolated Clusters Count \downarrow	0.00	0.00	0.00	0.00	0.01	0.00
	Force Path Cost Average Efficiency Ratio (%) \uparrow	96.47	98.72	98.63	91.79	95.40	97.22

3070
3071
3072
3073
3074
3075
3076
3077

3078 I ADDITIONAL PHYSICS-ENHANCED AND -NEUTRAL EXPERIMENT RESULTS 3079

3080 I.1 PROMPT AND COMPLETION - 1 RANDOM CELL EASY: PHYSICS-NETURAL 3081

3082 **Prompt and Completion - 1 Random Cell Easy: Physics-Netural** 3083

3084 **Prompt:**

3085 You are given a grid of cells. Each cell can have one of the following states:
 3086 - 'L' indicates a special marker.
 3087 - 'V' indicates an empty cell.
 3088 - 'S' indicates a fixed marker.

3089 The goal is to predict the correct grid configuration by filling in all 'V' cells with
 3090 either '1' (solid) or '0' (empty), based on the surrounding structure and general
 3091 consistency rules.

3092 Relevant rules for reasoning:
 3093

- 3094 - Filled cells should form continuous connections between relevant markers when necessary.
- 3095 - Avoid placing isolated filled cells that are not connected to anything meaningful.
- 3096 - Minimize the number of filled cells while maintaining a coherent and connected
 3097 structure.

3098 Below is the input grid with masked regions:
 3099

3100 L L L L 0 0 0 0 0
 3101 0 1 1 1 0 0 0 0 0 0
 3102 0 1 1 1 0 0 0 0 0 0
 3103 0 0 1 0 0 0 0 0 0 0
 3104 0 0 1 0 0 0 0 0 0 0
 3105 0 0 1 0 0 0 0 0 0 0
 3106 V 0 1 1 1 0 0 0 0 0
 3107 0 0 1 S S S 0 0 0 0

3108 Please output the completed grid by replacing all 'V' cells with either '1' (solid) or '0'
 3109 (empty).

3110 Maintain the same format as the input: one row per line, cells separated by spaces, and
 3111 the total number of rows and columns unchanged.

3112 Return only the completed grid without any additional explanation.

3113 **Model Completion (differences in red):**

3114 L L L L 0 0 0 0 0
 3115 0 1 1 1 0 0 0 0 0 0
 3116 0 1 1 1 0 0 0 0 0 0
 3117 0 0 1 0 0 0 0 0 0 0
 3118 0 0 1 0 0 0 0 0 0 0
 3119 0 0 1 0 0 0 0 0 0 0
 3120 0 0 1 0 0 0 0 0 0 0
 3121 0 0 1 1 1 0 0 0 0 0
 3122 0 0 1 S S S 0 0 0 0

3123 **Ground Truth:**
 3124

3125 L L L L 0 0 0 0 0
 3126 0 1 1 1 0 0 0 0 0 0
 3127 0 1 1 1 0 0 0 0 0 0
 3128 0 0 1 0 0 0 0 0 0 0
 3129 0 0 1 0 0 0 0 0 0 0
 3130 0 0 1 0 0 0 0 0 0 0
 3131 0 0 1 1 1 0 0 0 0 0
 3132 0 0 1 S S S 0 0 0 0

3132 I.2 PROMPT AND COMPLETION - 1 RANDOM CELL EASY: PHYSICS-ENHANCED
 3133

3134 **Prompt and Completion - 1 Random Cell Easy: Physics-Enhanced**

3135

3136 **Prompt:**

3137 You are given a structural material distribution represented as a grid. Each cell can
 have one of the following states:

- 'L' indicates applied load.
- 'V' indicates void.
- 'S' indicates support.

3140 The goal is to predict the correct material distribution by filling in all 'V' cells
 3141 with either '1' (solid) or '0' (empty), based on the surrounding structure and implicit
 3142 physical reasoning (such as load paths, supports, and forces).

3143

3144 Relevant physical knowledge for reasoning:

- Loads ('L') create forces that must be transferred through continuous material paths to supports ('S').
- Stress follows the shortest stiff path from loads to supports.
- Any material cell that is disconnected from both loads and supports does not carry force and should be avoided.
- Structures should satisfy equilibrium: all loads must eventually be resisted by at least one support.
- Use as little material as possible while still maintaining at least one valid load path.

3145

3146 Below is the input grid with masked regions:

3147

```
3148           0 0 L L L 0 0 0 0 0
  3149           0 0 0 1 0 0 0 0 0 0
  3150           0 0 0 V 0 0 0 0 0 0
  3151           0 0 0 1 0 0 0 0 0 0
  3152           0 0 0 1 0 0 0 0 0 0
  3153           0 0 0 1 0 0 0 0 0 0
  3154           0 0 0 1 0 0 0 0 0 0
  3155           0 0 1 1 0 0 0 0 0 0
  3156           0 0 1 1 1 0 0 0 0 0
  3157           0 0 1 1 1 0 0 0 0 0
  3158           S S S S S S S S S 0
```

3159

3160 Please output the completed grid by replacing all 'V' cells with either '1' (solid) or '0' (empty).

3161

3162 Maintain the same format as the input: one row per line, cells separated by spaces, and the total number of rows and columns unchanged.

3163

3164 Return only the completed grid without any additional explanation.

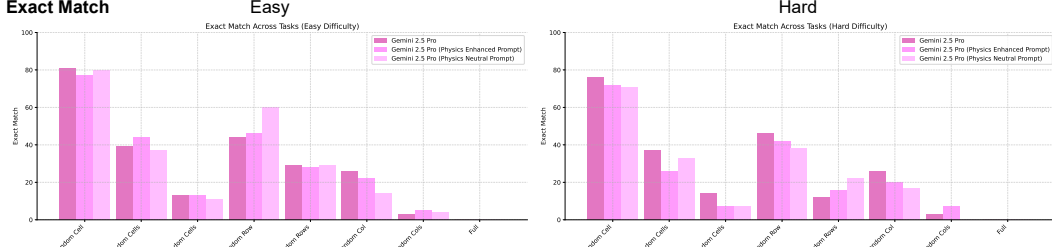
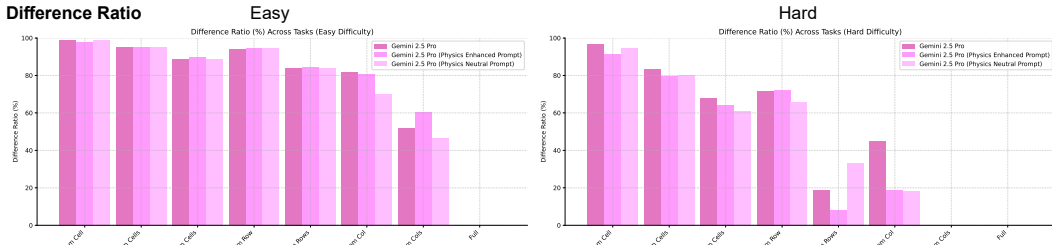
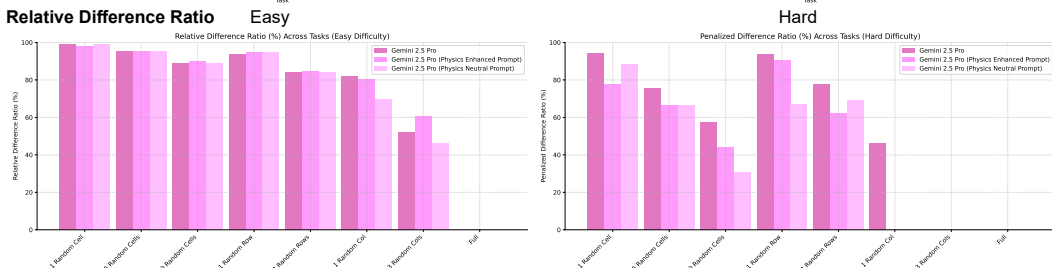
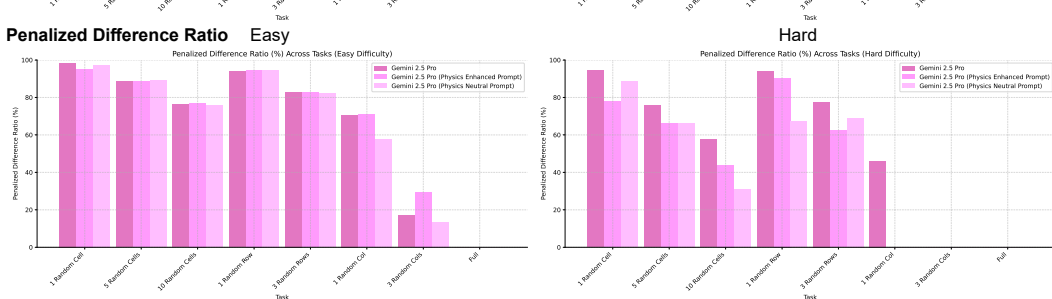
3165 **Model Completion (differences in red):**

```
3166           0 0 L L L 0 0 0 0 0
  3167           0 0 0 1 0 0 0 0 0 0
  3168           0 0 0 1 0 0 0 0 0 0
  3169           0 0 0 1 0 0 0 0 0 0
  3170           0 0 0 1 0 0 0 0 0 0
  3171           0 0 0 1 0 0 0 0 0 0
  3172           0 0 0 1 0 0 0 0 0 0
  3173           0 0 0 1 0 0 0 0 0 0
  3174           0 0 0 1 0 0 0 0 0 0
  3175           0 0 1 1 0 0 0 0 0 0
  3176           0 0 1 1 1 0 0 0 0 0
  3177           0 0 1 1 1 0 0 0 0 0
  3178           S S S S S S S S S 0
```

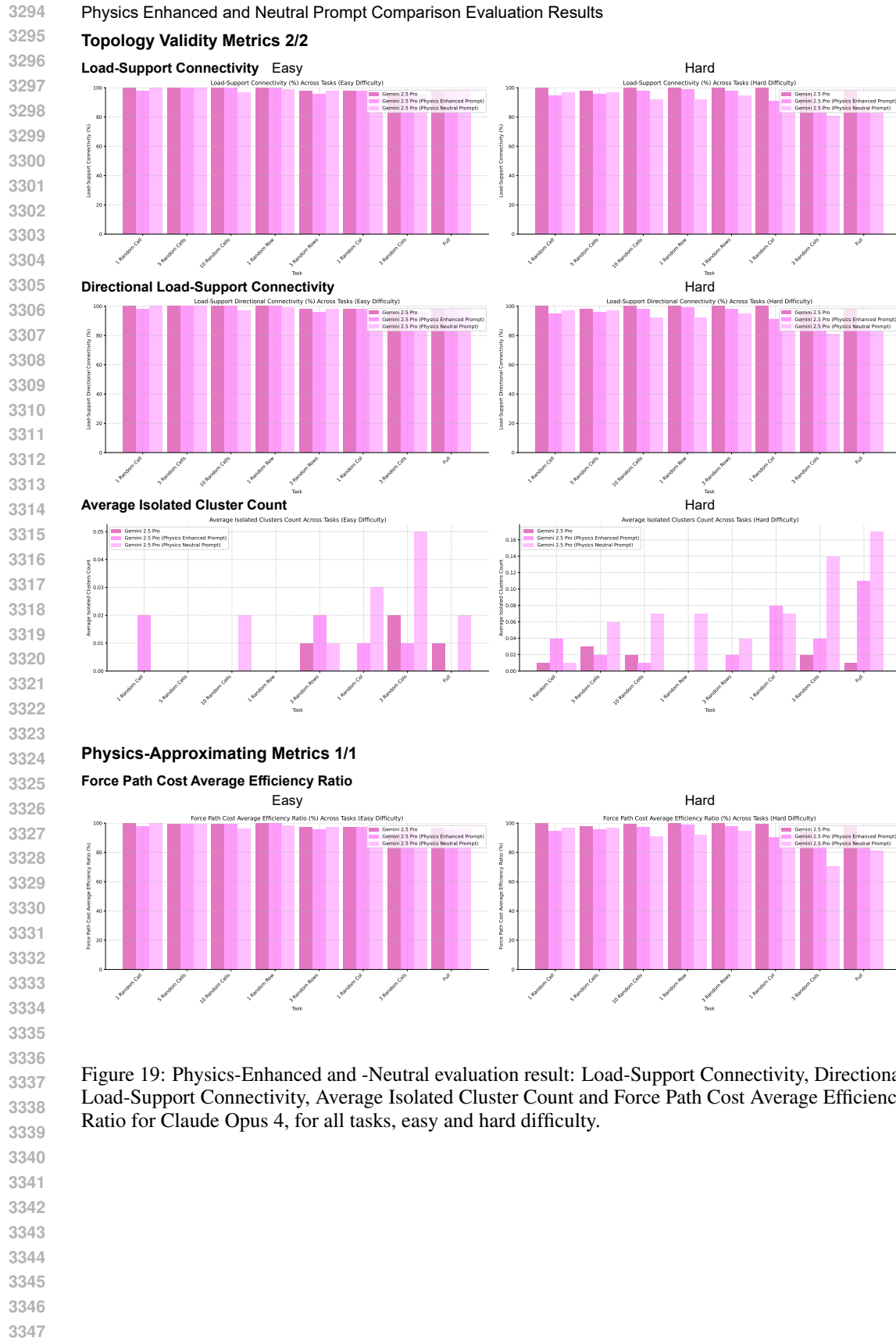
3179

3180 **Ground Truth:**

```
3181           0 0 L L L 0 0 0 0 0
  3182           0 0 0 1 0 0 0 0 0 0
  3183           0 0 0 1 0 0 0 0 0 0
  3184           0 0 0 1 0 0 0 0 0 0
  3185           0 0 0 1 0 0 0 0 0 0
  3186           0 0 0 1 0 0 0 0 0 0
  3187           0 0 0 1 0 0 0 0 0 0
  3188           0 0 0 1 0 0 0 0 0 0
  3189           0 0 1 1 0 0 0 0 0 0
  3190           0 0 1 1 1 0 0 0 0 0
  3191           0 0 1 1 1 0 0 0 0 0
  3192           0 0 1 1 1 0 0 0 0 0
  3193           S S S S S S S S S 0
```

3186 **I.3 RESULTS FOR CLAUDE OPUS 4 ON ALL TASKS**
31873188 **Physics Enhanced and Neutral Prompt Comparison Evaluation Results**
31893190 **Reconstruction Accuracy Metrics 1/2**
31913192 **Exact Match**
31933199 **Difference Ratio**
32003208 **Relative Difference Ratio**
32093217 **Penalized Difference Ratio**
32183226
3227
3228
3229
3230
3231 **Figure 17: Physics-Enhanced and -Neutral evaluation run metric: Exact Match, Difference Ratio, Relative Difference Ratio and Penalized Difference Ratio for Claude Opus 4, for all tasks, easy and hard difficulty.**
3232
32333234
3235
3236
3237
3238
3239





3348

Table 7: Physics-Enhanced and -Neutral evaluation results for all metrics, for Claude Opus 4, for all tasks, easy and hard difficulty.

Task	Metric	Easy			Hard		
		Gemini 2.5 Pro (Base)	Gemini 2.5 Pro (Physics-Enhanced Prompt)	Gemini 2.5 Pro (Physics-Neutral Prompt)	Gemini 2.5 Pro (Base)	Gemini 2.5 Pro (Physics-Enhanced Prompt)	Gemini 2.5 Pro (Physics-Neutral Prompt)
1 Random Cell	Exact Match \dagger	81	77	80	76	72	71
	Difference Ratio (%) \dagger	95.08	95.12	95.03	95.23	95.22	95.33
	Relative Difference Ratio (%) \dagger	99.03	97.87	98.93	97.88	92.22	95.33
	Penalized Difference Ratio (%) \dagger	98.37	95.26	97.20	94.31	77.77	88.60
	Average Difficulty Score	1.39	1.39	1.85	1.36	1.36	1.32
	Difficulty Weighted Difference Ratio (%) \dagger	65.47	64.69	60.78	58.87	59.00	59.30
	Difficulty Weighted Relative Difference Ratio (%) \dagger	65.47	64.69	60.78	60.01	60.03	60.11
	Valid Output Grid \dagger	100.00	100.00	100.00	100.00	100.00	99.00
	Load-Support Connectivity (%) \dagger	100.00	98.00	100.00	100.00	95.00	97.00
	Load-Support Directional Connectivity (%) \dagger	100.00	98.00	100.00	100.00	95.00	97.00
	Average Isolated Clusters Count \downarrow	0.01	0.02	0.03	0.01	0.04	0.01
	Force Path Cost Average Efficiency Ratio (%) \dagger	99.94	97.84	99.83	99.92	94.93	96.80
5 Random Cells	Exact Match \dagger	39	44	37	37	26	33
	Difference Ratio (%) \dagger	95.08	95.12	95.08	83.19	79.81	80.21
	Relative Difference Ratio (%) \dagger	99.03	94.32	95.98	89.95	85.92	83.99
	Penalized Difference Ratio (%) \dagger	88.59	88.62	89.15	75.62	66.34	66.29
	Average Difficulty Score	1.39	1.89	1.91	1.96	1.97	1.99
	Difficulty Weighted Difference Ratio (%) \dagger	59.45	59.26	60.93	52.69	51.32	51.35
	Difficulty Weighted Relative Difference Ratio (%) \dagger	59.45	59.26	60.93	57.87	55.88	55.77
	Valid Output Grid \dagger	100.00	100.00	100.00	99.00	98.00	99.00
	Load-Support Connectivity (%) \dagger	100.00	100.00	100.00	100.00	99.00	97.00
	Load-Support Directional Connectivity (%) \dagger	100.00	100.00	100.00	100.00	96.00	97.00
	Average Isolated Clusters Count \downarrow	0.01	0.02	0.03	0.02	0.04	0.06
	Force Path Cost Average Efficiency Ratio (%) \dagger	99.75	97.84	99.73	97.84	95.55	96.83
10 Random Cells	Exact Match \dagger	12	12	11	12	5	7
	Difference Ratio (%) \dagger	88.88	89.86	88.77	67.83	64.28	60.77
	Relative Difference Ratio (%) \dagger	88.88	89.86	88.77	82.80	77.50	72.96
	Penalized Difference Ratio (%) \dagger	73.21	73.11	75.70	57.60	44.06	30.78
	Average Difficulty Score	1.97	1.97	1.99	1.94	1.97	1.97
	Difficulty Weighted Difference Ratio (%) \dagger	59.48	59.26	60.93	41.99	41.53	38.61
	Difficulty Weighted Relative Difference Ratio (%) \dagger	59.48	59.26	60.93	52.66	41.13	47.43
	Valid Output Grid \dagger	100.00	100.00	100.00	100.00	99.00	99.00
	Load-Support Connectivity (%) \dagger	100.00	100.00	100.00	100.00	98.00	92.00
	Load-Support Directional Connectivity (%) \dagger	100.00	100.00	100.00	100.00	98.00	95.00
	Average Isolated Clusters Count \downarrow	0.00	0.00	0.02	0.02	0.01	0.07
	Force Path Cost Average Efficiency Ratio (%) \dagger	99.31	99.34	96.19	99.34	97.12	91.07
1 Random Row	Exact Match \dagger	45	46	46	42	38	38
	Difference Ratio (%) \dagger	93.90	94.56	94.59	71.69	72.25	65.84
	Relative Difference Ratio (%) \dagger	93.90	94.56	94.59	93.86	90.55	84.59
	Penalized Difference Ratio (%) \dagger	88.88	88.62	89.15	93.86	90.55	87.23
	Average Difficulty Score	1.97	1.97	1.99	1.94	1.97	1.99
	Difficulty Weighted Difference Ratio (%) \dagger	60.55	60.98	58.53	45.14	44.52	42.47
	Difficulty Weighted Relative Difference Ratio (%) \dagger	60.55	60.98	58.53	52.66	51.32	56.45
	Valid Output Grid \dagger	100.00	100.00	100.00	100.00	99.00	99.00
	Load-Support Connectivity (%) \dagger	100.00	100.00	100.00	100.00	99.00	92.00
	Load-Support Directional Connectivity (%) \dagger	100.00	100.00	100.00	100.00	98.00	95.00
	Average Isolated Clusters Count \downarrow	0.00	0.00	0.00	0.01	0.00	0.07
	Force Path Cost Average Efficiency Ratio (%) \dagger	99.99	99.84	98.65	99.99	99.00	91.96
3 Random Rows	Exact Match \dagger	29	28	39	12	16	22
	Difference Ratio (%) \dagger	84.09	84.46	83.85	10.25	9.35	33.21
	Relative Difference Ratio (%) \dagger	84.09	84.46	83.85	77.42	66.67	78.96
	Penalized Difference Ratio (%) \dagger	82.84	82.61	82.18	77.42	62.27	69.10
	Average Difficulty Score	1.94	1.94	1.95	1.95	1.94	1.94
	Difficulty Weighted Difference Ratio (%) \dagger	53.52	53.40	54.34	9.64	1.50	19.13
	Difficulty Weighted Relative Difference Ratio (%) \dagger	53.52	53.40	54.34	43.20	41.20	50.91
	Valid Output Grid \dagger	100.00	100.00	100.00	100.00	98.00	99.00
	Load-Support Connectivity (%) \dagger	100.00	100.00	100.00	100.00	98.00	95.00
	Load-Support Directional Connectivity (%) \dagger	100.00	100.00	100.00	100.00	98.00	95.00
	Average Isolated Clusters Count \downarrow	0.00	0.02	0.03	0.02	0.04	0.04
	Force Path Cost Average Efficiency Ratio (%) \dagger	99.74	95.88	97.43	99.87	97.97	94.45
1 Random Column	Exact Match \dagger	26	22	14	26	20	17
	Difference Ratio (%) \dagger	84.09	80.45	69.86	44.93	18.64	18.41
	Relative Difference Ratio (%) \dagger	84.09	80.45	69.86	72.25	28.65	42.16
	Penalized Difference Ratio (%) \dagger	84.09	80.45	70.83	46.17	2.29	5.47
	Average Difficulty Score	1.97	1.90	1.88	1.87	2.13	2.08
	Difficulty Weighted Difference Ratio (%) \dagger	48.21	48.24	48.35	15.91	2.54	0.84
	Difficulty Weighted Relative Difference Ratio (%) \dagger	48.21	48.24	48.35	40.27	29.14	22.96
	Valid Output Grid \dagger	98.00	99.00	100.00	100.00	99.00	100.00
	Load-Support Connectivity (%) \dagger	98.00	98.00	100.00	100.00	98.00	94.00
	Load-Support Directional Connectivity (%) \dagger	98.00	98.00	100.00	100.00	98.00	94.00
	Average Isolated Clusters Count \downarrow	0.00	0.01	0.03	0.02	0.04	0.07
	Force Path Cost Average Efficiency Ratio (%) \dagger	97.20	95.26	92.66	94.28	86.24	70.47
3 Random Columns	Exact Match \dagger	3	5	4	3	7	0
	Difference Ratio (%) \dagger	52.03	60.60	46.29	56.28	38.97	56.82
	Relative Difference Ratio (%) \dagger	52.03	60.60	46.29	20.85	16.32	31.7
	Penalized Difference Ratio (%) \dagger	70.55	70.83	57.94	46.17	316.57	358.96
	Average Difficulty Score	1.90	1.88	1.88	1.96	1.90	1.95
	Difficulty Weighted Difference Ratio (%) \dagger	31.14	36.00	28.05	50.66	32.81	37.68
	Difficulty Weighted Relative Difference Ratio (%) \dagger	31.14	36.00	28.05	77.2	4.18	43.02
	Valid Output Grid \dagger	98.00	99.00	100.00	100.00	99.00	100.00
	Load-Support Connectivity (%) \dagger	98.00	98.00	100.00	100.00	98.00	98.00
	Load-Support Directional Connectivity (%) \dagger	98.00	98.00	100.00	100.00	98.00	98.00
	Average Isolated Clusters Count \downarrow	0.02	0.01	0.05	0.02	0.04	0.14
	Force Path Cost Average Efficiency Ratio (%) \dagger	92.30	95.26	96.63	97.83	86.29	81.43
Full	Exact Match \dagger	0	0	0	0	0	0
	Difference Ratio (%) \dagger	25.03	39.34	-16.98	54.98	377.88	-439.73
	Relative Difference Ratio (%) \dagger	25.03	39.34	-16.98	-316.57	-358.96	-282.89
	Penalized Difference Ratio (%) \dagger	25.96	39.34	-17.62	-318.95	-391.30	-329.53
	Average Difficulty Score	1.91	1.93	1.91	1.94	1.94	1.96
	Difficulty Weighted Difference Ratio (%) \dagger	-14.61	-23.66	-10.88	-360.89	-380.19	-296.08
	Difficulty Weighted Relative Difference Ratio (%) \dagger	-14.61	-23.66	-10.88	-326.21	-329.96	-345.17
	Valid Output Grid \dagger	98.00	98.00	100.00	98.00	98.00	100.00
	Load-Support Connectivity (%) \dagger	98.00	98.00	100.00	100.00	98.00	83.00
	Load-Support Directional Connectivity (%) \dagger	98.00	98.00	100.00	100.00	98.00	83.00
	Average Isolated Clusters Count \downarrow	0.01	0.00	0.02	0.01	0.11	0.17
	Force Path Cost Average Efficiency Ratio (%) \dagger	97.87	97.89	97.06	98.57	91.43	89.43
Average	Exact Match \dagger	29.38	29.38	29.38	26.75	23.78	23.50
	Difference Ratio (%) \dagger	71.24	70.45	70.05	27.77	35.33	-17.95
	Relative Difference Ratio (%) \dagger	71.24	70.45	70.05	23.11	14.46	22.43
	Penalized Difference Ratio (%) \dagger	62.70	62.40	61.59	8.21	14.97	12.21
	Average Difficulty Score	1.92	1.92	1.91	1.94	1.98	1.98
	Difficulty Weighted Difference Ratio (%) \dagger	45.32	45.00	44.40	13.42	25.09	14.16
	Difficulty Weighted Relative Difference Ratio (%) \dagger	45.32	45.00	44.40	8.03	12.70	12.70
	Valid Output Grid \dagger	99.50	99.15	99.50	99.75	99.25	99.38
	Load-Support Connectivity (%) \dagger	98.75	98.38	98.00	99.00	94.35	91.38
	Load-Support Directional Connectivity (%) \dagger	98.75	98.38	98.00	99.00	94.25	91.38
	Average Isolated Clusters Count \downarrow	0.01	0.01	0.02	0.01	0.04	0.06
	Force Path Cost Average Efficiency Ratio (%) \dagger	96.85	95.30	96.63	97.83	86.29	81.43

3385

3386

3387

3388

3389

3390

3391

3392

3393

3394

3395

3396

3397

3398

3399

3400

3401

3402 **J SAMPLE PROMPTS & COMPLETIONS**
34033404 **J.1 CLAUDE 3.7 SONNET - 1 RANDOM CELL EASY: SAMPLE 1**
34053406 **Claude 3.7 Sonnet - 1 Random Cell Easy: Sample 1**
34073408 **Prompt:**3409 You are given a structural material distribution represented as a grid. Each cell can
3410 have one of the following states:
3411 - 'L' indicates applied load.
3412 - 'V' indicates void.
3413 - 'S' indicates support.3414 The goal is to predict the correct material distribution by filling in all 'V' cells
3415 with either '1' (solid) or '0' (empty), based on the surrounding structure and implicit
3416 physical reasoning (such as load paths, supports, and forces).3417 Important: The completed structure should use as little material as possible while
3418 remaining stable and plausible for carrying the applied forces. Minimize material usage
3419 unless necessary for structural support.3420 Below is the input grid with masked regions:
34213422 0 0 L L L 0 0 0 0 0
3423 0 0 0 1 0 0 0 0 0 0 0
3424 0 0 0 V 0 0 0 0 0 0 0
3425 0 0 0 1 0 0 0 0 0 0 0
3426 0 0 0 1 0 0 0 0 0 0 0
3427 0 0 0 1 0 0 0 0 0 0 0
3428 0 0 1 1 1 0 0 0 0 0 0
3429 0 0 1 1 1 0 0 0 0 0 0
3430 S S S S S S S S S 03431 Please output the completed grid by replacing all 'V' cells with either '1' (solid) or '0'
3432 (empty).3433 Maintain the same format as the input: one row per line, cells separated by spaces, and
3434 the total number of rows and columns unchanged.

3435 Return only the completed grid without any additional explanation.

3436 **Model Completion (differences in red):**
34373438 0 0 L L L 0 0 0 0 0
3439 0 0 0 1 0 0 0 0 0 0 0
3440 0 0 0 1 0 0 0 0 0 0 0
3441 0 0 0 1 0 0 0 0 0 0 0
3442 0 0 0 1 0 0 0 0 0 0 0
3443 0 0 1 1 1 0 0 0 0 0 0
3444 0 0 1 1 1 0 0 0 0 0 0
3445 0 0 1 1 1 0 0 0 0 0 0
3446 S S S S S S S S S 03447 **Ground Truth:**
34483449 0 0 L L L 0 0 0 0 0
3450 0 0 0 1 0 0 0 0 0 0 0
3451 0 0 0 1 0 0 0 0 0 0 0
3452 0 0 0 1 0 0 0 0 0 0 0
3453 0 0 0 1 0 0 0 0 0 0 0
3454 0 0 1 1 1 0 0 0 0 0 0
3455 0 0 1 1 1 0 0 0 0 0 0
3456 S S S S S S S S S 0

3456
3457

J.2 CLAUDE 3.7 SONNET - 1 RANDOM CELL EASY: SAMPLE 2

3458
3459**Claude 3.7 Sonnet - 1 Random Cell Easy: Sample 2**3460
3461**Prompt:**

You are given a structural material distribution represented as a grid. Each cell can have one of the following states:

- 'L' indicates applied load.
- 'V' indicates void.
- 'S' indicates support.

3464
3465
3466

The goal is to predict the correct material distribution by filling in all 'V' cells with either '1' (solid) or '0' (empty), based on the surrounding structure and implicit physical reasoning (such as load paths, supports, and forces).

3467
3468
3469

Important: The completed structure should use as little material as possible while remaining stable and plausible for carrying the applied forces. Minimize material usage unless necessary for structural support.

3470
3471

Below is the input grid with masked regions:

```
0 0 0 0 0 0 L L L 0
0 0 0 0 0 0 0 1 0 0
0 0 0 0 0 0 0 1 0 0
0 0 0 0 0 0 0 1 0 0
0 0 0 0 0 0 0 1 0 0
0 0 0 0 1 1 1 1 0 0
0 0 1 1 1 1 1 1 0 0
0 0 1 1 1 1 1 0 0 0
0 1 1 1 1 1 V 0 0 0
S S S S 1 0 0 0 0
```

3478
3479

Please output the completed grid by replacing all 'V' cells with either '1' (solid) or '0' (empty).

3480
3481

Maintain the same format as the input: one row per line, cells separated by spaces, and the total number of rows and columns unchanged.

Return only the completed grid without any additional explanation.

3482

Model Completion (differences in red):

```
0 0 0 0 0 0 L L L 0
0 0 0 0 0 0 0 1 0 0
0 0 0 0 0 0 0 1 0 0
0 0 0 0 0 0 0 1 0 0
0 0 0 0 0 0 0 1 0 0
0 0 0 0 1 1 1 1 0 0
0 0 1 1 1 1 1 1 0 0
0 0 1 1 1 1 1 1 0 0
0 1 1 1 1 1 1 0 0 0
S S S S 1 0 0 0 0
```

3490

Ground Truth:

```
0 0 0 0 0 0 L L L 0
0 0 0 0 0 0 0 1 0 0
0 0 0 0 0 0 0 1 0 0
0 0 0 0 0 0 0 1 0 0
0 0 0 0 0 0 0 1 0 0
0 0 0 0 1 1 1 1 0 0
0 0 1 1 1 1 1 1 0 0
0 0 1 1 1 1 1 1 0 0
0 1 1 1 1 1 1 0 0 0
S S S S 1 0 0 0 0
```

3498

3499

3500

3501

3502

3503

3504

3505

3506

3507

3508

3509

3564 J.4 CLAUDE 3.7 SONNET - FULL EASY

3565

3566 **Claude 3.7 Sonnet - Full Easy**

3567

3568 **Prompt:**3569 You are given a structural material distribution represented as a grid. Each cell can
have one of the following states:3570 - 'L' indicates applied load.
3571 - 'V' indicates void.
3572 - 'S' indicates support.3573 The goal is to predict the correct material distribution by filling in all 'V' cells
3574 with either '1' (solid) or '0' (empty), based on the surrounding structure and implicit
physical reasoning (such as load paths, supports, and forces).3575 Important: The completed structure should use as little material as possible while
3576 remaining stable and plausible for carrying the applied forces. Minimize material usage
3577 unless necessary for structural support.

3578 Below is the input grid with masked regions:

3579 0 L L L L L 0 0 0 0
3580 V V V V V V V V V V
3581 V V V V V V V V V V
3582 V V V V V V V V V V
3583 V V V V V V V V V V
3584 V V V V V V V V V V
3585 0 S S S S S S 0 0 03586 Please output the completed grid by replacing all 'V' cells with either '1' (solid) or '0'
3587 (empty).3588 Maintain the same format as the input: one row per line, cells separated by spaces, and
the total number of rows and columns unchanged.

3589 Return only the completed grid without any additional explanation.

3590 **Model Completion (differences in red):**3591 0 L L L L L 0 0 0 0
3592 0 1 1 1 1 1 0 0 0 0
3593 0 1 0 0 0 1 0 0 0 0
3594 0 1 0 0 0 1 0 0 0 0
3595 0 1 0 0 0 1 0 0 0 0
3596 0 1 0 0 0 1 0 0 0 0
3597 0 1 1 1 1 1 0 0 0 0
3598 0 S S S S S S 0 0 03599 **Ground Truth:**3600 0 L L L L L 0 0 0 0
3601 0 0 1 1 1 0 0 0 0 0
3602 0 0 1 1 1 0 0 0 0 0
3603 0 0 0 1 0 0 0 0 0 0
3604 0 0 0 1 0 0 0 0 0 0
3605 0 0 0 1 0 0 0 0 0 0
3606 0 0 0 1 0 0 0 0 0 0
3607 0 0 0 1 0 0 0 0 0 0
3608 0 0 0 1 0 0 0 0 0 0
3609 0 0 0 1 0 0 0 0 0 0
3610 0 0 0 1 0 0 0 0 0 0
3611 0 0 0 1 0 0 0 0 0 0
3612 0 0 0 1 0 0 0 0 0 0
3613 0 0 0 1 0 0 0 0 0 0
3614 0 0 0 1 0 0 0 0 0 0
3615 0 0 0 1 0 0 0 0 0 0
3616 0 0 0 1 0 0 0 0 0 0
3617 0 0 0 1 0 0 0 0 0 0

3618
3619

J.5 CLAUDE 3.7 SONNET - FULL HARD

3620

Claude 3.7 Sonnet - Full Hard

3621

Prompt:

3622

You are given a structural material distribution represented as a grid. Each cell can have one of the following states:

3623

- 'L' indicates applied load.
- 'V' indicates void.
- 'S' indicates support.

3624

3625

The goal is to predict the correct material distribution by filling in all 'V' cells with a floating point number between 0 and 1, with one decimal place (e.g., 0.0, 0.1, 0.2, ..., 1.0), based on the surrounding structure and implicit physical reasoning (such as load paths, supports, and forces).

3626

3627

Important: The completed structure should use as little material as possible while remaining stable and plausible for carrying the applied forces. Minimize material usage unless necessary for structural support.

3628

3629

Below is the input grid with masked regions:

3630

3631

```
0.0 L L L L L L L L
V V V V V V V V V V
V V V V V V V V V V
V V V V V V V V V V
V V V V V V V V V V
V V V V V V V V V V
V V V V V V V V V V
V V V V V V V V V V
V V V V V V V V V V
V V V V V V V V V V
0.0 0.0 S S S S S S 0.0 0.0 0.0
```

3632

3633

Please output the completed grid by replacing all 'V' cells with a floating point number between 0 and 1, with one decimal place (e.g., 0.0, 0.1, 0.2, ..., 1.0). Maintain the same format as the input: one row per line, cells separated by spaces, and the total number of rows and columns unchanged.

Return only the completed grid without any additional explanation.

3634

Model Completion (differences in red):

3635

```
0.0 L L L L L L L L
0.0 0.0 0.1 0.2 0.6 0.6 0.2 0.1 0.0 0.0
0.0 0.0 0.2 0.3 0.8 0.8 0.3 0.2 0.0 0.0
0.0 0.0 0.3 0.5 1.0 1.0 0.5 0.3 0.0 0.0
0.0 0.0 0.4 0.7 1.0 1.0 0.7 0.4 0.0 0.0
0.0 0.0 0.5 0.9 1.0 1.0 0.9 0.5 0.0 0.0
0.0 0.0 0.6 1.0 1.0 1.0 1.0 0.6 0.0 0.0
0.0 0.0 0.7 1.0 1.0 1.0 1.0 0.7 0.0 0.0
0.0 0.0 0.9 1.0 1.0 1.0 1.0 0.9 0.0 0.0
0.0 0.0 S S S S S S 0.0 0.0 0.0
```

3636

3637

Ground Truth:

```
0.0 L L L L L L L L
0.0 0.0 0.2 0.3 0.0 0.3 0.0 0.3 0.2 0.0
0.0 0.0 0.0 0.4 0.2 0.3 0.2 0.4 0.0 0.0
0.0 0.0 0.0 0.2 0.4 0.0 0.4 0.2 0.0 0.0
0.0 0.0 0.0 0.0 0.4 0.0 0.4 0.0 0.0 0.0
0.0 0.0 0.0 0.0 0.2 0.5 0.2 0.0 0.0 0.0
0.0 0.0 0.0 0.0 0.6 0.0 0.0 0.0 0.0 0.0
0.0 0.0 0.0 0.0 0.6 0.0 0.0 0.0 0.0 0.0
0.0 0.0 0.0 0.0 0.6 0.0 0.0 0.0 0.0 0.0
0.0 0.0 S S S S S S 0.0 0.0 0.0
```

3638

3639

3640

3641

3642

3643

3644

3645

3646

3647

3648

3649

3650

3651

3652

3653

3654

3655

3656

3657

3658

3659

3660

3661

3662

3663

3664

3665

3666

3667

3668

3669

3670

3671

3672 **J.6 DEEPSEEK-R1 - 1 RANDOM CELL EASY: SAMPLE 1**
 3673

3674 **DeepSeek-R1 - 1 Random Cell Easy: Sample 1**

3675 **Prompt:**

3676 You are given a structural material distribution represented as a grid. Each cell can
 3677 have one of the following states:

- 'L' indicates applied load.
- 'V' indicates void.
- 'S' indicates support.

3680 The goal is to predict the correct material distribution by filling in all 'V' cells
 3681 with either '1' (solid) or '0' (empty), based on the surrounding structure and implicit
 3682 physical reasoning (such as load paths, supports, and forces).

3683 Important: The completed structure should use as little material as possible while
 3684 remaining stable and plausible for carrying the applied forces. Minimize material usage
 3685 unless necessary for structural support.

3686 Below is the input grid with masked regions:

3687 0 0 L L L 0 0 0 0 0
 3688 0 0 0 1 0 0 0 0 0 0 0
 3689 0 0 0 V 0 0 0 0 0 0
 3690 0 0 0 1 0 0 0 0 0 0 0
 3691 0 0 0 1 0 0 0 0 0 0 0
 3692 0 0 1 1 1 0 0 0 0 0 0
 3693 0 0 1 1 1 0 0 0 0 0 0
 3694 S S S S S S S S S S 0

3695 Please output the completed grid by replacing all 'V' cells with either '1' (solid) or '0'
 3696 (empty).

3697 Maintain the same format as the input: one row per line, cells separated by spaces, and
 3698 the total number of rows and columns unchanged.

3699 Return only the completed grid without any additional explanation.

3700 **Model Completion (differences in red):**

3701 0 0 L L L 0 0 0 0 0
 3702 0 0 0 1 0 0 0 0 0 0
 3703 0 0 0 1 0 0 0 0 0 0
 3704 0 0 0 1 0 0 0 0 0 0
 3705 0 0 1 1 1 0 0 0 0 0
 3706 0 0 1 1 1 0 0 0 0 0
 3707 0 0 1 1 1 0 0 0 0 0
 3708 S S S S S S S S S S 0

3709 **Ground Truth:**

3710 0 0 L L L 0 0 0 0 0
 3711 0 0 0 1 0 0 0 0 0 0
 3712 0 0 0 1 0 0 0 0 0 0
 3713 0 0 0 1 0 0 0 0 0 0
 3714 0 0 1 1 1 0 0 0 0 0
 3715 0 0 1 1 1 0 0 0 0 0
 3716 0 0 1 1 1 0 0 0 0 0
 3717 S S S S S S S S S S 0

3718
 3719
 3720
 3721
 3722
 3723
 3724
 3725

3726 J.7 DEEPSEEK-R1 - 1 RANDOM CELL EASY: SAMPLE 2
 3727

3728 DeepSeek-R1 - 1 Random Cell Easy: Sample 2

3729
 3730 **Prompt:**
 3731 You are given a structural material distribution represented as a grid. Each cell can
 3732 have one of the following states:
 3733 - 'L' indicates applied load.
 3734 - 'V' indicates void.
 3735 - 'S' indicates support.

3736
 3737 The goal is to predict the correct material distribution by filling in all 'V' cells
 3738 with either '1' (solid) or '0' (empty), based on the surrounding structure and implicit
 3739 physical reasoning (such as load paths, supports, and forces).

3740 Important: The completed structure should use as little material as possible while
 3741 remaining stable and plausible for carrying the applied forces. Minimize material usage
 3742 unless necessary for structural support.

3743
 3744 Below is the input grid with masked regions:

3745 L L L L L L 0 0 0 0
 3746 0 1 1 1 1 0 0 0 0 0 0
 3747 0 0 1 1 0 0 0 0 0 0 0
 3748 0 0 1 1 0 0 0 0 0 0 0
 3749 0 0 1 1 1 0 0 0 0 0 0
 3750 V 0 0 1 1 1 1 0 0 0
 3751 0 0 0 1 1 1 1 1 0 0
 3752 0 0 0 0 0 1 S S S 0

3753 Please output the completed grid by replacing all 'V' cells with either '1' (solid) or '0'
 3754 (empty).
 3755 Maintain the same format as the input: one row per line, cells separated by spaces, and
 3756 the total number of rows and columns unchanged.
 3757 Return only the completed grid without any additional explanation.

3758
 3759 **Model Completion (differences in red):**

3760 L L L L L L 0 0 0 0
 3761 0 1 1 1 1 0 0 0 0 0 0
 3762 0 0 1 1 0 0 0 0 0 0 0
 3763 0 0 1 1 0 0 0 0 0 0 0
 3764 0 0 1 1 1 0 0 0 0 0 0
 3765 0 0 0 1 1 1 1 0 0 0 0
 3766 0 0 0 0 1 1 1 1 1 0 0
 3767 0 0 0 0 0 1 S S S 0

3768
 3769 **Ground Truth:**

3770 L L L L L L 0 0 0 0
 3771 0 1 1 1 1 0 0 0 0 0 0
 3772 0 0 1 1 0 0 0 0 0 0 0
 3773 0 0 1 1 0 0 0 0 0 0 0
 3774 0 0 1 1 1 0 0 0 0 0 0
 3775 0 0 0 1 1 1 1 0 0 0 0
 3776 0 0 0 0 1 1 1 1 1 0 0
 3777 0 0 0 0 0 1 S S S 0

3778

3779

3834 J.9 DEEPSEEK-R1 - FULL EASY
38353836 **DeepSeek-R1 - Full Easy**3837 **Prompt:**3838 You are given a structural material distribution represented as a grid. Each cell can
3839 have one of the following states:

- 'L' indicates applied load.
- 'V' indicates void.
- 'S' indicates support.

3842 The goal is to predict the correct material distribution by filling in all 'V' cells
3843 with either '1' (solid) or '0' (empty), based on the surrounding structure and implicit
3844 physical reasoning (such as load paths, supports, and forces).3845 Important: The completed structure should use as little material as possible while
3846 remaining stable and plausible for carrying the applied forces. Minimize material usage
3847 unless necessary for structural support.

3848 Below is the input grid with masked regions:

```
3849 0 L L L L 0 0 0 0
3850 V V V V V V V V V V
3851 V V V V V V V V V V
3852 V V V V V V V V V V
3853 V V V V V V V V V V
3854 V V V V V V V V V V
3855 0 S S S S S 0 0 0
```

3856 Please output the completed grid by replacing all 'V' cells with either '1' (solid) or '0'
3857 (empty).3858 Maintain the same format as the input: one row per line, cells separated by spaces, and
3859 the total number of rows and columns unchanged.

3860 Return only the completed grid without any additional explanation.

3861 **Model Completion (differences in red):**

```
3862 0 L L L L 0 0 0 0
3863 1 1 1 1 1 1 1 1 1
3864 1 1 1 1 1 1 1 1 1
3865 1 1 1 1 1 1 1 1 1
3866 1 1 1 1 1 1 1 1 1
3867 0 S S S S S 0 0 0
```

3868 **Ground Truth:**

```
3869 0 L L L L 0 0 0 0
3870 0 0 1 1 1 0 0 0 0 0
3871 0 0 1 1 1 0 0 0 0 0
3872 0 0 0 1 0 0 0 0 0 0
3873 0 0 0 1 0 0 0 0 0 0
3874 0 0 0 1 0 0 0 0 0 0
3875 0 S S S S S 0 0 0
```

3876

3877

3878

3879

3880

3881

3882

3883

3884

3885

3886

3887

3888
3889 J.10 DEEPSEEK-R1 - FULL HARD

3890 **DeepSeek-R1 - Full Hard**

3891 **Prompt:**

3892 You are given a structural material distribution represented as a grid. Each cell can
3893 have one of the following states:

- 'L' indicates applied load.
- 'V' indicates void.
- 'S' indicates support.

3894
3895
3896 The goal is to predict the correct material distribution by filling in all 'V' cells with
3897 a floating point number between 0 and 1, with one decimal place (e.g., 0.0, 0.1, 0.2, ...,
3898 1.0), based on the surrounding structure and implicit physical reasoning (such as load
paths, supports, and forces).

3899
3900 Important: The completed structure should use as little material as possible while
3901 remaining stable and plausible for carrying the applied forces. Minimize material usage
unless necessary for structural support.

3902 Below is the input grid with masked regions:

3903
3904 0.0 L L L L L L L L L L
3905 V V V V V V V V V V V V
3906 V V V V V V V V V V V V
3907 V V V V V V V V V V V V
3908 V V V V V V V V V V V V
3909 V V V V V V V V V V V V
3910 0.0 0.0 S S S S S S 0.0 0.0 0.0

3911 Please output the completed grid by replacing all 'V' cells with a floating point number
3912 between 0 and 1, with one decimal place (e.g., 0.0, 0.1, 0.2, ..., 1.0).

3913 Maintain the same format as the input: one row per line, cells separated by spaces, and
the total number of rows and columns unchanged.

3914 Return only the completed grid without any additional explanation.

3915 **Model Completion (differences in red):**

3916 0.0 L L L L L L L L L L
3917 0.0 0.0 0.0 0.0 0.0 0.0 0.0 0.0 0.0 0.0 0.0
3918 0.0 0.0 0.0 0.0 0.0 0.0 0.0 0.0 0.0 0.0 0.0
3919 0.0 0.0 0.0 0.0 0.0 0.0 0.0 0.0 0.0 0.0 0.0
3920 0.0 0.0 0.0 0.0 0.0 0.0 0.0 0.0 0.0 0.0 0.0
3921 0.0 0.0 0.0 0.0 0.0 0.0 0.0 0.0 0.0 0.0 0.0
3922 0.0 0.0 S S S S S S 0.0 0.0 0.0

3923 **Ground Truth:**

3924 0.0 L L L L L L L L L L
3925 0.0 0.0 0.2 0.3 0.0 0.3 0.0 0.3 0.2 0.0
3926 0.0 0.0 0.0 0.4 0.2 0.3 0.2 0.4 0.0 0.0
3927 0.0 0.0 0.0 0.2 0.4 0.0 0.4 0.2 0.0 0.0
3928 0.0 0.0 0.0 0.0 0.4 0.0 0.4 0.0 0.0 0.0
3929 0.0 0.0 0.0 0.0 0.2 0.5 0.2 0.0 0.0 0.0
3930 0.0 0.0 0.0 0.0 0.6 0.0 0.0 0.0 0.0 0.0
0.0 0.0 0.0 0.0 0.6 0.0 0.0 0.0 0.0 0.0
0.0 0.0 0.0 0.0 0.6 0.0 0.0 0.0 0.0 0.0
0.0 0.0 S S S S S S 0.0 0.0 0.0

3931
3932
3933
3934
3935
3936
3937
3938
3939
3940
3941

3942 J.11 GPT-4.1 - 1 RANDOM CELL EASY: SAMPLE 1
39433944 **GPT-4.1 - 1 Random Cell Easy: Sample 1**
39453946 **Prompt:**3947 You are given a structural material distribution represented as a grid. Each cell can
3948 have one of the following states:

- 'L' indicates applied load.
- 'V' indicates void.
- 'S' indicates support.

3950 The goal is to predict the correct material distribution by filling in all 'V' cells
3951 with either '1' (solid) or '0' (empty), based on the surrounding structure and implicit
3952 physical reasoning (such as load paths, supports, and forces).3953 Important: The completed structure should use as little material as possible while
3954 remaining stable and plausible for carrying the applied forces. Minimize material usage
3955 unless necessary for structural support.

3956 Below is the input grid with masked regions:

```

3957 0 0 L L L 0 0 0 0 0
3958 0 0 0 1 0 0 0 0 0 0 0
3959 0 0 0 V 0 0 0 0 0 0 0
3960 0 0 0 1 0 0 0 0 0 0 0
3961 0 0 0 1 0 0 0 0 0 0 0
3962 0 0 1 1 1 0 0 0 0 0 0
3963 S S S S S S S S S S 0
  
```

3964 Please output the completed grid by replacing all 'V' cells with either '1' (solid) or '0'
3965 (empty).3966 Maintain the same format as the input: one row per line, cells separated by spaces, and
3967 the total number of rows and columns unchanged.

3968 Return only the completed grid without any additional explanation.

3969 **Model Completion (differences in red):**

```

3970 0 0 L L L 0 0 0 0 0
3971 0 0 0 1 0 0 0 0 0 0 0
3972 0 0 0 1 0 0 0 0 0 0 0
3973 0 0 0 1 0 0 0 0 0 0 0
3974 0 0 0 1 0 0 0 0 0 0 0
3975 0 0 1 1 1 0 0 0 0 0 0
3976 S S S S S S S S S S 0
  
```

3977 **Ground Truth:**

```

3978 0 0 L L L 0 0 0 0 0
3979 0 0 0 1 0 0 0 0 0 0 0
3980 0 0 0 1 0 0 0 0 0 0 0
3981 0 0 0 1 0 0 0 0 0 0 0
3982 0 0 1 1 1 0 0 0 0 0 0
3983 0 0 1 1 1 0 0 0 0 0 0
3984 S S S S S S S S S S 0
  
```

3985

3986

3987

3988

3989

3990

3991

3992

3993

3994

3995

3996 J.12 GPT-4.1 - 1 RANDOM CELL EASY: SAMPLE 2
39973998 **GPT-4.1 - 1 Random Cell Easy: Sample 2**
39994000 **Prompt:**4001 You are given a structural material distribution represented as a grid. Each cell can
4002 have one of the following states:

- 'L' indicates applied load.
- 'V' indicates void.
- 'S' indicates support.

4004 The goal is to predict the correct material distribution by filling in all 'V' cells
4005 with either '1' (solid) or '0' (empty), based on the surrounding structure and implicit
4006 physical reasoning (such as load paths, supports, and forces).4007 Important: The completed structure should use as little material as possible while
4008 remaining stable and plausible for carrying the applied forces. Minimize material usage
4009 unless necessary for structural support.

4010 Below is the input grid with masked regions:

```

L L L L L L 0 0 0 0
0 1 1 1 1 0 0 0 0 0
0 0 1 1 0 0 0 0 0 0
0 0 1 1 0 0 0 0 0 0
0 0 1 1 1 0 0 0 0 0
0 0 1 1 1 1 0 0 0 0
V 0 0 1 1 1 1 0 0 0
0 0 0 1 1 1 1 1 1 0 0
0 0 0 0 1 1 1 1 0 0
0 0 0 0 0 1 S S S 0

```

4018 **Model Completion (differences in red):**

```

L L L L L L 0 0 0 0
0 1 1 1 1 0 0 0 0 0
0 0 1 1 0 0 0 0 0 0
0 0 1 1 0 0 0 0 0 0
0 0 1 1 1 0 0 0 0 0
0 0 1 1 1 1 0 0 0 0
1 0 0 1 1 1 1 0 0 0
0 0 0 1 1 1 1 1 1 0 0
0 0 0 0 1 1 1 1 1 0 0
0 0 0 0 0 1 S S S 0

```

4026 **Ground Truth:**

```

L L L L L L 0 0 0 0
0 1 1 1 1 0 0 0 0 0
0 0 1 1 0 0 0 0 0 0
0 0 1 1 0 0 0 0 0 0
0 0 1 1 1 0 0 0 0 0
0 0 1 1 1 1 0 0 0 0
0 0 0 1 1 1 1 0 0 0
0 0 0 0 1 1 1 1 1 0 0
0 0 0 0 0 1 1 1 1 0 0
0 0 0 0 0 1 S S S 0

```

4034
4035
4036
4037
4038
4039
4040
4041
4042
4043
4044
4045
4046
4047
4048
4049

4104 J.14 GPT-4.1 - FULL EASY
41054106 **GPT-4.1 – Full Easy**
41074108 **Prompt:**
41094109 You are given a structural material distribution represented as a grid. Each cell can
4110 have one of the following states:4110 - 'L' indicates applied load.
4110 - 'V' indicates void.
4111 - 'S' indicates support.4112 The goal is to predict the correct material distribution by filling in all 'V' cells
4113 with either '1' (solid) or '0' (empty), based on the surrounding structure and implicit
4114 physical reasoning (such as load paths, supports, and forces).4115 Important: The completed structure should use as little material as possible while
4116 remaining stable and plausible for carrying the applied forces.

4117 Below is the input grid with masked regions:

4118 0 L L L L L 0 0 0 0
4119 V V V V V V V V V V V V
4120 V V V V V V V V V V V V
4121 V V V V V V V V V V V V
4122 V V V V V V V V V V V V
4123 V V V V V V V V V V V V
4124 V V V V V V V V V V V V
4125 0 S S S S S S 0 0 04126 Please output the completed grid by replacing all 'V' cells with either '1' (solid) or '0'
(empty).4127 Maintain the same format as the input: one row per line, cells separated by spaces, and
4128 the total number of rows and columns unchanged.

4128 Return only the completed grid without any additional explanation.

4129 **Model Completion (differences in red):**4130 0 L L L L L 0 0 0 0
4131 1 1 1 1 1 1 0 0 0 0
4132 1 0 0 0 0 0 1 0 0 0
4133 1 0 0 0 0 0 0 1 0 0 0
4134 1 0 0 0 0 0 0 1 0 0 0
4135 1 0 0 0 0 0 0 1 0 0 0
4136 1 1 1 1 1 1 0 0 0 0
4137 0 S S S S S S 0 0 04138 **Ground Truth:**4139 0 L L L L L 0 0 0 0
4140 0 0 1 1 1 0 0 0 0 0
4141 0 0 1 1 1 0 0 0 0 0
4142 0 0 0 1 0 0 0 0 0 0
4143 0 0 0 1 0 0 0 0 0 0
4144 0 0 0 1 0 0 0 0 0 0
4145 0 S S S S S S 0 0 0

4146

4147

4148

4149

4150

4151

4152

4153

4154

4155

4156

4157

4158 J.15 GPT-4.1 - FULL HARD

4159

4160 **GPT-4.1 – Full Hard**

4161

Prompt:

4162

You are given a structural material distribution represented as a grid. Each cell can have one of the following states:

4163

- 'L' indicates applied load.
- 'V' indicates void.
- 'S' indicates support.

4164

4165

The goal is to predict the correct material distribution by filling in all 'V' cells with a floating-point number between 0 and 1, with one decimal place (e.g., 0.0, 0.1, ..., 1.0), based on the surrounding structure and implicit physical reasoning (such as load paths, supports, and forces).

4166

4167

Important: The completed structure should use as little material as possible while

4168

remaining stable and plausible for carrying the applied forces.

4169

4170

Below is the input grid with masked regions:

4171

4172

```
0.0 L L L L L L L L
V V V V V V V V V V
V V V V V V V V V V
V V V V V V V V V V
V V V V V V V V V V
V V V V V V V V V V
V V V V V V V V V V
V V V V V V V V V V
V V V V V V V V V V
0.0 0.0 S S S S S 0.0 0.0 0.0
```

4173

4174

4175

4176

4177

4178

4179

Please output the completed grid by replacing all 'V' cells with a floating-point number between 0 and 1, with one decimal place.

4180

4181

Maintain the same format as the input: one row per line, cells separated by spaces, and the total number of rows and columns unchanged.

4182

Return only the completed grid without any additional explanation.

4183

4184

Model Completion (differences in red):

4185

4186

4187

4188

4189

4190

4191

```
0.0 L L L L L L L L
0.0 0.4 0.6 0.8 1.0 1.0 0.8 0.6 0.4 0.0
0.0 0.3 0.5 0.7 0.9 0.9 0.7 0.5 0.3 0.0
0.0 0.2 0.4 0.6 0.8 0.8 0.6 0.4 0.2 0.0
0.0 0.1 0.3 0.5 0.7 0.7 0.5 0.3 0.1 0.0
0.0 0.1 0.2 0.4 0.6 0.6 0.4 0.2 0.1 0.0
0.0 0.1 0.2 0.3 0.5 0.5 0.3 0.2 0.1 0.0
0.0 0.1 0.2 0.2 0.4 0.4 0.2 0.2 0.1 0.0
0.0 0.1 0.1 0.1 0.3 0.3 0.1 0.1 0.1 0.0
0.0 0.0 0.0 S S S S S 0.0 0.0 0.0
```

4192

Ground Truth:

4193

4194

4195

4196

4197

4198

4199

```
0.0 L L L L L L L L
0.0 0.0 0.2 0.3 0.0 0.3 0.0 0.3 0.2 0.0
0.0 0.0 0.0 0.4 0.2 0.3 0.2 0.4 0.0 0.0
0.0 0.0 0.0 0.2 0.4 0.0 0.4 0.2 0.0 0.0
0.0 0.0 0.0 0.0 0.4 0.0 0.4 0.0 0.0 0.0
0.0 0.0 0.0 0.0 0.2 0.5 0.2 0.0 0.0 0.0
0.0 0.0 0.0 0.0 0.0 0.6 0.0 0.0 0.0 0.0
0.0 0.0 0.0 0.0 0.0 0.6 0.0 0.0 0.0 0.0
0.0 0.0 0.0 0.0 0.0 0.6 0.0 0.0 0.0 0.0
0.0 0.0 0.0 S S S S S 0.0 0.0 0.0
```

4200

4201

4202

4203

4204

4205

4206

4207

4208

4209

4210

4211

4212 J.16 GEMINI 2.5 PRO - 1 RANDOM CELL EASY: SAMPLE 1
42134214 **Gemini 2.5 Pro - 1 Random Cell Easy: Sample 1**
42154216 **Prompt:**4217 You are given a structural material distribution represented as a grid. Each cell can
4218 have one of the following states:

- 'L' indicates applied load.
- 'V' indicates void.
- 'S' indicates support.

4220 The goal is to predict the correct material distribution by filling in all 'V' cells
4221 with either '1' (solid) or '0' (empty), based on the surrounding structure and implicit
4222 physical reasoning (such as load paths, supports, and forces).4223 Important: The completed structure should use as little material as possible while
4224 remaining stable and plausible for carrying the applied forces.

4225 Below is the input grid with masked regions:

```

0 0 L L L 0 0 0 0 0
0 0 0 1 0 0 0 0 0 0
0 0 0 V 0 0 0 0 0 0 0
0 0 0 1 0 0 0 0 0 0
0 0 0 1 0 0 0 0 0 0
0 0 0 1 0 0 0 0 0 0
0 0 1 1 1 0 0 0 0 0
0 0 1 1 1 0 0 0 0 0
0 0 1 1 1 0 0 0 0 0
S S S S S S S S S 0

```

4233 Please output the completed grid by replacing all 'V' cells with either '1' (solid) or '0'
(empty).4234 Maintain the same format as the input: one row per line, cells separated by spaces, and
4235 the total number of rows and columns unchanged.

4236 Return only the completed grid without any additional explanation.

4237

4238 **Model Completion (differences in red):**

```

0 0 L L L 0 0 0 0 0
0 0 0 1 0 0 0 0 0 0
0 0 0 1 0 0 0 0 0 0
0 0 0 1 0 0 0 0 0 0
0 0 0 1 0 0 0 0 0 0
0 0 0 1 0 0 0 0 0 0
0 0 1 1 1 0 0 0 0 0
0 0 1 1 1 0 0 0 0 0
0 0 1 1 1 0 0 0 0 0
0 0 1 1 1 0 0 0 0 0

```

4245 **Ground Truth:**

```

0 0 L L L 0 0 0 0 0
0 0 0 1 0 0 0 0 0 0
0 0 0 1 0 0 0 0 0 0
0 0 0 1 0 0 0 0 0 0
0 0 0 1 0 0 0 0 0 0
0 0 0 1 0 0 0 0 0 0
0 0 1 1 1 0 0 0 0 0
0 0 1 1 1 0 0 0 0 0
0 0 1 1 1 0 0 0 0 0
S S S S S S S S S 0

```

4253

4254

4255

4256

4257

4258

4259

4260

4261

4262

4263

4264

4265

4266 J.17 GEMINI 2.5 PRO - 1 RANDOM CELL EASY: SAMPLE 2
 4267

4268 Gemini 2.5 Pro - 1 Random Cell Easy: Sample 2

4269 **Prompt:**

4270 You are given a structural material distribution represented as a grid. Each cell can
 4271 have one of the following states:

- 4272 - 'L' indicates applied load.
- 4273 - 'V' indicates void.
- 4274 - 'S' indicates support.

4275 The goal is to predict the correct material distribution by filling in all 'V' cells
 4276 with either '1' (solid) or '0' (empty), based on the surrounding structure and implicit
 4277 physical reasoning (such as load paths, supports, and forces).

4278 **Important:** The completed structure should use as little material as possible while
 4279 remaining stable and plausible for carrying the applied forces.

4280 Below is the input grid with masked regions:

4281 L L L L L 0 0 0 0
 4282 0 1 1 1 0 0 0 0 0
 4283 0 0 1 1 0 0 0 0 0
 4284 0 0 1 1 0 0 0 0 0
 4285 0 0 1 1 1 0 0 0 0
 4286 V 0 0 1 1 1 1 0 0 0
 4287 0 0 0 1 1 1 1 0 0 0
 4288 0 0 0 0 1 1 1 1 0 0 0
 4289 0 0 0 0 0 1 S S S 0

4290 Please output the completed grid by replacing all 'V' cells with either '1' (solid) or '0'
 4291 (empty).

4292 Maintain the same format as the input: one row per line, cells separated by spaces, and
 4293 the total number of rows and columns unchanged.

4294 Return only the completed grid without any additional explanation.

4295 **Model Completion (differences in red):**

4296 L L L L L 0 0 0 0
 4297 0 1 1 1 1 0 0 0 0 0
 4298 0 0 1 1 0 0 0 0 0
 4299 0 0 1 1 0 0 0 0 0
 4300 0 0 1 1 1 0 0 0 0
 4301 0 0 1 1 1 1 0 0 0 0
 4302 0 0 0 1 1 1 1 0 0 0
 4303 0 0 0 1 1 1 1 0 0 0
 4304 0 0 0 1 1 1 1 0 0 0
 4305 0 0 0 0 1 1 1 1 0 0 0
 4306 0 0 0 0 0 1 S S S 0

4307 **Ground Truth:**

4308 L L L L L 0 0 0 0
 4309 0 1 1 1 1 0 0 0 0 0
 4310 0 0 1 1 0 0 0 0 0 0
 4311 0 0 1 1 0 0 0 0 0 0
 4312 0 0 1 1 1 0 0 0 0 0
 4313 0 0 1 1 1 1 0 0 0 0
 4314 0 0 0 1 1 1 1 0 0 0
 4315 0 0 0 1 1 1 1 1 0 0 0
 4316 0 0 0 0 1 1 1 1 1 0 0
 4317 0 0 0 0 0 1 S S S 0

4318

4319

4320 J.18 GEMINI 2.5 PRO - 1 RANDOM CELL HARD
43214322 **Gemini 2.5 Pro - 1 Random Cell Hard**

4323

4324 **Prompt:**4325 You are given a structural material distribution represented as a grid. Each cell can
have one of the following states:4326 - 'L' indicates applied load.
4327 - 'V' indicates void.
4328 - 'S' indicates support.4329 The goal is to predict the correct material distribution by filling in all 'V' cells with
4330 a floating-point number between 0 and 1 (with one decimal place), based on the surrounding
4331 structure and implicit physical reasoning (such as load paths, supports, and forces).4332 **Important:** The completed structure should use as little material as possible while
4333 remaining stable and plausible for carrying the applied forces.

4334 Below is the input grid with masked regions:

4335 0.0 L V L L L L L 0.0
0.0 0.0 0.2 0.3 0.1 0.1 0.3 0.2 0.0 0.0
0.0 0.0 0.1 0.4 0.0 0.0 0.4 0.1 0.0 0.0
0.0 0.0 0.0 0.4 0.0 0.0 0.4 0.0 0.0 0.0
0.0 0.0 0.0 0.4 0.0 0.0 0.4 0.0 0.0 0.0
0.0 0.0 0.0 0.4 0.0 0.0 0.4 0.0 0.0 0.0
0.0 0.0 0.0 0.4 0.0 0.0 0.4 0.0 0.0 0.0
0.0 0.0 0.0 0.4 0.1 0.1 0.4 0.0 0.0 0.0
0.0 0.0 0.0 0.4 0.1 0.1 0.4 0.0 0.0 0.0
0.0 0.0 0.0 0.4 0.1 0.1 0.4 0.0 0.0 0.0
0.0 S S S S S S S S S 0.04336 **Model Completion (differences in red):**4337 0.0 L 0.2 L L L L L L 0.0
0.0 0.0 0.2 0.3 0.1 0.1 0.3 0.2 0.0 0.0
0.0 0.0 0.1 0.4 0.0 0.0 0.4 0.1 0.0 0.0
0.0 0.0 0.0 0.4 0.0 0.0 0.4 0.0 0.0 0.0
0.0 0.0 0.0 0.4 0.0 0.0 0.4 0.0 0.0 0.0
0.0 0.0 0.0 0.4 0.0 0.0 0.4 0.0 0.0 0.0
0.0 0.0 0.0 0.4 0.0 0.0 0.4 0.0 0.0 0.0
0.0 0.0 0.0 0.4 0.1 0.1 0.4 0.0 0.0 0.0
0.0 0.0 0.0 0.4 0.1 0.1 0.4 0.0 0.0 0.0
0.0 0.0 0.0 0.4 0.1 0.1 0.4 0.0 0.0 0.0
0.0 S S S S S S S S S 0.04338 **Ground Truth:**4339 0.0 L L L L L L L 0.0
0.0 0.0 0.2 0.3 0.1 0.1 0.3 0.2 0.0 0.0
0.0 0.0 0.1 0.4 0.0 0.0 0.4 0.1 0.0 0.0
0.0 0.0 0.0 0.4 0.0 0.0 0.4 0.0 0.0 0.0
0.0 0.0 0.0 0.4 0.0 0.0 0.4 0.0 0.0 0.0
0.0 0.0 0.0 0.4 0.0 0.0 0.4 0.0 0.0 0.0
0.0 0.0 0.0 0.4 0.1 0.1 0.4 0.0 0.0 0.0
0.0 0.0 0.0 0.4 0.1 0.1 0.4 0.0 0.0 0.0
0.0 0.0 0.0 0.4 0.1 0.1 0.4 0.0 0.0 0.0
0.0 S S S S S S S S S 0.0

4340

4341

4342

4343

4344

4345

4346

4347

4348

4349

4350

4351

4352

4353

4354

4355

4356

4357

4358

4359

4360

4361

4362

4363

4364

4365

4366

4367

4368

4369

4370

4371

4372

4373

4374 J.19 GEMINI 2.5 PRO - FULL EASY

4375

4376 **Gemini 2.5 Pro – Full Easy**

4377

4378 **Prompt:**4379 You are given a structural material distribution represented as a grid. Each cell can
have one of the following states:4380 - 'L' indicates applied load.
4381 - 'V' indicates void.
4382 - 'S' indicates support.4383 The goal is to predict the correct material distribution by filling in all 'V' cells
4384 with either '1' (solid) or '0' (empty), based on the surrounding structure and implicit
physical reasoning (such as load paths, supports, and forces).4385 Important: The completed structure should use as little material as possible while
4386 remaining stable and plausible for carrying the applied forces.

4387 Below is the input grid with masked regions:

4388 0 0 0 L L L L 0 0 0
4389 V V V V V V V V V V V V
4390 V V V V V V V V V V V V
4391 V V V V V V V V V V V V
4392 V V V V V V V V V V V V
4393 V V V V V V V V V V V V
4394 V V V V V V V V V V V V
4395 0 0 0 0 S S S 0 0 04396 **Model Completion (differences in red):**4397 0 0 0 L L L L 0 0 0
4398 0 0 0 1 1 1 0 0 0
4399 0 0 0 0 1 1 1 0 0 0
4400 0 0 0 0 1 1 1 0 0 0
4401 0 0 0 0 1 1 1 0 0 0
4402 0 0 0 0 1 1 1 0 0 0
4403 0 0 0 0 S S S 0 0 04404 **Ground Truth:**4405 0 0 0 L L L L 0 0 0
4406 0 0 0 0 1 1 0 0 0 0
4407 0 0 0 0 1 1 0 0 0 0
4408 0 0 0 0 1 1 0 0 0 0
4409 0 0 0 0 1 1 0 0 0 0
4410 0 0 0 0 1 1 0 0 0 0
4411 0 0 0 0 S S S 0 0 0

4412

4413

4414

4415

4416

4417

4418

4419

4420

4421

4422

4423

4424

4425

4426

4427

4428 J.20 GEMINI 2.5 PRO - FULL HARD
 4429

Gemini 2.5 Pro - Full Hard

4430 **Prompt:**

4431 You are given a structural material distribution represented as a grid. Each cell can
 4432 have one of the following states:

- 'L' indicates applied load.
- 'V' indicates void.
- 'S' indicates support.

4433 The goal is to predict the correct material distribution by filling in all 'V' cells with
 4434 a floating-point number between 0 and 1 (with one decimal place), based on the surrounding
 4435 structure and implicit physical reasoning.

4436 Below is the input grid with masked regions:

4437 0.0 0.0 L L L 0.0 0.0 0.0 0.0 0.0 0.0
 4438 V V V V V V V V V V V V
 4439 V V V V V V V V V V V V
 4440 V V V V V V V V V V V V
 4441 V V V V V V V V V V V V
 4442 V V V V V V V V V V V V
 4443 V V V V V V V V V V V V
 4444 V V V V V V V V V V V V
 4445 V V V V V V V V V V V V
 4446 S S S S S S S S S 0.0

4447 **Model Completion (differences in red):**

4448 0.0 0.0 L L L 0.0 0.0 0.0 0.0 0.0 0.0
 4449 0.0 0.1 1.0 1.0 1.0 0.1 0.0 0.0 0.0 0.0 0.0
 4450 0.0 0.2 1.0 1.0 1.0 0.2 0.0 0.0 0.0 0.0 0.0
 4451 0.1 0.3 1.0 1.0 1.0 0.3 0.1 0.0 0.0 0.0 0.0
 4452 0.2 0.4 1.0 1.0 1.0 0.4 0.2 0.0 0.0 0.0 0.0
 4453 0.3 0.5 1.0 1.0 1.0 0.5 0.3 0.1 0.0 0.0 0.0
 4454 0.4 0.6 1.0 1.0 1.0 0.6 0.4 0.2 0.0 0.0 0.0
 4455 0.5 0.7 1.0 1.0 1.0 0.7 0.5 0.3 0.1 0.0 0.0
 4456 0.6 0.8 1.0 1.0 1.0 0.8 0.6 0.4 0.2 0.0 0.0
 4457 S S S S S S S S S 0.0

4458 **Ground Truth:**

4459 0.0 0.0 L L L 0.0 0.0 0.0 0.0 0.0 0.0
 4460 0.0 0.0 0.0 0.9 0.0 0.0 0.0 0.0 0.0 0.0 0.0
 4461 0.0 0.0 0.0 0.8 0.0 0.0 0.0 0.0 0.0 0.0 0.0
 4462 0.0 0.0 0.0 0.8 0.0 0.0 0.0 0.0 0.0 0.0 0.0
 4463 0.0 0.0 0.0 0.9 0.0 0.0 0.0 0.0 0.0 0.0 0.0
 4464 0.0 0.0 0.1 0.8 0.1 0.0 0.0 0.0 0.0 0.0 0.0
 4465 0.0 0.0 0.1 0.8 0.1 0.0 0.0 0.0 0.0 0.0 0.0
 4466 0.0 0.0 0.2 0.8 0.2 0.0 0.0 0.0 0.0 0.0 0.0
 4467 S S S S S S S S S 0.0

4468

4469

4470

4471

4472

4473

4474

4475

4476

4477

4478

4479

4480

4481